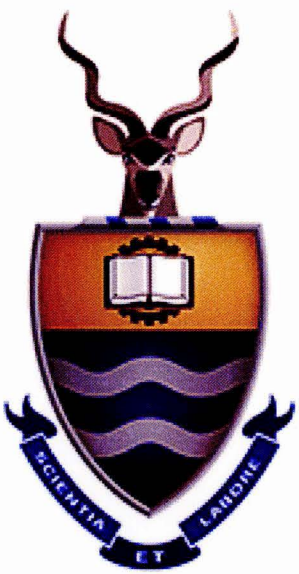
The Effect of imidazo[1,2-a]pyridine amines on MCF-7 and MDA-MB-231 Breast Cancer Cells

Taurai Flloyd Kurebwa



WITS
UNIVERSITY

A dissertation submitted to the Faculty of Health Sciences, University of the Witwatersrand, Johannesburg, in fulfilment of the requirements for the degree of Masters of Science in Medicine (Pharmacology)

Johannesburg, 2015

Declaration

I declare that the work presented in this Dissertation is, to the best of my knowledge and belief, original, except as acknowledged in the text, and that the material has not been submitted for a degree at this or any other university. It is being submitted for the degree of Master of Science in Medicine (Pharmacology) at the University of the Witwatersrand, Johannesburg.

I acknowledge that I have read and understood the University's rules, requirements, procedures and policy relating to my Dissertation. I certify that I have complied with the rules, requirements, procedures and policy of the University.

Signature:.....

On this 15th day of February 2016

Dedication

I dedicate this thesis to the following people:

- My supervisor **Dr Leonie Harmse** for her continued patience and support and nurturing of my scientific methods and writing method. She has constantly been a pillar throughout my dissertation and I cannot thank her enough, I am a better scientist because of her.

- My parents **Mr** and **Mrs Kurebwa** for believing in me when I didn't believe in myself.

    - My mom for all her hard work, you spent time away from your husband in a foreign land just to get me through university, I am forever grateful for your sacrifice and love.

    - My dad, for all the pep talks, for the sacrifice and for faith in me ever since I was in high school, even when I believed I couldn't do it you believed in me before it happened. Thank you for your unconditional love.

- My brothers **Francis** and **Frank Kurebwa**, you guys are the coolest brothers a guy could ask for, thank you for your support, for setting the standard and for constantly reminding me that I am going to get this done.

- My colleagues **Zeenat Ismail** and **Somayya Ragie** for your constant encouragement sharing the burden of laboratory work. For reading my work time and time again, for being my writing buddies and proofreading champions. I appreciate and treasure your friendship.

- Last but not definitely not least I would like to thank my number one fan and girlfriend **Babalwa May**, you saw me at my lowest and could always brighten up my day. Thanks for reading the boring science and being ever interested in my work. Thank you for your patience with the long hours, your understanding and most of all your love.

Abstract

Breast cancer, is the most frequently diagnosed cancer in women and is associated with high mortality rates in South Africa. There is a high prevalence of metastatic breast cancer and triple negative tumours, which are associated with poor prognosis. In this study, the response of two breast cancer cell lines, MCF-7 and MDA-MB-231, were evaluated when treated with novel imidazo[1,2-a]pyridine amines.

The compounds were synthesized by the School of Chemistry of the University of the Witwatersrand using the Groebke-Blackburn-Bienaymé multicomponent reaction and tested for purity by elemental analysis. The MTT (3-(4,5-dimethylthiazol-2-yl)-2,5-diphenyltetrazolium bromide) assay was used to determine the cytotoxic effects of test compounds on breast cancer cells and the toxic effect of compounds on non-tumorigenic unstimulated peripheral leukocytes. IC_{50} values of test compounds were calculated from sigmoidal dose response curves. The morphology of cells exposed to test compounds was assessed by fluorescent microscopy using Hoechst 33342, acridine orange and ethidium bromide. The ability of test compounds to induce apoptosis was measured by a colorimetric caspase-3 assay and a fluorometric Annexin-V-FITC assay. Monodansylcadaverine was used to determine if autophagic vacuoles were formed after exposure to test compounds.

Three imidazo[1,2-a]pyridine amines, JD88, JD253 and JD256, were more cytotoxic to MCF-7 than to MDA-MB-231 cells. MCF-7 cells showed morphological features associated with apoptosis, and proteolysis by caspase-3/7 was observed after MCF-7 cells were exposed to JD88 for two hours. Vacuole formation induced by these compounds was not autophagic in since they did not co-localize with MDC florescent clusters. This together with the exposure of phosphatidylserine to the outer surface of MCF-7 cells suggests that apoptosis is induced in these cells. There was no evidence of cytochrome c translocation to the cytoplasm, which indicates that the intrinsic pathway of apoptosis is not activated. MDA-MB-231 cells treated with JD88, JD253 and JD256 were large with multiple nuclei and decondensed chromatin, morphological features associated with mitotic catastrophe. The cells also showed morphological features associated with necrosis and apoptosis, which include loss of cell membrane integrity and cell membrane blebbing respectively. MDA-MB-231 cells exposed to JD88 showed marked exposure of phosphatidylserine and this was observed to a minor extent in cells exposed to JD253 and JD256. Proteolysis by caspase-3/7 was activated in MDA-MB-231 cells exposed to JD88 as early as 2 hours after exposure.

In conclusion three compounds; JD88, JD253 and JD256 were able to induce apoptosis in MCF-7 cells. These compounds were selectively toxic against MCF-7 cells compared to MDA-MB-231 cells and JD256 in particular was less toxic to leukocytes, which may translate to fewer serious adverse effects. Addition of a copper dioxygen complex to these compounds increases activity against both breast cancer cells. JD88 in particular has shown effective induction of apoptosis and this merits further investigation into its potential as a lead compound in breast cancer therapy.

Acknowledgements

This dissertation could not have been completed without the support and input of different people and organisations.

I would like to thank Dr Leonie Harmse my supervisor for her constant support and mentorship. Thank you for helping me improve my writing and critical thinking skills, for always being available to assist and guide me throughout my Masters.

I sincerely thank our collaborators from the Wits School of Chemistry, Professor Charles de Koning and Jean Dam. Thank you for your foresight in developing the compounds for this study, for assistance in understanding the chemistry, for continued support at conference presentations. Thank you very much for all your intellectual and financial support.

I am grateful to the National Research Foundation Niche Areas Program for their financial support during this study.

Many thanks to the Andrew T. Mellon Foundation for financial support during this study and intellectual support during my writing process. I would sincerely like to thank my Mellon Mays Undergraduate Fellowship cohort Tiffany, Jonathan, Sifiso and Genevieve for all the guidance and support during my masters.

I would like to thank Professor Robyn van Zyl for your continued support and assistance during this entire process.

Special thanks to the staff from the Division of Pharmacology and my 2013 masters cohort for all your assistance, be it in helping me write better, supporting my laboratory procedures or the many printing jobs that needed to be done. I am forever grateful for all of you.

I am forever grateful to my family for all their support, emotionally, financially and intellectually. I would not have made it to this point without all of you.

Research Outputs

Conference Proceedings

Kurebwa TF, de Koning CB, Dam J, Harmse LH. Novel 6-substituted imidazoles as potential chemotherapeutic agents in breast cancer. Oral presentation at the School of Therapeutic Sciences Research Day 2015, held on the 8th of September 2015 at the Wits Education Campus Khanya Block, Johannesburg South Africa.

Kurebwa TF, de Koning CB, Dam J, Harmse LH. Novel imidazoles induce apoptosis in breast cancer cells. Oral presentation at the SASBCP-TOXSA-WITS Congress 2015, held from the 31st of August to the 2nd of September 2015 at the Wits Club, Johannesburg South Africa.

Kurebwa TF, de Koning CB, Dam J, Harmse LH (2015). The effect of compounds based on novel 7-azaindoles and 6-substituted imidazoles on MCF-7 breast cancer cells. *Southern African Journal of Infectious Diseases (Abstract)* **30**(1): 26

Kurebwa TF, de Koning CB, Dam J, Harmse LH. An In-vitro study on the effects of compounds based on novel 7-azaindoles and 6-substituted imidazoles in MCF-7 breast cancer cells. An oral presentation at the WITS Cross-Faculty Graduate Symposium 2014, held from the 29th to the 30th of October 2014 at the Senate House, Wits University, Johannesburg South Africa.

Kurebwa TF, de Koning CB, Dam J, Harmse LH (2014). The effects of novel 7-azaindoles and 6-substituted imidazoles on MCF-7 breast cancer cells. *Journal of Basic & Clinical Pharmacology & Toxicology (Abstract)* **115**(s1): 154

Table of Contents

	Page
Declaration	i
Dedication	ii
Abstract	iii
Acknowledgements	iv
Research Outputs	v
Table of Contents	vi
List of Figures	ix
List of Tables	xii
List of Abbreviations, Acronyms and Symbols	xiv

CHAPTER 1 – INTRODUCTION **1**

1.1 Statistics **1**
1.1.1 Global Cancer Statistics 1
1.1.2 Global Breast Cancer Statistics 2
1.1.3. South African Breast cancer Statistics 2

1.2 Cancer classification **3**
1.2.1 General cancer classification 3
1.2.2 Breast cancer histological classification 3
1.2.2.1 In-situ carcinomas 3
1.2.2.2 Invasive carcinomas 4
1.2.2.2 Molecular classification 4
1.2.3 Breast Cancer Staging 7
1.2.3.1 Size of tumour at primary site (T) 7
1.2.3.2 Regional lymph node metastases (N) 7
1.2.3.3 Distant metastases (M) 7
1.2.3.4 Prognostic stages 8

1.3 Molecular basis of cancer **8**
1.3.1 The Cell Cycle 8
1.3.2 The Clonal genetic model 10

1.4 Breast cancer therapy **12**
1.4.1 Surgery and radiation therapy 12
1.4.2 Chemotherapy 12
1.4.2.1 Taxanes and anthracyclines 13
1.4.2.2 Other agents 14
1.4.2.3 Hormone therapy 15
1.4.2.4 Targeted therapy 16

1.5 Cancer cell death **17**
1.5.1 Autophagy 18
1.5.2 Regulated Necrosis 18
1.5.3 Mitotic catastrophe 18
1.5.4 Apoptosis 19
1.5.1.1 Death receptor pathway 19
1.5.1.2 Mitochondrial Pathway 20

1.6 Apoptosis in Breast cancer 22
1.6.1 p53 and breast cancer 22
1.6.2 Bcl-2 and breast cancer 24

1.7 Drug discovery 24
1.7.1 Target-based screening 24
1.7.2 Phenotypic screening 25
1.7.3 Novel Compounds 26
1.7.4 Cell Lines 26
1.7.4.1 MCF-7 cell line 26
1.7.4.2 MDA-MB-231 cell line 26

1.8 Aim and Objectives 27

CHAPTER 2 - METHODS 28

2.1 Cell culture 28
2.1.1 Cell culture initiation 28
2.1.2 Cell culture maintenance 29
2.1.3 Cell sub-culturing 29
2.1.4 Cryopreservation 30

2.2 Cell viability assays 30
2.2.1 MTT Cell Viability Assay 30
2.2.2 Leucocyte toxicity assay 32

2.3 Cell morphology assays 33
2.3.1 Phase contrast and Fluorescence microscopy 33
2.3.1.1 Effect of novel compounds on cell morphology (AO-EB-HO staining) 33
2.3.1.2 Effect of test compounds on autophagic vacuole formation in MCF-7 cells 34

2.4 Apoptotic biomarker assays 35
2.4.1 Caspase-3/7 colorimetric assay 35
2.4.1.1 Assay procedure 35
2.4.1.2 Bradford protein determination assay 36
2.4.1.3 Standard curve 36
2.4.2 Annexin-V Assay 37
2.4.3 Effect of test compounds on the cytoskeleton of MCF-7 cells 37
2.4.4 Cytochrome c ELISA assay 38
2.4.4.1 Lysate preparation 38
2.4.4.2 ELISA assay procedure 39
2.5.2.3 Standard Curve 40

CHAPTER 3 – RESULTS 41

3.1 Solubilisation of imidazo[1,2-a]pyridine amines 41

3.2 Effect of the test compounds on cell viability 41
3.2.1 MCF-7 IC_{50} values of active compounds 44
3.2.2 MDA-MD-231 IC_{50} values of active compounds 45
3.2.3 Dose response curves for MCF-7 and MDA-MB-231 cells 46
3.2.4 Effect of test compounds on leukocyte viability 48
3.2.5 Statistical analysis of cell viability 48
3.3 Morphology of cells exposed to test compounds 50
3.3.1 Effect of test compounds on MCF-7 cell morphology 50
3.3.1.1 Effect of test compounds on MCF-7 morphology at concentrations equal to their IC_{50} values 50
3.3.1.2 Effect of test compounds on MCF-7 morphology at 25 μM 52
3.3.2 Effect of test compounds on MDA-MB-231 cell morphology 53
3.3.3 Effect of test compounds on cell and nuclear morphology 55
3.3.3.1 Effect of test compounds on MCF-7 cell and nuclear morphology 55

3.3.3.2 Effects on MDA-MB-231 cell and nuclear morphology 57

3.4 Identity of vacuoles formed in MCF-7 cells treated with test compounds 60

3.5 Effect on test compounds on biochemical markers 62
3.5.1 Effect of test compounds on caspase-3/7 activity 62
3.5.1.1 Caspase-3/7 activity in MCF-7 cells 62
3.5.1.2 Caspase-3/7 activity in MDA-MB-231 cells 63
3.5.2 Exposure of phosphatidylserine on the surface of the cell membrane 64
3.5.2.1 Exposure of phosphatidylserine on the cell membrane of MCF-7 cells 64
3.5.2.2 Exposure of phosphatidylserine on the cell membrane of MDA-MB-231 cells 66
3.5.3 Effect of active test compounds on the cytoskeleton of MCF-7 cells 68
3.5.4 Effect of test compounds on mitochondrial integrity in MCF-7 cells 70

3.6 Effect of copper containing imidazo[1,2-a]pyridine analogues on MCF-7 and MDA-MB-231 cells 71
3.6.1 Effect of copper containing imidazo[1,2-a]pyridine amine analogues on cell viability 71
3.6.2 Structural activity relationships (SARs) of imidazo[1,2-a]pyridine amines 74

CHAPTER 4 – DISCUSSION 78

4.1 Effect of imidazo[1,2-a]pyridine amines on cell viability of MCF-7, MDA-MB-231 cells and leukocytes 78

4.2 Effect of active test compounds on programmed cell death in MCF-7 cells 81
4.2.1 Effect of active test compounds on cell morphology of MCF-7 cells 81
4.2.2 Effect of active test compounds on nuclear morphology of MCF-7 cells 83
4.2.3 Effect of active test compound on caspase-7 activity and phosphatidylserine exposure in MCF-7 cells 83
4.2.4 Effect of active test compounds on cytochrome c translocation in MCF-7 cells 85

4.3 Effect of active test compounds on programmed cell death in MDA-MB-231 cells 86
4.3.1 Effect of active test compounds on cell morphology of MDA-MB-231 cells 87
4.3.2 Effect of active test compounds on nuclear morphology of MDA-MB-231 cells 87
4.3.3 Effect of active test compound on caspase-3/7 activity and phosphatidylserine exposure in MDA-MB-231 cells 88

4.4 Structure activity relationships of active test compounds 89

CHAPTER 5 – CONCLUSION 91

CHAPTER 6 – REFERENCES 93

CHAPTER 7 – APPENDIX 110

Appendix A: Additional Documents 110

Appendix B: Standard Curves 115

Appendix C: Microscopy 119

Appendix D: Protein Concentration 126

List of Figures

Figure		Page
	Chapter 1 – Introduction and Literature Review	
Figure 1.1	Global estimations of new cases (thousands) of cancer in 2012	1
Figure 1.2	Key steps in the development of cancerous cells through cell cycle dysregulation	9
Figure 1.3	The clonal genetic model	11
Figure 1.2	Schematic of the death receptor and mitochondrial pathways of apoptosis	21
Figure 1.3	Schematic diagram of the role of p53 in the mitochondrial pathway	23
	Chapter 3 – Results	
Figure 3.1	The effect of test compound on cell viability of MCF-7 cells after 48 hours exposure at 100 µM	42
Figure 3.2	The effect of test compound on cell viability of MDA-MB-231 cells after 48 hours exposure at 100 µM	43
Figure 3.3	Summary of IC_{50} values of MCF-7 cells exposed to active test compounds for 48 hours	44
Figure 3.4	Summary of IC_{50} values of MDA-MB-231 cells exposed to active test compounds for 48 hours	45
Figure 3.5	Representative dose response curves of test compounds and camptothecin (CAM) for MCF-7 and MDA-MB-231 cells	47
Figure 3.6	Effect of test compounds on leukocyte cell viability at MCF-7 and MDA-MB-231 at 15 and 25 µM after 48 hours	48
Figure 3.7	Effect of test compounds on MCF-7 cell morphology at IC_{50} values	51
Figure 3.8	Effect of test compounds on MCF-7 cell morphology at 25 µM	52
Figure 3.9	Effect of test compounds on MDA-MB-231 cell morphology at IC_{50} values	54
Figure 3.10	Effect of test compounds on cell and nuclear morphology of MCF-7 cells after 24 hours at 400x magnification	56

Figure 3.11 Effect of test compounds on cell and nuclear morphology of MDA-MB-231 cells after 24 hours at 400x magnification 58

Figure 3.12 Monodansylcadaverine fluorescent clustering in MCF-7 cells treated with test compounds for 20 hours 61

Figure 3.13 The effect of test compounds on caspase-3/7 activity in MCF-7 cells at various exposure times 63

Figure 3.14 The effect of test compounds on caspase-3/7 activity in MDA-MB231 cells at various exposure times 64

Figure 3.15 The effect of test compounds on phosphatidylserine exposure in MCF-7 cells at 400X magnification 66

Figure 3.16 The effect of test compounds on phosphatidylserine exposure in MDA-MB-231 cells at 400X magnification 67

Figure 3.17 Effect of test compounds on the cytoskeleton of MCF-7 cells at 24 hours of exposure 69

Figure 3.18 The effect of test compounds on the translocation of cytochrome c to the cytoplasm in MCF-7 cells 71

Figure 3.19 Summary of IC_{50} values of copper containing compounds against MCF-7 after 48 hours 72

Figure 3.20 Summary of IC_{50} values of copper containing compounds against MDA-MB-231 after 48 hours 73

Chapter 7 – Appendices

Figure B7.1 Standard curve for MCF-7 cells using the MTT assay 115

Figure B7.2 Standard curve for MDA-MB-231 cells using the MTT assay 115

Figure B7.3 Caspase assay pNa standard curve 116

Figure B7.4 Standard curves for protein concentrations in the caspase assay (Experiment 1-4) 116

Figure B7.5 Standard curves for protein concentrations in the caspase assay (Experiment 5-8) 117

Figure B7.6 Standard curves for protein concentrations (Experiment 9-11) 117

Figure B7.7 pNA standard curve for cytochrome c assay 118

Figure C7.8 Effect of test compounds at IC50 values on MCF-7 cell morphology after 2 and 6 hours 119

Figure C7.9 Effect of test compounds at 25 μM on MCF-7 cell morphology at 2, 6 and 8 hours 120

Figure C7.10 Effect of test compounds on MDA-MB-231 cell morphology at 2 and 8 hours 121

Figure C7.11 Effect of test compounds on nuclear morphology in MCF-7 cells at 24 hours 122

Figure C7.12 Effect of test compounds on nuclear morphology in MDA-MB-231 cells after 24 hours 123

Figure C7.13 Effect of active test compounds on MCF-7 cells at 100X magnification 124

Figure C7.14 Effect of active test compounds on MDA-MB-231 cells at 100X magnification 125

List of Tables

Table		Page
	Chapter 2 – Methods	
Table 2.1	Reaction volume for caspase assay in 96 well plate	36
	Chapter 3 – Results	
Table 3.1	Summary of structures and IC_{50} values of active test compounds	46
Table 3.2	Statistical comparisons of IC_{50} values of test compounds and positive control camptothecin (CAM)	49
Table 3.3	Effect of test compounds on MCF-7 cell nuclear length and induction of apoptosis and necrosis	57
Table 3.4	Effect of test compounds on MDA-MB-231 cell nuclear length and induction of apoptosis and necrosis	59
Table 3.5	The effect of test compounds on phosphatidylserine exposure in MCF-7 cells (IC75 value)	65
Table 3.6	The effect of test compounds on phosphatidylserine exposure in MDA-MB-231 cells (IC75 value)	68
Table 3.7	Statistical significance of effect of imidazo[1,2-a]pyridine amine analogues in MCF-7 cells	73
Table 3.8	Statistical significance of effect of imidazo[1,2-a]pyridine amine analogues in MDA-MB-231 cells	74
Table 3.9	Comparison of base structure and structures containing transition metal complexes	75
Table 3.10	Comparison of copper containing structures and substitutions on the amidogen group	75
Table 3.11	Structure activity relationships of imidazo[1,2-a]pyridine amines and analogues	76
	Chapter 4 – Discussion	
Table 4.1	Summary of effect of active test compounds on MCF-7 programmed cell death	81
Table 4.2	Summary of effect of active test compounds on MDA-MB-231 programmed cell death	86

Chapter 7 – Appendix

Table D7.1 Effect of active test compounds on protein concentration in MCF-7 cells 126

Table D7.2 Effect of active test compounds on protein concentration in MDA-MB-231 cells 126

List of Abbreviations and Acronyms

Abs	–	Absorbance
AO	–	Acridine orange
AIF	–	Apoptosis inducing factor
Apaf-1	–	Apoptosis protease activating factor 1
Bcl-2	–	B-cell lymphoma-2
Bcl-X_L	–	B-cell lymphoma-extra large
BH3	–	B-cell lymphoma-2 homology domain 3
BID	–	BH3 interacting-domain
BSA	–	Bovine serum albumin
CHAPS	–	3-[(3-Cholamidopropyl)dimethylammonio]-1 propanesulfonate
CO_2	–	Carbon dioxide
DMEM	–	Dulbecco's Modified Eagle's Medium
DMSO	–	Dimethyl sulfoxide
DNA	–	Deoxyribonucleic acid
DR3	–	Death receptor 3
EB	–	Ethidium bromide
EDTA	–	Ethylenediaminetetraacetic acid
EGFR	–	Epidermal growth factor receptor
FADD	–	Fas associated death domain
FasL	–	Fas ligand
FBS	–	Foetal bovine Serum
FDA	–	Food and Drug Administration
FITC	–	Fluorescein isothiocyanate
HEPES	–	4-(2-hydroxyethyl)-1-piperazine ethanesulfonic acid
HO	–	Hoechst 33342
ICAD	–	Inhibitor of caspase-activated DNase
IC_{50}	–	50 % inhibitory concentration
M	–	Molar
MDC	–	Monodansylcadaverine
mM	–	Millimolar
µM	–	Micromolar
µL	–	Microliter

mL	–	Milliliter
µm	–	micrometre
MTT	–	3-(4,5-dimethylthiazol-2-yl)-2,5-diphenyltetrazolium bromide
O_2	–	Oxygen
ONC	–	Oncogene
PARP	–	Poly(ADP-ribose) polymerase
PBS	–	Phosphate Buffered Saline
PUMA	–	p53 upregulated modulator of apoptosis
PI	–	propidium iodide
pNa	–	p-nitroanilide
PS	–	Phosphatidylserine
RIP	–	Receptor interacting protein
rpm	–	Rotations per minute
SDS	–	Sodium dodecyl sulfate
SEM	–	Standard error of the mean
Smac	–	Second mitochondria-derived activator of caspases
tBid	–	Truncated Bid
TNF	–	Tumour necrosis factor
TRAIL	–	Tumour necrosis factor–related apoptosis-inducing ligand
TSG	–	Tumour suppressor gene
v/v	–	Volume per volume
w/v	–	Weight per volume
XIAP	–	x-linked Inhibitor-of-apoptosis

Chapter 1 – Introduction

1.1 Statistics

1.1.1 Global Cancer Statistics

Non-communicable diseases have become the dominant cause of death worldwide according to the World Health Organisation's 2010 study (Lozano *et al.*, 2012). Cancer related death, one of the major contributors to mortality, increased by 38% between 1990 and 2010. An increase in 200 000 deaths was observed from 2008 to 2012 in the GLOBOCAN 2012 study.

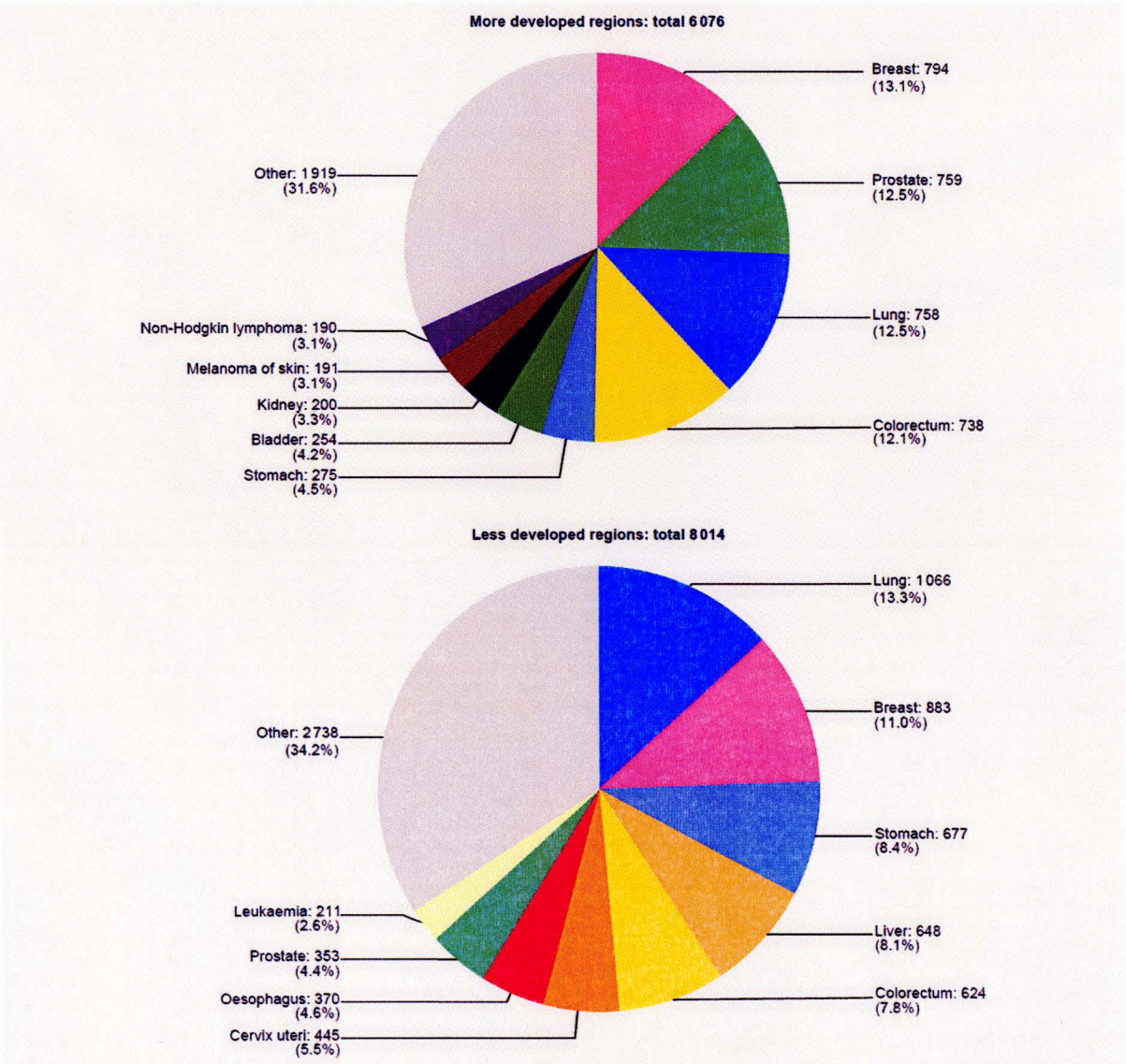


Figure 1.1 Global estimations of new cases (thousands) of cancer in 2012 (Ferlay *et al.*, 2015) The two pie charts represent total new cases of cancer in developed and less developed regions worldwide respectively. Each section of the pie represents the proportion of new cases for each cancer.

GLOBOCAN 2012 also showed that in 2012 breast cancer was the most diagnosed cancer and the most prominent cause of cancer related death among women. In the same year lung cancer was the most prominent cause of cancer death in men. The five cancers with the highest mortality rates in 2012 were breast, liver, stomach, colorectal and lung cancer (Ferlay *et al.*, 2015; Jemal *et al.*, 2011).

1.1.2 Global Breast Cancer Statistics

Breast cancer is globally the most commonly diagnosed cancer in women. It is the most common cause of death in women in underdeveloped countries and the second most common in the developed world. In a 2012 GLOBOCAN study, breast cancer accounted for 25% of all diagnosed cancer with approximately 1.67 million new cases reported in that year (Ferlay *et al.*, 2015). In Southern Africa, breast cancer significantly contributes to the incidence and mortality rates of cancer (Ferlay *et al.*, 2013).

1.1.3. South African Breast cancer Statistics

South Africa is the greatest contributor to breast cancer mortality and incidence in Southern Africa (Ferlay *et al.*, 2013). In the last two decades breast cancer has overtaken cervical cancer as the most diagnosed cancer in Asian and mixed race women, and is also the second most diagnosed in black and white women in South Africa (Vorobiof *et al.*, 2001). The mortality rate and incidence of breast cancer has increased in women over the age of 30 according to the latest cancer registry of 2010. The latest cancer registry of South Africa in 2010 observed that there were 6125 cases of breast cancer with the majority of the cases in women over 35 years of age. Although 65% of the cases occurred in postmenopausal women, younger women aged between 35 and 49 years accounted for 27.5% of breast cancer incidence in 2010. Black women accounted for 47.5% of breast cancer cases in 2010 and 39% of these women were below the age of 50 (National Health Laboratory Services, 2010).

A variety of factors increase the risk of breast cancer incidence. These risk factors include early onset of menstruation, extensive use of oral contraceptives, family history of the disease, genetic predisposition and late maternal age at first birth (Jemal *et al.*, 2011). In terms of mortality two main factors play a role, the stage of

breast cancer at first diagnosis and, the histological (Ellis *et al.*, 1992) and molecular features of the tumour (Weigel *et al.*, 2010; Weigelt *et al.*, 2008). Poor prognosis in breast cancer is therefore associated with certain tumour types and late stage diagnosis (Reis-Filho *et al.*, 2011; Weigel *et al.*, 2010). The different types of tumours will be reviewed in the following section.

1.2 Cancer classification

1.2.1 General cancer classification

There are different ways of classifying cancer. One of the main methods, as described by the five most dominant cancer types listed earlier, is by site of origin (e.g. breast, liver, lung). However, cancer can also be classified according to the histology of the tumour. The three histological classifications in cancer are sarcomas, carcinomas and leukaemia. Sarcomas originate from connective or muscular tissue cells, while carcinomas are derived from epithelial tissue cells and leukaemia is composed of all other non-solid tissue type cells for example blood cells (Alberts *et al.*, 2007b). Breast cancer is a carcinoma that has distinct classifications based on histology and molecular characteristics.

1.2.2 Breast cancer histological classification

The first model for breast cancer classification describes the histological presentation of the tumours, while the second describes molecular markers (Elston *et al.*, 1991; Reis-Filho *et al.*, 2011; Weigelt *et al.*, 2008). Breast cancer is a highly heterogeneous cancer with a variety of histological types associated with tumours. All breast cancer tumours are carcinomas with two main classifications, in-situ carcinomas and invasive (infiltrating) carcinomas (Malhotra *et al.*, 2010).

1.2.2.1 In-situ carcinomas

In-situ carcinomas are described according to their site of origin in the breast tissue. The two breast tissue sites are known as lobular and ductal. Ductal forms of in-situ carcinomas are the most common and are divided into five sub-categories, comedo, cribiform, micropapillary, papillary and solid tumours. Lobular in-situ carcinomas are less common with little to no histological heterogeneity (Malhotra *et al.*, 2010; Weigelt *et al.*, 2008). In-situ carcinomas constitute approximately 5% of breast cancer histology observed (Bertos *et al.*, 2011).

1.2.2.2 Invasive carcinomas

Invasive carcinomas are commonly known as infiltrating carcinomas and divided into either lobular or ductal forms. Infiltrating ductal carcinomas and infiltrating lobular types make up 75% and 10% of breast cancer cases observed respectively (Bertos *et al.*, 2011; Malhotra *et al.*, 2010). Infiltrating ductal carcinomas, the most common breast cancer histology type, can be further differentiated through the grading of the tumours as described below.

Tumours are graded as either well, moderately or poorly differentiated according to scores obtained from three features. These features are the mitotic rate, tubule formation and nuclear polymorphisms. The mitotic rate is determined by observing the mitotic count (number of cells that are dividing in a defined region of the tumour) and a score of 1 to 3 is given depending on the number of mitotic counts observed. The greater the mitotic count the higher the score. The morphology of the nuclei is graded from 1 to 3 depending on how closely the tumour cell nuclei resembles normal nuclei with a low score for normal-like nuclei. Finally tubule formation is given a score of 1 to 3 depending of the percentage of tumour with tubules. Tumours with less than 10% of defined tubular structures a score of 3 is given, while tumours with more than 75% defined tubules are given a score of 1 (Ellis *et al.*, 2006; Elston *et al.*, 1991; Lester *et al.*, 2009).

The combined score therefore distinguishes between well, moderately and poorly differentiated tumours. Tumours with a higher score are poorly differentiated and called high-grade tumours. Infiltrating ductal carcinomas are high-grade tumours and form the most aggressive tumour types. They are associated with poor prognosis and are the only histological tumour type that is co-classified using molecular factors (Malhotra *et al.*, 2010).

1.2.2.2 Molecular classification

Classification of infiltrating ductal carcinomas can be expanded by the use of molecular classes and these are currently in use in clinical practice (Malhotra *et al.*, 2010). There are currently six molecular classes for breast cancer, which are Luminal A and B types, Claudin low, normal breast like, basal-like and HER2 enriched tumours. These molecular sub-types are differentiated according to their clinical features, genetic profile and treatment profile. The most clinically significant aspect of

these tumours is their genetic profile. There are three genes that code for molecular receptors involved in the growth and proliferation of the tumours. These genes are for the estrogen (ERα) and progesterone receptor (PR), and the human epidermal growth factor receptor 2 (HER2/neu) (Perou *et al.*, 2000; Sørlie *et al.*, 2001).

Luminal type tumours are mainly characterised by the expression of genes that are present in cells in the luminal epithelium of the breast tissue. They also account for 60% of infiltrating ductal carcinomas (Perou *et al.*, 2000). The expression levels of the ERα and *Erb-B2* (*HER2/neu*) genes help differentiate between the luminal subtypes. Luminal A tumours express high levels of the ERα gene and low levels of the *HER/neu* while the Luminal B subtype expresses low levels of ERα and *HER/neu*. Luminal subtypes are therefore often referred to as hormone receptor positive sub-types and their genetic profile is associated with a good prognostic outcome (Reis-Filho *et al.*, 2011; Weigel *et al.*, 2010). Luminal B tumours have a poorer prognosis as compared to luminal A due to genes that allow their cells to proliferate at the higher rate than luminal A tumours (Sørlie *et al.*, 2001; Sørlie *et al.*, 2003). Although luminal subtypes represent the majority of molecular subtypes observed, there are other tumour subtypes that have become increasingly prominent in breast cancer.

Basal-like and Claudin low tumours form a group of tumours known as triple negative tumours and represent about 20-30% of tumour observed in breast cancer cases (Malhotra *et al.*, 2010). A large cohort study in Soweto, South Africa found that triple negative breast cancer is the most common cancer in black women (Cubasch *et al.*, 2013). These tumours are referred to as triple negative because they do not express the three genes ERα (ER), *Erb-B2* (*HER2/neu*) and *PGR* (PR). Triple negative tumours are the most aggressive tumours observed and are associated with a poor prognosis (Perou, 2011; Reis-Filho *et al.*, 2011).

The basal-like subtype tumours express some of the genes that are observed in the basal epithelium of the breast tissue (Perou *et al.*, 2000; Sørlie *et al.*, 2001; Sørlie *et al.*, 2003). Claudin-low subtype tumours are the most aggressive of the triple negative tumours with a lower pathological complete response than the basal-like tumours (Perou, 2011). The pathological complete response is defined as the absence of residual invasive tumours and lymph node metastasis after adjuvant

treatment (von Minckwitz *et al.*, 2012). Claudin-low tumour cells express transcription factors that are expressed at high levels in stem cells and tumour initiating cells. Stem cells are resistant to chemotherapy and expression stem cell features in Claudin-low tumours may be associated with poor prognosis (Perou, 2011; Prat *et al.*, 2010).

Triple negative tumours are associated with poor prognosis. This is attributed to the association of basal-like tumours and Claudin-low tumours with treatment resistance properties attributed to their stem cell like features and mutations in *TP53* (codes for p53 protein) and *BRCA1* genes (codes for BRCA1) (Perou, 2011; Prat *et al.*, 2010; Sørlie *et al.*, 2001). BRCA1 is a tumour suppressor protein belonging to the BRCA family and it is implicated in breast cancer. BRCA1 has a variety of function including repair or destruction of damaged DNA in cells of the breast and female reproductive system. A mutation in the the gene *BRCA1* significantly increases the risk of developing breast or ovarian cancer in women (Balmaña, *et al.,* 2011 King *et al.,* 2003; Venkitaraman, 2001). The identification of potential drug targets and new therapeutic agents against triple negative tumours are therefore an important endeavour.

The final two categories of breast cancer molecular subtypes collectively represent approximately 10% of breast cancer cases observed (Malhotra *et al.*, 2010). The two subtypes are referred to as HER2-enriched and normal-like tumours (Perou *et al.*, 2000). HER2-enriched tumours are characterised by high expression levels of the *Erb-B2* gene. This gene encodes the HER/neu receptor protein that is a growth factor receptor implicated in the progression of breast cancer tumours. Survival and relapse free survival outcomes of HER2-enriched tumours are low and this is attributed to the greater frequency of mutations in the gene coding for the tumour suppressor p53 and a low pathological complete response (Prat *et al.*, 2010; Sørlie *et al.*, 2001). Normal-like tumours are characterised by expression of genes usually expressed by non-epithelial and adipose tissue in the normal breast (Sørlie *et al.*, 2001).

Prognosis of breast cancer is determined by molecular and histological classification and the stage of disease progression upon diagnosis. The following section will describe the different disease stages of breast cancer.

1.2.3 Breast Cancer Staging

Tumour staging is standardised across most cancers and is based on the size of the tumour at the primary site (T), the presence of lymph node metastases (N) and the presence of distant metastases (M), forming the TNM system. This system was unified by the International Union Against Cancer and the American Joint Committee on Cancer in 1987 and is updated periodically. The TNM system is applied differently in breast cancer, which has seen various revisions to its TNM classification system (International Union Against Cancer, 1959; Singletary *et al.*, 2003b; Sobin, 2001).

1.2.3.1 Size of tumour at primary site (T)

The determination of the size of the tumour at the primary site is complex and several revisions have been made from the original TNM system to accommodate advances in our knowledge of breast cancer. There are basically four main subgroups T1-T4 that describe the tumour size and they are primarily differentiated by the extension of the tumour from less than 2cm to greater than 5cm. T1 and T4 subgroups are further divided qualifying the size of the tumour for T1 and describing the extent of tumour invasion of the chest wall and/or skin (American Joint Committee on Cancer, 2012; Singletary *et al.*, 2003a; Singletary *et al.*, 2003b).

1.2.3.2 Regional lymph node metastases (N)

The second component is the presence of metastases in regional lymph nodes. There are 3 main subgroups, which describe the extent to which the metastases have invaded regional lymph nodes. These are denoted as N1, N2 and N3 from the least to the most affected lymph node status respectively. Lymph node status is also pathologically assessed and is accorded the subgroups pN0-pN3 from the least extensive to the most extensive lymph node metastases respectively (American Joint Committee on Cancer, 2012; Singletary *et al.*, 2003a; Singletary *et al.*, 2003b).

1.2.3.3 Distant metastases (M)

The final component of the TNM cancer staging system is the assessment of distant metastases. This final component only has 3 subgroups in breast cancer; the main ones are M0 and M1. M0 denotes the lack of any observable clinical or radiological evidence of distant tumour metastases and M1 denotes the evidence of distant metastases. The third subgroup describes the molecular detection of distant metastases in body fluids although no radiological or clinical evidence is observed,

and this group is called cM0(i+) (American Joint Committee on Cancer, 2012; Singletary *et al.*, 2003a). The three components of the TNM system are only the first part of staging and the second part defines the actual prognostic stages.

1.2.3.4 Prognostic stages

Prognostic staging of breast cancer has transformed from the initial four stages (Stage I-IV) described by International Union Against Cancer (1959) to a total of nine stages that are currently clinically used. These nine stages are made up of various combinations of the T, N and M subgroups. The stage with the poorest prognosis is Stage IV that is described by the presence of distance metastases (M1) regardless of the T and N status (American Joint Committee on Cancer, 2012). An understanding of cancer on the molecular level has been important in the development of therapeutic interventions. The following section will therefore review the molecular origins of cancer.

1.3 Molecular basis of cancer

The eukaryotic cell is the basic unit of multicellular living organisms and has the ability to grow and replicate through a well-regulated process known as the cell cycle (Alberts *et al.*, 2007c). The dysregulation of this process is observed to begin the process of transformation of cells to become cancerous (Alberts *et al.*, 2007b). To understand how this transformation results in cancer a discussion on the cell cycle is essential.

1.3.1 The Cell Cycle

The cell cycle describes the process that governs the growth and proliferation of a cell. It is a divided into four main phases, the first growth phase (G_1), the DNA replication phase (S), the second growth phase (G_2) and the division phase (M). The G_1-phase involves the growth of the cell in size and protein production essential for cellular replication. This is followed by the S-phase, which is the process of duplication of the cell's DNA. During the S-phase any damage to the DNA is detected and repair enzymes are recruited to fix damages. Any DNA damages beyond repair result in cell death initiation and degradation of the cell. The G_2-phase is the second growth phase where rapid growth occurs in the cell and protein is synthesised as the cell prepares for the cellular division phase, mitosis (Alberts *et al.*, 2007c).

The final phase of the cell cycle is the M-phase where the cell divides to form daughter cells that are identical to each other. Mitosis in eukaryotic cells is divided into five main stages, prophase, prometaphase, metaphase, anaphase and telophase. Prophase is characterised by condensation of chromatin to form chromosomes while the mitotic spindle begins to form. This is followed by prometaphase where the nuclear envelope disassembles and the mitotic spindle expands to opposite poles of the cell invading the nuclear region. During the prometaphase stage the spindle fibres attach to the kinetochores, points of attachment on the chromosome. This leads to the metaphase stage where chromosome centromeres align at the equator of the mitotic spindle (Alberts *et al.*, 2007c).

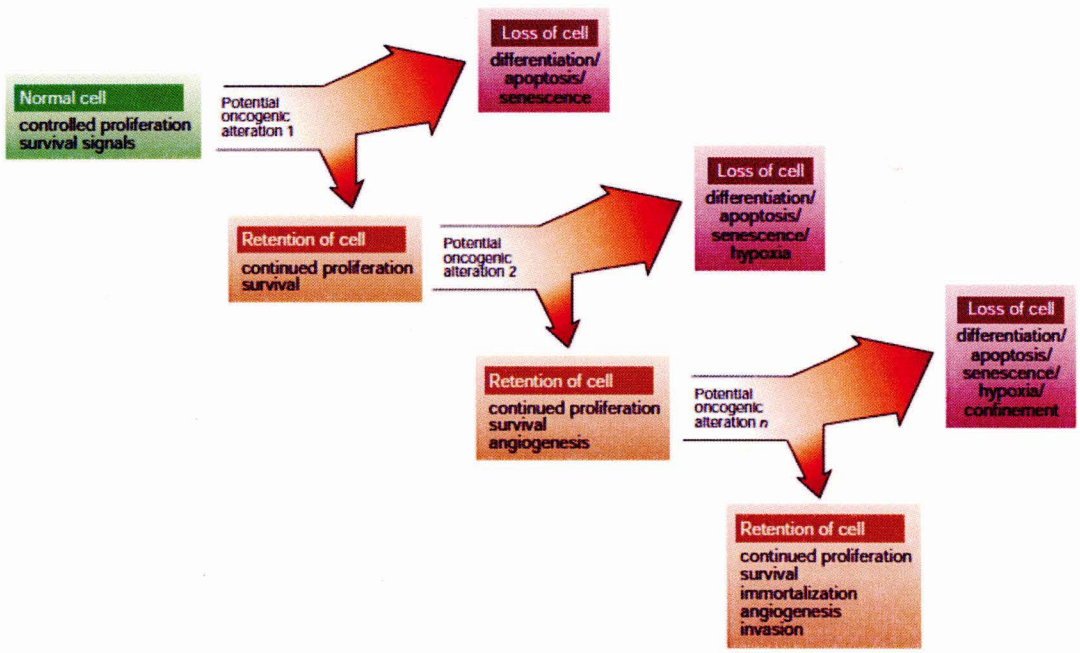


Figure 1.2 Key steps in the development of cancerous cells through cell cycle dysregulation (Evan *et al.*, 2001) A normal cell undergoes genetic alteration and dysregulation of the cell cycle results in it surviving and having increased survival and proliferation potential. Due to the initial genetic alteration the cell is more likely to undergo a second genetic mutation resultion in its increased survival and potential to stimulate development of new blood vessel to aid its survival. Subsequent genetic mutations in the cell result in features of immortality and an increased ability to invade surrounding and distant tissue

After the cells have properly aligned to the equator of the mitotic spindle, anaphase begins. The mitotic spindle begins to contract, separating sister chromatids to opposite poles of the spindle network. The final stage of mitosis is telophase when

the sister chromatids organise on opposite poles of the cell, the nuclear envelope begins to form around the chromosomes and the chromatids then decondense. When mitosis is complete cytokinesis occurs which separates the cytoplasm into two identical daughter cells (Alberts *et al.*, 2007c).

The cell cycle is therefore a complex process that requires regulation to ensure the integrity of all cells that pass through the cycle. This is made possible by two sets of proteins known as gatekeepers and caretakers (Alberts *et al.*, 2007c). Gatekeepers are sometimes referred to as tumour suppressor genes and they regulate the growth and proliferation of cells (Kinzler *et al.*, 1997). Caretakers are encoded by genes that maintain the integrity of DNA through the action of repair enzymes. They can also delay the cell cycle through various checkpoints (Kinzler *et al.*, 1997; Levitt *et al.*, 2002).

There are three main checkpoints within the cell cycle, the G_1/S, G_2/M and M checkpoints. The intrinsic base error rate of DNA is approximately 10^{-5} and the G_2/M checkpoint reduces this error rate to 10^{-9} by ensuring DNA integrity through the action of DNA repair enzymes. The G_1/S checkpoint determines whether a cell goes through another round of the cell cycle or to the quiescence phase (G_0). Finally the M-phase checkpoint ensures that chromosomes are aligned properly at the equator of the spindle during anaphase of nuclear division (Coop *et al.*, 2003; Elledge, 1996; Kunkel, 2004). The cell cycle is therefore important for cell growth and proliferation and its dysregulation results in a variety of health disorders, cancer being the most prominent. The clonal genetic model is used to explain how this dysregulation occurs.

1.3.2 The Clonal genetic model

The clonal genetic model is the most commonly accepted, and therefore the classic template, for the development of cancer. The model begins with a normal cell that through a particular sequence of mutations results in benign tumours, then these become malignant and finally develop metastatic and drug resistance resistant properties as displayed in figure 2 (Feinberg *et al.*, 2006).

This model is supported by the existence of gatekeeper and caretaker genes and has been observed in colon cancer development. A caretaker gene is initially mutated

resulting in loss of DNA integrity and genetic instability. Genetic instability is key in the development of cancer through inducing somatic mutations. Somatic mutations occur in both gatekeeper and caretaker genes but the knockout of both alleles of a gatekeeper gene is the rate-limiting step in tumour formation (benign stage). Successive replication cycles knockout more regulatory genes and the transformed cells acquire new functions like the ability to metastasize and resist drug action (Feinberg *et al.*, 2006; Kinzler *et al.*, 1997).

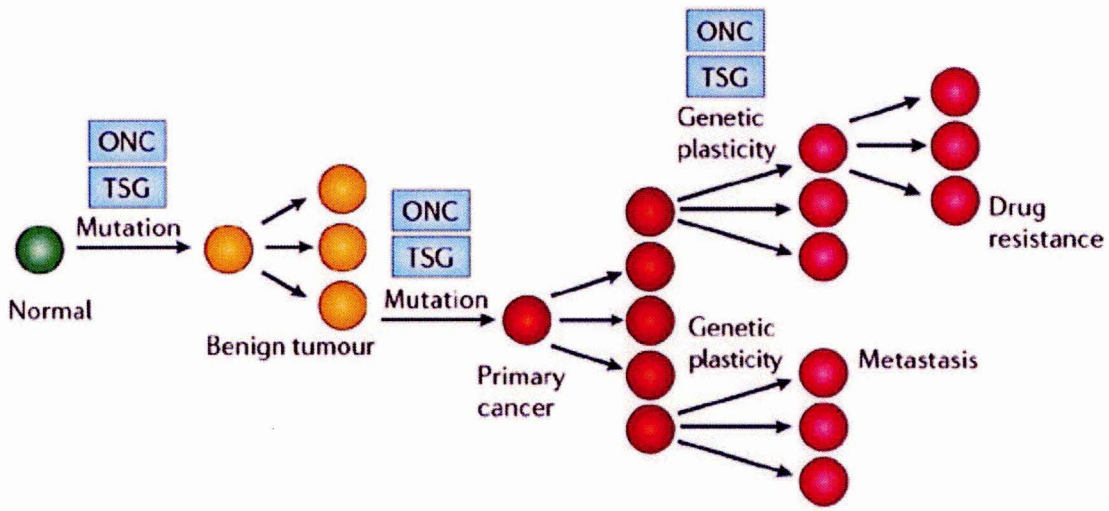


Figure 1.3 The clonal genetic model (Feinberg *et al.*, 2006)

A normal cell undergoes initial oncogene (ONC) and tumour suppressor gene (TSG) mutation, which knockout their function resulting in a transformed cell. This cell divides and proliferates uncontrollably forming a benign tumour. A second generation of mutations of the ONC and TSG in the cells result in the formation of cells that proliferate to form malignant tumours. A third round of mutations in ONC and TSG are required for cells in malignant tumours to become metastatic and acquire drug resistance (Feinberg et al., 2006).

This model can be applied generally to cancer but distinctive differences can be observed in different cancer types. Some cancers do not originate from a single cell type to become cancerous, but due to the makeup of their tissue, they are heterogeneous in origin and morphology. One such cancer is breast cancer, which will be the focus of this study. Classification and staging of breast cancer reviewed earlier provides details that are important in providing effective treatment for each individual diagnosed with breast cancer. Treatment for breast cancer is mainly through surgery (mastectomy or breast conserving surgery) together with adjuvant chemotherapy. Late stage (metastatic) breast cancer can only be treated through chemotherapy. In South Africa this is of importance since most newly made

diagnosis are stage III and IV tumours (Cubasch *et al.*, 2013; Loubser, 2008). Therefore a review on the type of therapy used in breast cancer, particularly chemotherapy, currently used to treat metastatic breast cancer is important for this study.

1.4 Breast cancer therapy

1.4.1 Surgery and radiation therapy

Early stage breast cancer (Stage 0 - II) commonly consists of resectable tumours. These tumours are commonly treated by means of surgery and radiation therapy as an adjunct. There are two types of breast cancer surgery available, mastectomy (removal of the entire breast tissue) and breast conservation therapy (Kalogerakos *et al.*, 2008). Breast conservation therapy involves the resection of tumorous breast tissue with minimal loss of normal breast tissue (Goldhirsch *et al.*, 2013; Kalogerakos *et al.*, 2008). Breast conservation therapy has become more common than a mastectomy in clinical practice and several studies have shown the benefit of breast conservation surgery with radiation therapy and chemotherapy as an adjunct (Benson, 2012; Goodwin *et al.*, 2009; Litière *et al.*, 2012). Despite advances in surgery techniques and adjunct treatments the risk of recurrence is high in patients treated by mastectomy or breast conserving therapy and this recurrence has been observed to be particularly prominent in triple negative and HER2 expressing tumours (Lowery *et al.*, 2012). Recurrence in patients treated through surgery and radiation therapy or chemotherapy normally presents as metastatic disease.

1.4.2 Chemotherapy

The treatment of metastatic breast cancer, an advanced stage of breast cancer, is palliative. Chemotherapy achieves this by treating the symptoms and increasing survival of an individual with breast cancer. The word chemotherapy in this study is used to refer to cytotoxic and other drugs that are used to reduce the tumour burden and growth fraction. In breast cancer there are three main groups of chemotherapy: hormone therapy (depending on receptor expression), cytotoxic chemotherapy and targeted biological therapy.

Breast cancer is not considered to be a single disease but is a collection of multiple heterogeneous diseases and therefore it is hard to prescribe standard treatment

regimens as health professionals seek to tailor specific treatment regimens for individual patients and their type of cancer. Clinical trials on breast cancer therapy continue to be conducted showing various treatments that have been effective in certain types of breast cancer (Pagani *et al.*, 2010). The following section will review chemotherapy options currently in use clinically.

1.4.2.1 Taxanes and anthracyclines

Cytotoxic chemotherapy is used in metastatic breast cancer when there is therapeutic failure in hormone therapy, rapidly progressive disease and extensive visceral disease (Beslija *et al.*, 2009). In their reviews on treatment of metastatic breast cancer Carrick *et al.* (2009) and Dear *et al.* (2013) argue that there is benefit on progression free survival for sequential treatment with single agents and a high response rate for combination therapies. However combination therapies are associated with a higher risk of development of febrile neutropenia (Carrick *et al.*, 2009; Dear *et al.*, 2013). The following section will review cytotoxic treatments currently in use against metastatic breast cancer.

Anthracyclines are considered the most effective agents for use as part of a single sequential regimen in the treatment of metastatic breast cancer and as adjuncts in early breast cancer (Beslija *et al.*, 2009; Cardoso *et al.*, 2014; Mayer *et al.*, 2007; Pagani *et al.*, 2010). The anthracycline group consists mainly of three drugs, doxorubicin, daunorubicin and epirubicin, which are used as first-line therapy for tumours that are receptor negative. These agents act in a number of ways, which include, intercalation with DNA, complexation with topoisomerase II and DNA and production of free radicals. These mechanisms result in DNA damage and cell death in tumours (Kim *et al.*, 2002; Laurent *et al.*, 2001; Minotti *et al.*, 2004). The use of anthracyclines in metastatic breast cancer is associated with adverse effects like, increased cardiotoxicity, nausea, vomiting, alopecia and neutropenia (Mayer *et al.*, 2007). The associated cardiac effects of anthracyclines may limit their use in patients with pre-existing cardiac disease therefore taxanes are also indicated as first line agents for metastatic breast cancer that is receptor negative (Beslija *et al.*, 2009).

Taxanes are used to treat receptor negative breast cancer or breast cancer that has failed to respond to anthracycline therapy. They are plant derived and act by binding β-tubulin thus stabilising and promoting microtubule formation. Aberrant microtubules structures are therefore formed and this stops mitosis and retards the growth of

breast cancer tumours (Abal *et al.*, 2003; Beslija *et al.*, 2009). The two main drugs indicated for use in breast cancer are docetaxel and paclitaxel. Docetaxel is the more effective of the two agents and is used as the first option in metastatic breast cancer (Nabholtz *et al.*, 2002). Adverse effects associated with taxanes are neuropathy and neutropenia. Despite the adverse effects, taxanes have proved effective in increasing the time to progression, and are an important group of drugs for the induction of remission. However like anthracyclines, resistance eventually develops and effectiveness decreases significantly with recurrence of disease (Ghersi *et al.*, 2005; Ghersi *et al.*, 2015; Jones, 2008; Mayer *et al.*, 2007).

The extensive use of anthracyclines and taxanes as first-line chemotherapy in progressive metastatic disease usually leads to their disuse in patients that have relapsed. Therefore there are other options for refractory metastatic breast cancer in patients previously on anthracyclines or taxanes (Beslija *et al.*, 2009).

1.4.2.2 Other agents

Vinorelbine is a vinca alkaloid that is used in metastatic breast cancer for patients that have previously been treated with anthracyclines and taxanes. It is particularly active as an adjunct in HER2 positive tumours (Cardoso *et al.*, 2014; Saeki *et al.*, 2000). It functions by inhibiting the cell cycle at the G2-M phase therefore stopping cell division in breast cancer tumours. Vinorelbine can be taken as an oral treatment and is associated mainly with neutropenia (Aapro *et al.*, 2012; Degardin *et al.*, 1994; Montemurro *et al.*, 2008).

Despite advances in the treatment of breast cancer and high response rates in early stage breast cancer, the likelihood of recurrence of disease remains high (O'Shaughnessy, 2005). Survival over a five-year period remains low for stage IV breast cancer and toxicity profiles hamper the tolerability of combination therapy (Carrick *et al.*, 2009; Siegel *et al.*, 2015). The major side effect of effective treatments like anthracyclines and taxanes is neutropenia (Mayer *et al.*, 2007). Neutropenia is a disorder caused by the reduction of neutrophils within the blood. Neutrophils account for approximately 60% of white blood cells contributing to the bulk of the body's immune response to infection (Blumberg *et al.*, 1990; Li *et al.*, 2002; Pizzo, 1993). This is particularly important in South Africa because of the high prevalence of HIV and AIDS in black women and the increasing likelihood of concomitant breast cancer

and HIV (Cubasch *et al.*, 2013; Simbayi *et al.*, 2014). Therefore, even though these treatments are effective in breast cancer and induce apoptosis in tumour cells (Binaschi *et al.*, 2001; Ghersi *et al.*, 2015), there is a continual need for agents that can specifically induce cell death in cancerous cells with minimal effect on non-tumorigenic cells.

1.4.2.3 Hormone therapy

Hormone therapy is indicated for use in patients who are estrogen (ER) or progesterone receptor (PR) positive or have an unknown ER/PR status (National Cancer Institute, 2013). Hormone therapy is indicated in cases where there is insignificant visceral metastasis, slow disease progression and a long disease free interval (Beslija *et al.*, 2009). Hormone therapy is divided into two main treatments, which are tamoxifen and aromatase inhibitors (Bertos *et al.*, 2011).

Tamoxifen is a partial agonist on the estrogen receptor that for many years has been used as a single agent for the first line treatment for ER/PR positive metastatic breast cancer. The primary mechanism of action for tamoxifen is competitive inhibition of the effects of estrogen on the estrogen receptor therefore retarding the growth of breast cancer cells. The partial agonistic effect of tamoxifen on the ER helps relieve symptoms like osteoporosis in postmenopausal women but can increase the likelihood of thromboembolic events and endometrial cancer (Kalogerakos *et al.*, 2008; National Cancer Institute, 2013).

In the past decade aromatase inhibitors have become favourable alternatives to tamoxifen due to better toxicity profile (Beslija *et al.*, 2009; Gibson *et al.*, 2009). Agents used in the clinical setting; anastrozole, letrozole and exemestane, are used as single agents because no significant increase in benefit is observed in combination therapy (Carrick *et al.*, 2009). These treatments act through the inhibition of the aromatase enzyme. Aromatase enzyme is a cytochrome P450 enzyme that converts testosterone into estrogen and progesterone (Simpson *et al.*, 1994). Therefore aromatase inhibitors decrease the production of estrogen and progesterone resulting in the inhibition of growth in hormone receptor positive tumours (Czajka-Oraniec *et al.*, 2010; Gibson *et al.*, 2009). Patients treated with aromatase inhibitors have an increased risk of bone fractures and osteoporosis than

those treated with tamoxifen, however they exhibit fewer thromboembolic events (Gibson *et al.*, 2009; National Cancer Institute, 2013).

Hormone therapy results in initial tumour response but the disease usually progresses leading to therapeutic failure in metastatic breast cancer (Carrick *et al.*, 2009). Therapeutic failure in hormone therapy, like other treatments for metastatic breast cancer, could be due to the increased use of these treatments as adjuncts in early stage breast cancer (Kalogerakos *et al.*, 2008). Due to the progressive nature of breast cancer, the tumours can develop resistance to these treatments due to previous use (Jones, 2008). The criteria mentioned earlier for use of hormonal therapy in metastatic breast cancer makes its use limited to a small number of patients even within the ER/PR positive population. This is particularly important in South Africa as a majority of cases are newly diagnosed at stage III and IV, and are highly progressive with significant visceral metastases (McCormack *et al.*, 2013). Therefore research into new therapies is essential to augment current therapeutic options available for metastatic breast cancer.

1.4.2.4 Targeted therapy

Tumours that are hormone receptor negative but positive for human epidermal growth factor receptor 2 (HER2) are treated with a combination of targeted therapy and cytotoxic chemotherapy. The first agent to be approved for use in metastatic breast cancer that is HER2 positive is trastuzumab. Trastuzumab is a monoclonal antibody that binds and blocks the action of HER2. HER2 is a growth factor receptor belonging to the human epithelial growth factor receptor family that is overexpressed in breast cancer and linked to progression of tumours (Bertos *et al.*, 2011; Outhoff, 2011).

A second agent lapatinib was approved in 2007 for the use in the treatment of breast cancer that overexpresses HER2 and is refractory to trastuzumab (Higa *et al.*, 2007; Moy *et al.*, 2007). Lapatinib is a tyrosine kinase inhibitor that binds to the tyrosine kinase domain of HER1 and HER2 receptors inhibiting their function (Higa *et al.*, 2007; Wood *et al.*, 2004). It is also indicated for use in combination with letrozole for post-menopausal patients with hormone receptor and HER2 positive tumors. (US Food and Drug Administration, 2010). A recent clinical trial has shown efficacy of

lapatinib in combination with captecitabine in breast cancer patients with brain metastases (Bachelot *et al.*, 2013).

Since their introduction, trastuzumab and lapatinib have significantly improved the treatment of metastatic breast cancer. Trastuzumab extends the time to progression and overall survival in patients with metastatic breast cancer while lapatinib extends the time to progression (Higa *et al.*, 2007; Pagani *et al.*, 2010). Treatment with lapatinib does not show any life-threatening side effects and the most significant side effect is sever diarrhoea, which could lead to therapy discontinuation (Higa *et al.*, 2007). However, trastuzumab is associated with cardiotoxicity in metastatic breast cancer (Balduzzi *et al.*, 2014; Outhoff, 2011).

The high cost of these targeted therapies have made them inaccessible to most patients, even in the developed world where patients have substantial medical aid benefits (Outhoff, 2011). In 2011, approval for bevacizumab, a monoclonal antibody inhibiting angiogenesis, was withdrawn from the treatment of metastatic breast cancer as it did not improve the quality of life of individuals and caused haemorrhaging (Woolston, 2011). The following year a Cochrane review on benefits of bevacizumab as an adjunct in first and second line treatment of metastatic breast cancer found that it did not improve quality of life or overall survival in patients (Wagner *et al.*, 2012). The benefit of targeted therapy like trastuzumab as first line therapy in metastatic breast cancer has not been determined and its use beyond progression is not well supported by evidence (Balduzzi *et al.*, 2014). These challenges highlight the continuous need for development of new therapeutic agents that are cost-effective and safe.

1.5 Cancer cell death

Cell death can be classified morphologically into four processes; necrosis, autophagy, apoptosis and death linked to failed mitosis (mitotic catastrophe) (Kroemer *et al.*, 2009; Majno *et al.*, 1995). A number of biochemical markers can be used to identify cell death but some of these are reversible, like caspase activation and exposure of phosphatidylserine. Therefore the end point of cell death is usually determined by the loss of cell membrane integrity as viewed by vital stains and disintegration of the cell and its nucleus to apoptotic bodies (Kroemer *et al.*, 2009). Apoptosis an important process in the growth and development of multicellular

organisms and is often considered synonymous with programmed cell death, however there are other types of cell death which are considered programmed (Galluzzi *et al.*, 2012; Kroemer *et al.*, 2009). Some of these modes of cell death will be discussed in the following section.

1.5.1 Autophagy

Autophagy is a process characterised by the digestion of the cells contents in order to provide energy in response to nutrient deprivation and in some cases exposure to chemotherapy (Childs, 2004; Meijer *et al.*, 2009; Ouyang *et al.*, 2012). The most prominent morphological features of autophagy are extensive formation of double membrane autophagic vacuoles and lack of chromatin condensation (Kroemer *et al.*, 2009). In response to cancer chemotherapy cells that lack caspases and regulators of apoptosis like BAX are often observed to exhibit characteristics consistent with autophagy. However it remains difficult to identify whether activation of autophagy in these cells is due to cell's normal response to stress. Therefore inhibition of autophagy pathway can be useful in identifying cell death mediated by autophagy (Galluzzi *et al.*, 2012).

1.5.2 Regulated Necrosis

Necrosis, once considered the accidental death of cells characterised by cell membrane rupture and cell swelling, has been shown to occur through regulated processes (Kroemer *et al.*, 2009). It has been observed that when caspases are inhibited receptor interacting protein kinases (RIPK) influence downstream events that result in necrotic cell death. Pathways activated by tumour necrosis factor (TNF) have shown features consistent with necrosis further highlighting its regulated nature (Festjens *et al.*, 2007; Galluzzi *et al.*, 2012).

1.5.3 Mitotic catastrophe

Cell death that occurs during the disruption of cell division by mitosis is referred to as mitotic catastrophe (Kroemer *et al.*, 2009). Some studies do not consider mitotic catastrophe as a mode of cell death but a precursor to cell death by apoptosis and necrosis (Galluzzi *et al.*, 2012; Mansilla *et al.*, 2005). However there is evidence to suggest that mitotic catastrophe causes cell death without the activation of apoptosis or necrosis (Portugal *et al.*, 2010; Vakifahmetoglu *et al.*, 2008). Mitotic catastrophe is morphologically characterised by large cells that contain multiple decondensed nuclei

(Castedo *et al.*, 2004; Kroemer *et al.*, 2009; Vakifahmetoglu *et al.*, 2008). Normally considered a mode of cell death induced by irradiation of cells, there is evidence of mitotic catastrophe induced by chemotherapy, particularly in breast cancer cells (Eom *et al.*, 2005; Ianzini *et al.*, 2006; Portugal *et al.*, 2010; Roninson *et al.*, 2001).

Approximately 50% of cancer tumours contain mutations that prolong survival of tumour cells through enhanced proliferation and inhibition of apoptotic pathways (Kumar *et al.*, 2000; Lowe *et al.*, 2000; Makin *et al.*, 2000; Reed, 1999; Wong, 2011). Induction of apoptosis is therefore a key target for cancer chemotherapy. The following section will review the features and pathways involved in apoptosis and how this process is dysregulated in breast cancer cells.

1.5.4 Apoptosis

Apoptotic cells have distinct morphological and biochemical features. Morphological features include a reduction in cell size known as cell shrinkage due to condensation of the cytoplasm, degradation of the nucleus observed as chromatin condensation and cleavage of the DNA, and protrusions of the cell membrane called blebs containing pieces of cellular material. The final stages of apoptosis involve the formation of apoptotic bodies that are usually engulfed by surrounding macrophages as part of homeostasis (Kroemer *et al.*, 2009).

Biochemical features include the degradation of nuclear DNA, the externalisation of the protein phosphatidyl-serine from the inner leaflet of the plasma membrane to the outer leaflet, the change in electric potential of the mitochondrial membrane, and the release of cytochrome c from the mitochondria to the cytosol (Alberts *et al.*, 2007a; Kerr *et al.*, 1972; Majno *et al.*, 1995; Saraste *et al.*, 2000). The two main signalling pathways in which apoptosis can be induced are known as the death receptor and the mitochondrial pathways or the intrinsic and extrinsic pathways (Earnshaw *et al.*, 1999; Lowe *et al.*, 2000).

1.5.1.1 Death receptor pathway

The death receptor pathway (extrinsic pathway) is activated through the binding of a ligand to a death receptor resulting in a signalling cascade that leads to apoptosis. There are a number of death receptors, CD95/Fas, TNF-related apoptosis inducing ligand receptor 1 (TRAIL1), tumour necrosis factor (TNF) receptor 1 & 2 and death

receptor 3, located on the surface of the plasma membrane and activated by many different ligands whose stimulation triggers death signal cascades (Wajant, 2003). The best understood of these pathways is the one which is due to binding of the ligand FasL to Fas (Dickens *et al.*, 2012; Earnshaw *et al.*, 1999; Ouyang *et al.*, 2012; Wajant, 2003).

The binding of FasL to Fas recruits the Fas-associated death domain (FADD), an adaptor protein that completes the scaffold required to activate the inactive initiator caspase called procaspase-8, to its active form caspase-8. Caspase-8 activates downstream proteins and cleaves executioner procaspases for caspase-3, -6 and -7, to their active form. These executioner caspases activate proteins responsible for DNA degradation and damage of intracellular proteins resulting in apoptotic features. Activation of caspase-8 cleaves the pro-apoptotic protein BH3 interacting-domain (bid) to its active form therefore activating the mitochondrial pathway (**Figure 1.2**) (Alberts *et al.*, 2007a; Dickens *et al.*, 2012; Earnshaw *et al.*, 1999).

1.5.1.2 Mitochondrial Pathway

The mitochondrial pathway (intrinsic pathway) can be activated either by the death receptor pathway through Bid or cell damage due to chemicals or irradiation (Alberts *et al.*, 2007a). The Bcl-2-associated X protein (BAX) oligomerises leading to the release of cytochrome c from the mitochondria to the cytoplasm. Cytochrome c release leads to a conformational change in the Apoptotic protease-activating factor 1 (Apaf1) allowing it to bind to caspase-9 forming an apoptosome in the presence of adenosine triphosphate. The apoptosome recruits effector caspases-3 and -7 while activating caspase-9. The effector caspases then cleave structural and regulatory proteins resulting in the biochemical and morphological features associated with apoptosis (**Figure 1.2**) (Alberts *et al.*, 2007a; Earnshaw *et al.*, 1999; Ouyang *et al.*, 2012).

Caspase-3 has been implicated in both the death receptor and mitochondrial pathway as terminal effector caspase. It can cleave the protein inhibitor of caspase-activated dNase (iCAD), which activates CAD resulting in the condensation of chromatin and DNA fragmentation (Alberts *et al.*, 2007a). Other effector caspases (caspase-6 and -7) are involved in cleaving of the regulatory regions of protein kinases in the cell leading to the damage of cell monitoring network and cytoskeleton

survival pathways. These kinases also degrade lamins thereby disassembling the nuclear envelope (Earnshaw *et al.*, 1999; Ouyang *et al.*, 2012). Studies on dysregulation of apoptosis in cancer have yielded insights into possible therapeutic targets. The following section will review the various regulatory proteins affected in breast cancer cells.

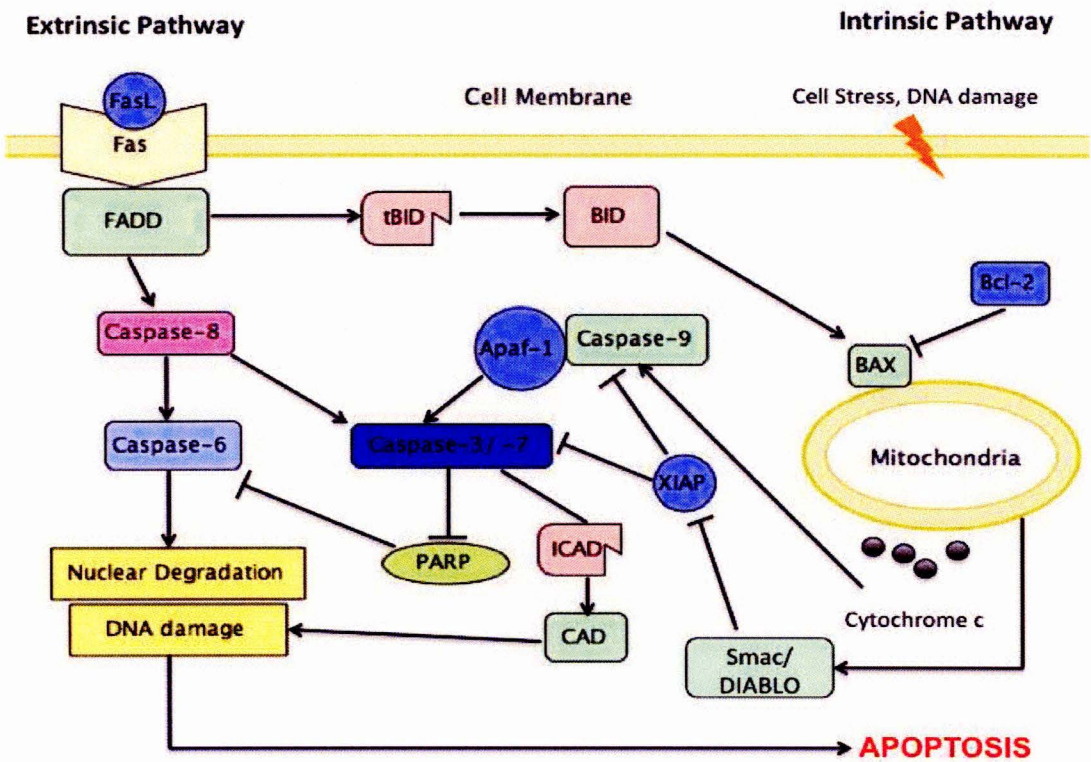


Figure 1.2 Schematic of the death receptor and mitochondrial pathways of apoptosis

Extrinsic Pathway: Fas the ligand binds to its receptor resulting in the recruitment of the Fas-associated death domain (FADD). The FADD scaffold can bind caspase-8 activating it. Caspase 8 in turn cleaves caspase-3, -6, -7 activating them. Caspase-6 leads to nuclear degradation and DNA damage resulting in apoptotic cell death. Caspase-3/7 cleaves inhibitor of caspase activated DNase (ICAD), which activates caspase activated DNase (CAD) resulting in DNA damage and apoptosis.

Intrinsic pathway: The intrinsic pathway can be activated either through caspase-8. Caspase-8 cleaves truncated BH3 interacting-domain (tBID) to its active form BID. This results in the release of cytochrome c from the mitochondria. Cytochrome c facilitates the formation of the apoptosome consisting of Apoptotic protease-activating factor 1 (Apaf1) and caspase-9. This apoptosome activates caspase-3/7 resulting in DNA degradation and apoptosis cell death. In response to cell stress and damage Bcl-2-associated X protein (BAX) oligomerises leading to the release of cytochrome c and second mitochondria-derived activator of caspases (Smac) also known as DIABLO from the mitochondria (Salvesen et al., 2002). Smac/DIABLO inhibits the action of XIAP therefore augmenting

apoptosis. When overexpressed B-cell lymphoma 2 (Bcl-2) can inhibit the action of BAX on the mitochondria, therefore inhibiting apoptosis (Ouyang *et al.*, 2012; Salvesen *et al.*, 2002).

1.6 Apoptosis in Breast cancer

Dysregulation and inhibition of apoptosis in breast cancer is hypothesized to occur during progression of breast cancer cells to form an invasive ductal carcinoma (Parton *et al.*, 2001). This is important to review because the majority of breast cancer cases are invasive ductal carcinomas especially in South Africa (Bertos *et al.*, 2011; McCormack *et al.*, 2013). Evidence to support this hypothesis includes the presence of reduced apoptosis in poorly differentiated ductal carcinoma in-situ ((DCIS) (Mommers *et al.*, 1999) and high expression levels of mutated p53 in invasive ductal carcinomas (Allred *et al.*, 2008; Umekita *et al.*, 1994). This inhibition of apoptosis in breast cancer cells is associated with various factors such as the estrogen receptor status (ER) and expression of biochemical markers p53 and Bcl-2 (Gandhi *et al.*, 1998; Kumar *et al.*, 2000; Yamamoto *et al.*, 2014). This section will review the role of p53 and Bcl-2 dysregulation of apoptosis in breast cancer tumours.

1.6.1 p53 and breast cancer

The p53 protein, encoded by the p53 gene is known as a tumour suppressor due to its ability to regulate cell proliferation and inhibit tumour cell growth. The main characteristic of the wild-type p53 protein is the inhibition of tumour formation in animal models and cell culture by suppressing mitosis at the G1-phase. Wild-type p53 activated by the cell's stress response induces apoptosis by activating the transcription of BAX and inhibiting the action of Bcl-2 and B-cell lymphoma-extra large (Bcl-X_L) proteins. This leads to activation of the mitochondrial apoptotic pathway (**Figure 1.3**). p53 has also shown the ability to activate the death receptor pathway through death receptor 3 and increasing expression of Fas on the cell surface (Amaral *et al.*, 2010).

Studies in breast cancer have shown marked expression of mutated p53 in invasive ductal carcinomas with this expression absent in benign and ductal hyperplasias (Allred *et al.*, 2008; Umekita *et al.*, 1994). The presence of p53 mutants could explain the resistance to apoptotic cell death of invasive carcinomas when they are treated with chemotherapy. In their review on the role of p53 in breast cancer, Walerych *et al.* (2012) argue that p53 mutants play a key role in progression and resistance in

triple negative breast cancer. This evidence supports the hypothesis that mutation of p53 is involved in the development and progression of breast cancer.

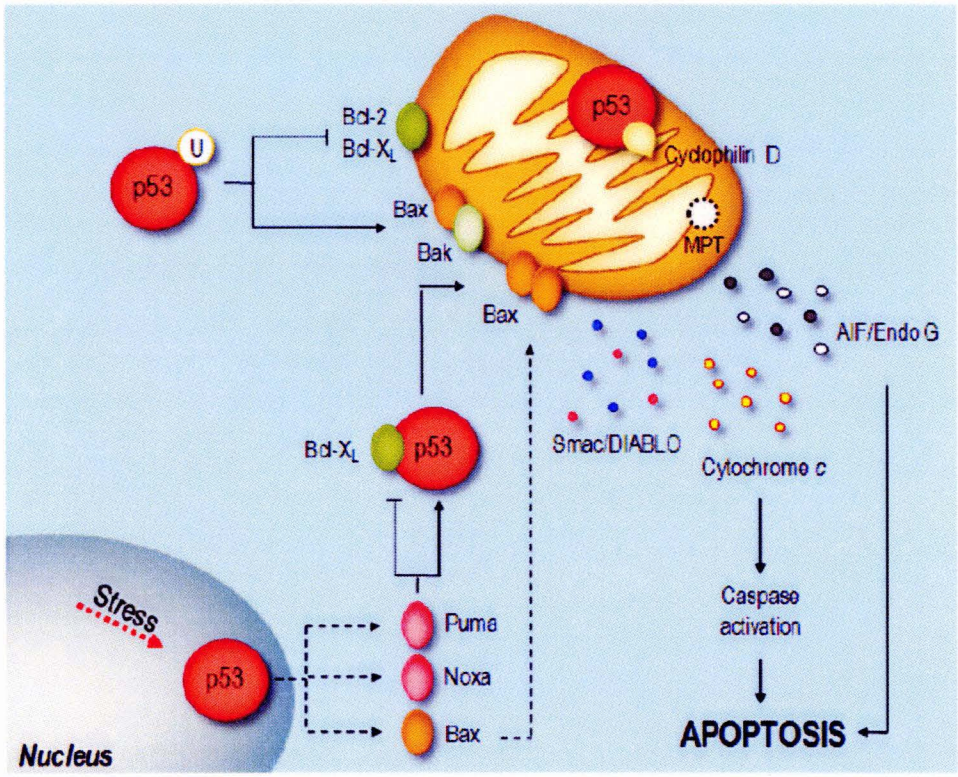


Figure 1.3 Schematic diagram of the role of p53 in the mitochondrial pathway (Amaral *et al.*, 2010)

p53 induces apoptosis through activation of the mitochondrial pathway. p53 is present in the nucleus, ubiquitous in the cytosol bound to Bcl-X_L or in its free form, and in the mitochondria bound to cyclophilin D. In response to cellular stress nuclear p53 activates the transcription of p53 upregulated modulator of apoptosis (Puma), Noxa and Bax. Puma and noxa then facilitate the dissociation of cytosolic p53 from Bcl-X_L activating p53. Activated p53 then inhibits anti-apoptotic proteins Bcl-X_L and Bcl-2. This activated p53 also initiates the formation of Bak/Bax and Bax/Bax protein oligomers. These oligomers together with p53 bound to cyclophilin D in the mitochondria alter the mitochondrial membrane potential resulting in the release of cytochrome c to the cytosol. Cytochrome c release results in the downstream effects of caspase activity and apoptosis. Smac/DIABLO is released together with cytochrome c from the mitochondria and inhibits the action of Bcl-2 and Bcl-X_L augmenting apoptosis. Apoptosis inducing factor (AIF) is released from the mitochondria and maintains mitochondrial permeability during apoptosis as well as triggering DNA fragmentation in a caspase-independent manner. Endonuclease G (Endo G) is released from the mitochondria and migrates to the nucleus where it degrades DNA (Amaral *et al.*, 2010; Hangen *et al.*, 2010; Vařecha *et al.*, 2012; Yu *et al.*, 2006).

1.6.2 Bcl-2 and breast cancer

B-cell lymphoma 2 (Bcl-2) was first characterised from a B-cell leukemia cell line (Tsujimoto *et al.*, 1984) and has since been described as a modulator of apoptosis through the mitochondrial pathway (Yip *et al.*, 2008). Bcl-2 is an important regulatory protein during apoptosis and functions as an inhibitor of apoptosis, particularly through the mitochondrial pathway (**Figure 1.3**). The relationship between breast cancer and Bcl-2 expression tends to have two divergent outcomes. In terms of prognostic outcome, Bcl-2 overexpression is associated with good survival outcomes and hormone receptor positive tumours (Binder *et al.*, 1995; Kumar *et al.*, 2000; Martin *et al.*; Vakkala *et al.*, 1999).

However, histological studies show that overexpression of Bcl-2 is associated with poorly differentiated tumours and high proliferation rates despite a high rate of cell death (Gandhi *et al.*, 1998; van Slooten *et al.*, 1998). The presence of Bcl-2 overexpression is also associated with resistance to breast cancer chemotherapy (Kumar *et al.*, 2000). Furthermore, inhibition of Bcl-2 sensitizes breast cancer cells to chemotherapy (Oakes *et al.*, 2012; Vaillant *et al.*, 2013). The seemingly contradictory role of Bcl-2 in breast cancer pathogenesis could therefore be due to localization of Bcl-2 in cells. Portier *et al.* (2006) argue that localization of Bcl-2 regulates its activity with cytoplasmic Bcl-2 performing an antiapoptotic function while nuclear Bcl-2 has a proapoptotic function.

1.7 Drug discovery

Drug discovery is an important part of the discipline of pharmacology and novel screening of compounds has proven effective in isolating agents for use in cancer chemotherapy (Boyd, 1997; Swinney *et al.*, 2011). There are two main techniques used in novel screening of compounds, target-based screening and phenotypic screening. Target-based screening aims at developing therapies by targeting specific disease associated proteins while phenotypic screening identifies therapies that can favourable modification of the disease phenotype without prior knowledge of a disease target (Swinney *et al.*, 2011).

1.7.1 Target-based screening

Target-based screening is an approach to drug discovery that makes use of bio-intelligence to identify the specific molecular signature in a disease. Specific disease

associated proteins generally become the target for drug design with the aim to interfere with the function of the target structure. Inhibition of target structure function then translates to a cure for the specific disease of a disease-modifying target. The structure of this target is used to design a compound that will bind complementarily to a region on the target thereby effecting the desired change in the disease (Lindsay, 2003).

1.7.2 Phenotypic screening

Phenotypic screening identifies compounds that modify the disease in the desired way without prior knowledge of their specific molecular target. The use of this approach identifies small molecules that affect a previously unknown target or has multiple target effects (Kotz, 2012; Swinney, 2013; Swinney, 2014).

Over the past three decades, target-based screening has overtaken phenotypic screening as an approach to drug discovery in cancer and other diseases. This has been largely due to the development of bioinformatics that aids the identification of disease-modifying targets (Lindsay, 2003). However, target-based screening has been plagued by high attrition rates due to safety concerns and lack of proof of biological hypotheses. This has led to an average of 1-3 molecules annually that are approved through this system and maintains the advantages of phenotypic screening (Swinney, 2013; Swinney, 2014). In their review on drugs approved by the FDA over a 10-year period from 1999-2008, Swinney *et al.* (2011) showed that phenotypic screening contributed more to new medicines approved by the FDA. The review also showed that less than 20% of these new medicines were for cancer and none of them for breast cancer (Lindsay, 2003).

The aggressive nature of metastatic breast cancer, its increase in South Africa, and the lack of development of effective new treatment therapies highlights the need for identifying new lead compounds for breast cancer therapy. The statistically high success rate of phenotypic screening over target-based screening maintains it as the better approach to discovering lead compounds for breast cancer. This study therefore will use phenotypic screening to assess the effectiveness of novel compounds on two breast cancer cell lines, the MCF-7 and the MDA-MB-231 cell line using novel compounds based on an imidazo[1,2-a]pyridine amine scaffold.

1.7.3 Novel Compounds

The novel imidazole compounds to be used in this study are imidazo[1,2-a]pyridine amines. Studies on compounds based on an imidazo[1,2-a]pyridine scaffold caused the induction of cell death in HT-29 and Caco-2 cell lines through activation of caspases-3 and -8 as well as release of cytochrome c, which are all markers for apoptotic cell death (Dahan-Farkas *et al.*, 2011). Other compounds based an imidazopyridine structure have shown an ability to induce cell growth arrest and apoptosis (Martínez-Urbina *et al.*, 2010). The coordination of transitional metals to heterocyclic compounds has yielded compounds with increased activity against cancer cell lines when compared to their uncoordinated analogues (Martinez-Bulit *et al.*, 2015). Coordination of heterocyclic compounds, including imidazopyridine amines, with copper-II has created compounds active against cancer cells with some inducing programmed cell death consistent with mitotic catastrophe (Dallavalle *et al.*, 2002; Tardito *et al.*, 2006).

1.7.4 Cell Lines

1.7.4.1 MCF-7 cell line

In the 1970s at the Michigan Cancer Foundation, the MCF-7 cell line was developed to become a model for hormone receptor positive breast cancer tumours (Levenson *et al.*, 1997). MCF-7 cells were initially described to express a large number of estrogen receptors (ERs) and they were later observed to express progesterone, androgens and glucocorticoid receptors (Brooks *et al.*, 1973; Horwitz *et al.*, 1975). These features are similar to those observed in ER+ tumours and therefore the MCF-7 cancer cell line is a good model for ER+ breast cancer (Holliday *et al.*, 2011; Lacroix *et al.*, 2004).

1.7.4.2 MDA-MB-231 cell line

The second cell line to be used in this study is the MDA-MB-231 cell line originating from a pleural effusion of a breast cancer patient, which had become poorly differentiated and aggressive (Lacroix *et al.*, 2004). These cells show molecular features that are mesenchymal in nature and therefore aggressive which is indicative of triple negative tumours. Currently MDA-MB-231 cell line is arguably the best in-vitro model available for triple negative breast cancer (Holliday *et al.*, 2011). These two cells lines are therefore suitable in-vitro models to determine the effect of the novel compounds on metastatic breast cancer, as they closely resemble ER+ breast

cancer and triple-negative breast cancer, which contribute to the majority of breast cancer cases in South African women (Cubasch *et al.*, 2013; McCormack *et al.*, 2013).

These two cell lines were chosen as models for breast cancer in this study because they are good models for the two most common breast cancer types, triple negative and hormone receptor positive. Therefore to evaluate the efficacy of compounds based on an imidazo[1,2-a]pyridine amines in breast cancer the use of cell lines that represent the majority of breast cancer tumours observed is ideal. Leukocytes were used to represent non-tumoregenic cells in the study because current side effect profile for standard cytotoxic agents against breast cancer show mild to severe neutropenia. Therefore the effect of compounds based on imidazo[1,2-a]pyridines amines on leukocytes is important to assess.

1.8 Aim and Objectives

Despite advancements in breast cancer treatment and improvement in survival outcomes in early breast cancer, the risk of recurrence is high and survival in metastatic cancer remains low. This is particularly a problem in South Africa where the majority of breast cancer cases occur in black women and new diagnoses are already advanced (Stage III and IV). A large percentage of these cases are triple negative breast cancer, which is particularly aggressive and resistant to a variety of chemotherapeutic interventions. The most effective chemotherapy treatments cause severe neutropenia, which is a problem in South Africa given the high prevalence of HIV in black women.

Therefore considering the evidence, this study aims to observe the potential anticancer effects of test compounds based on an imidazo[1,2-a]pyridine amine scaffold in two breast cancer cell lines, MCF-7 and MDA-MB-231. To achieve the aim, the objectives of the study will be to:

- Determine the effect of test compounds on cell viability in MCF-7 and MDA-MB-231 cells.
- Measure the effect of highly active test compounds on leukocyte cell viability
- To describe and evaluate the effect of test compounds on induction of programmed cell death

Chapter 2 - Methods

A total of 27 compounds were evaluated against breast cancer cell lines MCF-7 and MDA-MB-231. These compounds were synthesised using the Groebke-Blackburn-Bienaymé multicomponent reaction and evaluated for purity by elemental analysis. Test compounds were tested for their ability to inhibit cell growth at a concentration of 100 μM. Stock solutions of the tests compounds imidazo[1,2-a]pyridine amine derivatives were prepared in 100% ethanol (v/v) at a concentration of 10 μM, except for $JDPtCl_2$ which was dissolved in DMSO at 10 μM, and stored at 4°C. The IC_{50} (half maximal inhibitory concentration) value of compounds was determined over a range of test compound concentrations (0.001 - 100 μM) using the MTT assay. Compounds that showed the greatest activity (IC_{50} < 10 μM in MCF-7 and < 30 μM in MDA-MB-231 cells) were tested for their ability to induce apoptosis. This was achieved through several experiments, which assessed different aspects of apoptotic cell death. All aqueous solutions were prepared using of double distilled Milli-Q^{TM} water unless otherwise stated (Millipore Elix 3 Water Purification System).

2.1 Cell culture

2.1.1 Cell culture initiation

Cells stored in liquid nitrogen were rapidly thawed in a water bath at 37°C. Once thawed, the cell suspension was transferred to a 25 cm^2 Greiner bio-one culture flask (Lasec) containing 2 mL of culture medium composed of Dulbecco's Modified Eagle's Medium (DMEM) (Sigma-Aldrich). DMEM was supplemented with 100 μg/mL of carbenicillin, 10 μg/mL of ciprofloxacin (Sigma-Aldrich) and 10% (v/v) of fetal bovine serum (FBS) (Celtic Molecular Diagnostics) for MCF-7 cells. MDA-MB-231 cells were grown in a 1:1 (v:v) solution of DMEM and Hams F12 media (Sigma-Aldrich), 15% (v/v) FBS and 100 μg/mL of carbenicillin. Two millilitres of culture media was added at two-minute intervals to a total volume of 10 mL in the flask. The cells media was the replaced with fresh media every second day for seven days. Ciprofloxacin was not added to MCF-7 culture media after seven days of culture growth. The Human Research Ethics Committee (Medical) approved the use of the cell lines in this study, ethic waiver number: **W-CJ-130311-2**.

DMEM powder (with 4.5 g/L glucose, L-glutamine) was dissolved in water at a concentration of 13.5 g/L and supplemented with 3.5 g/L of $NaHCO_3$ (Merck). This solution was then sterile filtered through a Sterivex 0.22 µm membrane (Merck/Millipore) and incubated for 48 hours at 37°C to detect if any microorganisms were still present.

FBS purchased was heat-inactivated by placing a sealed 500 mL bottle in a 4°C fridge overnight. The sealed bottle was then placed in a 56°C water bath for 60 minutes with mixing at regular intervals. The bottle was aliquoted into 50 mL falcon tubes under sterile conditions and stored at -20°C. Heat-inactivation of the heat labile complement in the FBS reduces the haemolytic activity of the serum and promoting cell growth (Freshney, 2010; Triglia *et al.*, 1980).

2.1.2 Cell culture maintenance

Cells were grown in 75 cm^2 Greiner bio-one culture flasks (Lasec) containing 25 mL of culture medium. Culture medium was replaced by washing the cells with phosphate buffered saline (PBS) and adding fresh media every third day. PBS consisted of 1.37 M NaCl (Merck), 27 mM KCl, 100 mM Na_2HPO_4 and 18 mM KH_2PO_4 (Sigma-Aldrich) in a 1L solution at a pH between 7.2 – 7.4. The PBS solution was autoclaved at 121°C before use in any experiments.

2.1.3 Cell sub-culturing

When cells had reached 70% confluency, the culture media was aspirated and cells were washed once with 3 mL of PBS. The cells were detached from the growth surface by adding 3 mL of 0.25% trypsin-ethylenediaminetetraacetic (Trypsin-EDTA) (Sigma-Aldrich) and placing the flask in a 37°C incubator for 10 – 15 minutes. The cells were then separated into single cells by pipetting up and down gently before adding 7 mL of culture media. The serum in the culture media contains trypsin inhibitors that inactivate trypsin-EDTA reaction (Quigley Iii *et al.*, 1995). MDA-MB-231 cells were detached by adding 0.05% Trypsin-EDTA and incubating for 5 minutes.

Cells were then counted using the trypan blue exclusion assay. This involved adding 20 µL of trypan blue solution (Sigma-Aldrich) to 20 µL of the cell suspension followed by thorough mixing. Twenty microlitres of this mixture was added to the

haemocytometer and the cells were counted. Cells numbers were counted on each quadrant of the haemocytometer and an average calculated. This average was multiplied by the dilution factor (x2) and multiplied by the 10^4 to obtain the number of cells per millilitre. The cells were then reseeded at 1 x 10^6 cells per flask. The trypan blue exclusion assay is based on the staining of dead cells by trypan blue due to the loss of integrity of their cell membrane. Therefore dead cells are stained blue while live cells are lightly stained on their cell membrane (Strober, 2001). Only live cells are counted on the haemocytometer under a light microscope (100x magnification).

Trypan blue was dissolved to a final concentration of 0.2% (w/v) in PBS, which was subsequently sterile filtered through a 0.22 µm membrane and stored in a dark cupboard at room temperature.

2.1.4 Cryopreservation

Cells extracted from the base of the flask were placed in a 14 mL falcon tube and centrifuged at 200 x *g* for 5 minutes. The supernatant was carefully removed and 5 mL of PBS was added to wash the cells and the cells centrifuged for 5 minutes. The supernatant was discarded and the pellet resuspended in 10 mL of freezing media composed of culture media specific to each cell line supplemented with dimethylsulfoxide (DMSO) (5% v/v) (Sigma-Aldrich) for preservation. The solution was then aspirated and aliquoted equally into 2 mL cryotubes. The cryotubes were placed for 72 hours in a -70°C freezer allowing for the slow decrease in temperature (1°C per minute) of the freezing solution so as to ensure maximal survival of the cells under cryopreservation (Freshney, 2006) before being transferred to liquid nitrogen. Cryopreservation is useful for the long-term storage of cells in a state that protects from contamination and aging during a period in which they are not used and also as a stock for future use (Freshney, 2006).

2.2 Cell viability assays

2.2.1 MTT Cell Viability Assay

MTT (3-[4,5-dimethylthiazol-2-yl]-2,5- diphenyltetrazolium bromide) (Sigma-Aldrich) was prepared to a 5 mg/mL solution and sterile filtered through a 0.22 µm membrane. This solution was prepared fresh and could be used for a maximum of seven days after preparation.

Cells were seeded at 5000 cells/well for MCF-7 cells and 25 000 cells/well for MDA-MB-231 cells in 96 well plates, in a volume of 180 µL. These cells numbers were determined to be representative of the linear relationship between cell number and absorbance values in MTT standardisation experiments. Cells were then incubated in a humidified incubator at 37°C and 5% CO_2 for 2 hours for MCF-7 cells and overnight for MDA-MB-231 cells to allow attachment to the growth surface. Cells were then exposed to 100 µM per well of test compounds for basic screening, and a range of concentrations (0.001 – 100 µM) for determining the IC_{50} values (half maximal inhibitory concentration). These concentrations are recommended for pure compound testing by the National Cancer Institute (Monks *et al.*, 1991). Camptothecin was used as the positive control for all experiments.

The exposed cells were then incubated for 48 hours at 37°C followed by addition of MTT solution. Treated and untreated cells were then exposed to 40µL of MTT solution per well and incubated for 2 hours at 37°C and 5% CO_2. The culture media-MTT solution was then completely aspirated from each well and the formazan crystals dissolved by addition of 200 µL of DMSO. The absorbance was read on an iEMS micro-plate reader at a wavelength of 540nm and a reference wavelength of 690nm. The MTT assay distinguishes viable from non-viable cells. Viable cells are able to transform the yellow methylthiazolyldiphenyl-tetrazolium bromide through mitochondrial succinate dehydrogenase to purple formazan crystals (Mosmann, 1983).

The following formula was used to calculate the cell viability when MCF-7 and MDA-MB-231 cells were exposed to test compounds. The blank well only contained DMSO.

Key: Abs - Absorbance

$$\text{Cell Viability (\%)} = \frac{\text{Average Abs (treated cells)} - \text{Average Abs (Blank)}}{\text{Average Abs (untreated cells)} - \text{Average Abs (Blank)}}$$

The statistical significance of the mean IC_{50} values of test compounds compared to the control and between cell lines were determined using a student-t test with the significance set at $p < 0.05$. The IC_{50} values were expressed as the mean ± the standard error of the mean.

2.2.2 Leucocyte toxicity assay

Whole blood was collected in heparin containing blood collecting tubes. White blood cells were isolated from whole blood using Histopaque-1077 (Sigma-Aldrich) solution. Leukocytes are isolated from whole blood by aggregation of erythrocytes and granulocytes in the polysaccharide and salt matrix. Centrifugation creates a layer of leukocytes in the middle of the histopaque and plasma while erythrocytes and granulocytes sediment at the bottom (Boyum, 1976). An ethics approval was obtained from the Human Research Ethics Committee (Medical) for the use of leukocytes in this study (Clearance number: **M140669**).

The histopaque solution was brought to room temperature and 15 mL was transferred into a 50 mL falcon tube. An equal volume of whole blood was layered onto the surface of the histopaque. The tube was then centrifuged for 30 minutes at 250 x *g*. The upper layer of the solution was then carefully aspirated and discarded and the opaque interface was aspirated and transferred to a new 50mL tube.

Ten millilitres of PBS was added to the histopaque cell mixture and resuspended followed by centrifugation at 250 x *g* for 10 minutes. The supernatant was carefully discarded and replaced with 5 mL of culture medium (1:1 DMEM and Hams F12 media supplemented with 100 µg/mL carbenicillin solution and 20% (v/v) of FBS). The pellet was resuspended and the solution was centrifuged for 10 minutes at 200 x *g*. This was repeated once more and the pellet was then resuspended in 2 mL of culture medium and the cells counted on a haemocytometer using trypan blue. The cells were counted in order to determine the percentage recovery of live cells from whole blood.

The white blood cells were seeded in a 96 well plate at 40 000 cells/well and exposed to active test compounds at 15 and 25 µM concentrations, and concentrations equal to the IC_{50} value of the test compounds. The plate was then placed in a humidified incubator at 37°C and 5% CO_2 for 48 hours. The MTT assay was then performed on the cells as described in section 2.3.1 and the results were analysed.

2.3 Cell morphology assays

2.3.1 Phase contrast and Fluorescence microscopy

Glass cover slips were soaked in 100% ethanol (v/v) and then flamed immediately before being placed in a 6 well plate. This was done in order to sterilize the cover slips where the cells would attach. Cells were then seeded at 100 000 cells/coverslip for fluorescence microscopy. Cells were seeded at 25 000 cells/well in 24 well plates for phase microscopy and the plates were incubated at 37°C and 5% CO_2 in a humidified incubator overnight.

2.3.1.1 Effect of novel compounds on cell morphology (AO-EB-HO staining)

Ethidium bromide and acridine orange (AO-EB) staining is based on the ability of AO and EB to cross the cell membrane and bind to DNA. In living cells, AO is taken up and binds to DNA fluorescing green under a wide-band blue excitation filter (McMaster *et al.*, 1977; Rigler, 1966). Dead cells allow the entry of ethidium bromide and the nucleus is stained purple to red under a wide-band UV excitation and wide-band blue excitation filter respectively (Lepecq *et al.*, 1967; Waring, 1965). Hoechst 33258 (HO) (Sigma-Aldrich) dye stains the nucleus of viable cells blue under a wide-band UV excitation filter through binding DNA (Arndt-Jovin *et al.*, 1977).

Therefore a combination of these dyes is useful is distinguishing between apoptotic and non-apoptotic cells. Apoptotic cells contain fragmented nuclei that fluoresce blue with HO stain and green with AO. These cells may also stain red and pink under AO and HO respectively during late apoptosis when they lose their cell membrane integrity and allow the entry of ethidium bromide. Necrotic cells will stain red due to entry of EB and pink with HO staining without any associated fragmentation. Living cells stain green with AO and blue with HO without any associated nuclei fragmentation (Mpoke *et al.*, 1997). All phase contrast and fluorescent images were viewed under an Olympus BX41 fluorescent microscope.

Cells grown on coverslips for fluorescence were exposed to the concentrations equal to the IC_{75} value of active test compound and then incubated for 24 hours at 37°C and 5% CO_2. Cells were then washed three times by adding 2mL of PBS to each well per wash. To each coverslip 100 µL of HO (10 µg/mL) was added and the plate incubated for 20 minutes in the dark. Each well was then washed once with 2mL of PBS, which was then aspirated and discarded.

To a normal microscope slide, 10 µL of solution (AO/EB) (10 µg/mL) (Sigma-Aldrich) was added and the cover slips were carefully removed one at a time from the base of the well using a sterile surgical blade and a pair of forceps. The blade was used to elevate the coverslip from the base of the well while the forceps were used to transfer the coverslip to a slide and immediately viewed under an Olympus BX41 fluorescent microscope. Fluorescent images were viewed under a wide-band UV excitation and blue excitation filter at both a 100x and 400x magnification. Phase contrast images were taken under the bright field view at a 100x and 400x magnification.

The fluorescent images at 100x magnification were used to calculate the apoptotic and necrotic index of the active test compounds in MCF-7 and MDA-Mb-231 cells. This was calculated according to the formula below:

$$\text{Index (Apoptotic/Necrotic)} = \frac{\text{Number of cells (Apoptotic/Necrotic) in field of view}}{\text{Total Cell Population in field of view}}$$

2.3.1.2 Effect of test compounds on autophagic vacuole formation in MCF-7 cells

Autophagy is a type of cell death that is usually induced in cells that are nutrient deprived. One of the morphological features observed during autophagy is the formation of vacuoles that ingest cytoplasmic components that are digested to provide energy (Meijer *et al.*, 2009). Monodansylcadaverine is a non-specific acidotrophic dye that is incorporated into the cytoplasmic vesicles and can be used to identify autophagic vacuoles (Klionsky *et al.*, 2012).

MCF-7 cells were seeded on a cover slip at 100 000cells/well and incubated overnight at 37°C in a humidified incubator. The cells were then treated with active test compounds at a concentration of 20 µM for 20 hours. The cell media was then carefully aspirated before being washed three times with 1mL of PBS in each wash per well. The cells were then exposed to 500 µL per well of a 50 µM solution of monodansylcadaverine (MDC). MDC was prepared by diluting a 50 mM solution of MDC in DMSO to a concentration 50 µM in PBS. The cells were then incubated for 15 minutes in a humidified incubator and then viewed under a wide-band UV excitation filter on a fluorescence microscope.

2.4 Apoptotic biomarker assays

2.4.1 Caspase-3/7 colorimetric assay

Caspase-3 and -7 are recognised as executioner caspase that are activated as part of apoptotic cell death. The Sigma-Aldrich colorimetric assay used is based on the ability of caspase-3/7 to cleave the substrate acetyl-Asp-Glu-Val-Asp p-nitroanilide (Ac-DEVD-pNA) releasing p-nitroaniline a coloured product, whose absorbance can be measured spectrophotometrically at 405 nm (Earnshaw *et al.*, 1999).

2.4.1.1 Assay procedure

Cells were grown in 24 well plates at 1 x 10^6 cells per well and then exposed to active test compounds at the IC_{75} concentration and incubated for a range of time periods between 2 and 32 hours at 37°C and 5% CO_2. Cells were washed with 150 µL of PBS and then 150 µL of Trypsin-EDTA was added to each well to detach the cells from the bottom of the well. The cell solution was aspirated into microcentrifuge tubes and centrifuged at 250 x *g* for 5 minutes. The supernatant was carefully discarded, 1 mL of cold PBS was added and the pellet was resuspended. The solution was re-centrifuged (600 x *g*, 5 minutes) and the supernatant discarded before the pellet was resuspended in 50 µL of 1X Lysis buffer (50 mM HEPES (4-(2-hydroxyethyl)-1-piperazineethanesulfonic acid), 5 mM CHAPS (3-[(3-cholamidopropyl) dimethylammonio]-1-propanesulfonate), 50 mM DTT (Dithiothreitol), 20 mM EDTA (pH 7.4). This solution was then incubated for 20 minutes on ice and the tubes were centrifuged at 20000 x *g* (4°C) for 15 minutes. The supernatant was then aspirated and placed in a new tube on ice.

A 96 well plate was used to setup the reaction scheme for the Sigma-Aldrich Caspase-3 Colorimetric Assay Kit (CASP-3-C). The 96 well plate was divided into one treatment well and four control wells. The four control wells were composed of untreated cells, well with no cells, caspase-3 positive control and the caspase-3 positive control with a caspase inhibitor. The well contents were added as specified in the **Table 2.1** below and the plate was covered with a lid and sealed using

parafilm. The plate was then incubated at 37°C overnight and then analysed at 405 nm on a Multiskan™ GO Microplate Spectrophotometer.

Table 2.1: Reaction volume for caspase assay in 96 well plate

Well No	Cell Lysate (µL)	Caspase-3 5µg/mL (µL)	1X Assay buffer (µL)	Inhibitor AC-DEVD-CHO (µL)	Substrate AC-DEVD-pNA (µL)
1	--	--	90	--	10
2	5	--	85	--	10
3	5	--	85	--	10
4	--	5	85	--	10
5	--	5	75	10	10

All experiments were done independently and in triplicate for both MCF-7 and MDA-MB-231 cells.

2.4.1.2 Bradford protein determination assay

The BIO-RAD protein assay mixture was purchased from Bio-Rad laboratories and used to determine the amount of protein in the cell lysates. This protein assay kit is based on the principle of the Bradford method for protein determination. This method makes use of a protein binding dye known as coomassie blue that when bound to protein is rapidly altered from an excitation maximum of 465 nm to 595 nm. This change can be measured on a spectrophotometer and a standard curve can be used to determine the protein concentration in a sample (Bradford, 1976).

The assay was carried out in 96-well microtiter plates. In each well, 10 µL of each test sample was added followed by 200 µL of the reagent dye coomassie blue. Each well was mixed thoroughly using the Multiskan™ GO Microplate Spectrophotometer at 300 rpm for 15 minutes at room temperature and then analysed at 595 nm.

2.4.1.3 Standard curve

Stock concentrations of p-nitroaniline (pNA) were used to construct a standard curve. In order to make the stock solution p-nitroaniline was dissolved in 720 µL of DMSO in an epperndorf tube and from this 100 µL was transferred into a new microcentrifuge tube. To this new tube 900 µL of 1X assay buffer (20 mM HEPES, 2 mM EDTA, 0.1%

CHAPS, 5mM DTT) was added and the solution was thoroughly mixed. This test solution was then aliquoted into 5 new microcentrifuge tubes. These tubes were diluted to a concentration 10%, 20%, 40% 60% 80% (v/v) respectively in a final volume of 300 µL. A 96 well plate was used for the reaction and 100 µL of each dilution was added to a well in triplicate. The plate was then read in a Multiskan™ GO Microplate Spectrophotometer at 405 nm and the results were used to construct a standard curve. Each data point for the standard curve was calculated using the formula below.

Average Net Abs = Average Abs (Standard) – Average Abs (Blank)

To calculate the caspase activity in the samples, the formula below used the reaction time in minutes, the volume of the sample in millilitres and the protein concentration in milligrams.

$$\text{Specific Activity} = \frac{\mu\text{mol pNA x dilution factor}}{\text{reaction time(t) x volume of sample x protein concentration}}$$

2.4.2 Annexin-V Assay

An Invitrogen Alexa Fluor® 488 annexin V/Dead Cell Apoptosis Kit was used to determine the presence of phosphatidyl serine exposed on the cell membrane of cells exposed to active test compounds. Cells grown on cover slips in six well plates were exposed to the active test compound at a concentration equal to the IC_{50} for 18 and 24 hours. The cover slips were washed as described in section 2.4.1.1. After this 30 µL of a staining solution containing Alexa Fluor® 488 (6% v/v) and propidium iodide (1% v/v) was placed on a normal microscope slide and the cover slip gently placed on top. The slide was incubated for 15 minutes and the cells viewed at 400x magnification under a wide-band blue excitation filter for fluorescence and at 400x magnification under the bright light for phase contrast microscopy.

2.4.3 Effect of test compounds on the cytoskeleton of MCF-7 cells

One of the major components of the eukaryotic cytoskeleton is F-actin. Several changes to cytoskeleton occur during apoptotic cell death including the loss of F-actin and therefore the ability to probe F-actin is helpful in identifying apoptotic cells. Phalloidin is a peptide that is part of the phallotoxin family of toxins that has the ability

to bind to F-actin. When phalloidin is conjugated with a FITC probe, F-actin can be identified in cells using fluorescence microscopy (Bursch *et al.*, 2000; Endresen *et al.*, 1995).

MCF-7 cells were seeded at 100 000 cells/well on coverslips as described in section 3.4.1 and incubated overnight in a humidified incubator at 37°C. These cells were then treated to active test compounds at a concentration equal to the IC_{75} value for each compound for 24 hours. The cells were then washed twice with PBS warmed to 37°C. A fresh solution of 3.7% (v/v) formaldehyde was prepared by diluting a 20% (v/v) formaldehyde solution with PBS. The cells were then fixed by adding 500 µL of 3.7% formaldehyde, and incubating at room temperature for 10 minutes.

The cells were then washed twice with PBS supplemented with 0.5% (v/v) of bovine serum albumin (BSA) (BioRad) to reduce non-specific staining of the phalloidin. The fixed cells were then permeabilized by adding 0.1% (v/v) Triton-X-100 (Sigma-Aldrich) in PBS for 5 minutes. The cells were then washed twice with PBS supplemented with 0.5% BSA before 120 µL of Cytopainter Phalloidin-iFluor 488 (Abcam) conjugate was added to each coverslip. Cytopainter Phalloidin-iFluor 488 was prepared by adding 1µL of 1000X of the phalloidin conjugate in 1mL of PBS supplemented with 1% (v/v) BSA.

The coverslips were incubated for 60 minutes at room temperature in the dark in a container layered with damp filter paper to avoid the cover slips drying out. The cover slips were then washed twice with PBS before being mounted on the slide with Fluoromount™ (Sigma-Aldrich). The cover slips were then incubated for two hours to allow Fluoromount™ to dry and then viewed under a wide-band blue excitation filter. The slides can be stored for up to 6 months at 4°C.

2.4.4 Cytochrome c ELISA assay

2.4.4.1 Lysate preparation

Cells were seeded in a 24 well plate at $1x10^6$ cells per well and incubated overnight in a humidified incubator at 37°C and 5% CO_2. MCF-7 cells were then exposed to the IC_{75} concentration of each active compound for 24 hours. These cells were then washed thoroughly (al least three times) with PBS and 500 µL of trypsin-EDTA was pipetted into each well. After the cells had detached from the bottom of the growth

surface, 500 µL of culture media was added to each well and the solution was transferred into new microcentrifuge tubes for each well.

The microcentrifuge tubes were centrifuged at 800 x *g* for 5 minutes and the resulting supernant was discarded. The cells were then washed with PBS by resuspending the pellet in 1 mL of PBS into each tube and centrifuging the tubes at 800 x *g* for 5 minutes and then discarding the supernatant. This wash step was repeated at least three times. Each pellet was then resuspended in 500 µL of the Digitonin Cell Permeabilization Buffer (250 mM Sucrose, 137 mM NaCl, 70 mM KCl, 4.3 mM Na2HPO4, 1.4 mM K2HPO4, 0.2 mg/mL Digitonin and 0.1% Hydorol M) and placed on ice for 5 minutes. The tubes were then vortexed and centrifuged at 1000 x *g* for 5 minutes at 4°C. The supernatant was transferred into a new microcentrifuge tube and stored at -70°C. This was the cytosolic lysate.

The remaining pellet was resuspended in 500 µL of RIPA Cell Lysis Buffer (50 mM Tris HCl, pH 7.4, 150 mM NaCl, 1 mM EDTA, 1 mM EGTA, 1% Triton X-100, 1% Sodium Deoxycholate and 0.1% SDS) and placed on ice for 5 minutes before being vortexed and centrifuged at 10 000 x *g* for 10 minutes. The supernatant which consisted of the mitochondrial fraction was transferred into a new tube and stored at -70°C.

2.4.4.2 ELISA assay procedure

An assay layout sheet provided in the cytochrome c (human) EIA kit (Enzo Life Sciences) was used to allocate wells in the 96 well plate for the lysates and the standards. Lysates were thawed on ice and 10 µL of each transferred into new microcentrifuge tubes. The lysates were then diluted 200X and then 100 µL of each lysate placed in appropriate wells in duplicate. The plate was then tapped gently to ensure that the contents were mixed thoroughly.

After the hour had passed, the plate was emptied and washed with 400 µL/well, of wash solution (Tris buffer with detergents) and this was repeated a three more times. Traces of wash buffer were removed by tapping the plate firmly on a paper towel and 100 µL of yellow antibody was added to each well excluding the blank. The plate was then sealed and incubated for 60 minutes on a plate shaker at room temperature and 500 rpm.

The plate was then washed and dried as described above and 100 µL of blue conjugate was added to each well excluding the blank. The plate was sealed for 30 minutes on a plate shaker at room temperature and 500 rpm. The plate was washed again four times as described above and 100 µL of substrate solution (p-nitrophenyl phosphate solution) was pipetted into each well. The plate was then incubated for 45 minutes at 500 rpm and room temperature after which 25 µL of stop solution (trisodium phosphate solution) was added to each well. The plate was then read at a test wavelength of 405 nm and a reference wavelength of 590 nm using a Multiskan™ GO Microplate Spectrophotometer.

2.5.2.3 Standard Curve

The standards were prepared by first adding 500 µL of Assay buffer 13 (Tris buffered saline, protein and protease inhibitor) to the lyophilized cytochrome c. This was vortexed and labelled Standard #1 (S#1). Thereafter 250 µL of S#1 was transferred to a microcentrifuge tube and vortexed to make S#2. This serial dilution was repeated to make S#3 to S#6. The final concentrations for S#1 to S#6 were 900, 450, 225, 112.5, 56.25 and 28.13 pg/mL respectively. A standard curve for pNA was then constructed for the cytochrome c assay by adding 100 µL of each standard in the appropriate well as outlined in the assay layout sheet and conducting the assay procedure as described in section 2.4.2.2. The concentration of cytochrome c was then extrapolated from the standard curve using the equation from the linear line. The concentration of cytochrome c per milligram of protein was calculated using the formula below.

$$\text{Net Cytochrome c} = \frac{\text{Concentration of cytochrome c}}{\text{Concentration of protein}} \times \text{Dilution factor}$$

Chapter 3 – Results

A total of 35 imidazo[1,2-a]pyridine amines were synthesised by the Chemistry department of the University of the Witwatersrand. These test compounds were arbitrarily given the name JD after the initial of the chemist Jean Dam who synthesised them, followed by a number. These imidazo[1,2-a]pyridine amines will be referred to as test compounds throughout this dissertation.

3.1 Solubilisation of imidazo[1,2-a]pyridine amines

The test compounds proved difficult to solubilise in an aqueous medium. Therefore, a variety of solvents were evaluated to identify those that were able to solubilise the test compounds without causing a decrease in cell viability. Acetone was initially considered as a potential solvent but only a few compounds showed solubility in acetone. Furthermore, cell viability studies using various concentrations of acetone revealed that this solvent was toxic to the cells at concentrations of 5-10% (v/v) and therefore was not suitable as a solvent for the test compounds.

Dimethyl sulfoxide (DMSO) was then considered as a possible solvent for the test compounds as it is a known organic solvent. DMSO did not dissolve any of the test compounds except JDPtCl2 and therefore it was not used as a solvent for all the test compounds. Finally, almost all the compounds, except the platinum containing compound JDPtCl2, were soluble in ethanol. Ethanol was not toxic to the cells at relatively high concentrations (10-15% v/v) and concentrations (1-5% v/v) were used for testing. A total of 26 compounds were soluble in ethanol and one was soluble in DMSO, the remainder of the compounds were insoluble in organic or aqueous solvents.

3.2 Effect of the test compounds on cell viability

The effects of novel test compounds were evaluated at a concentration of 100 µM against MCF-7 and MDA-MB-231 cells for 48 hours. This initial investigation identified 12 test compounds that were active against MCF-7 cells (**Figure 3.1**) and 10 test compounds that were active against MDA-MB-231 cells (**Figure 3.2**). These active test compounds (cell viability < 95% in MCF-7 and MDA-MB-231 cells) were then further tested to determine their IC_{50} (half maximal inhibitory concentration) values against the two breast cancer cell lines.

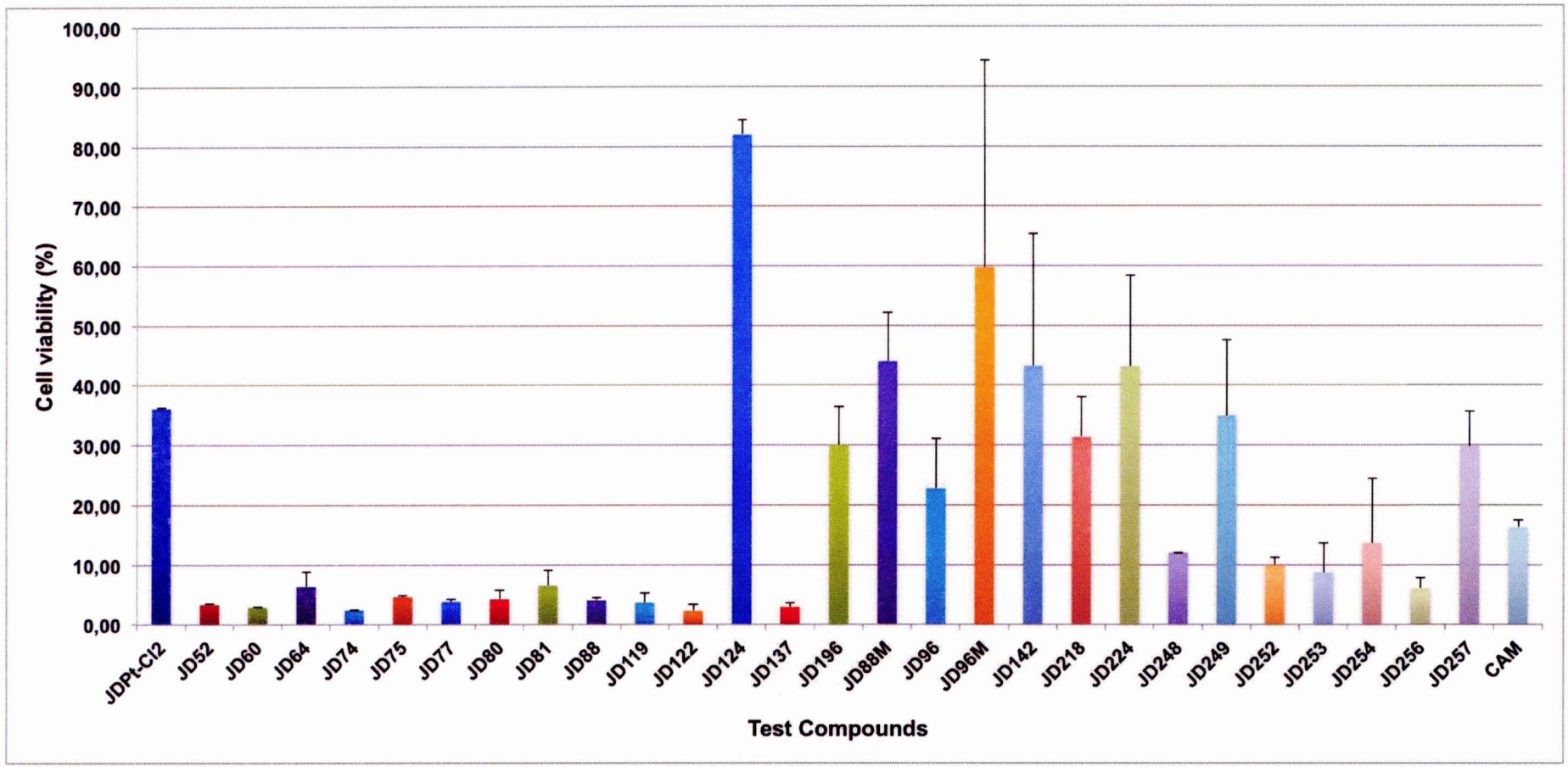


Figure 3.1 The effect of test compound on cell viability of MCF-7 cells after 48 hours exposure at 100 µM Each column represents the mean of at least three independent experiments. The bars represent the standard error of the mean for each mean value. A total of 13 compounds reduced cell viability by more than 90%, a further three compounds reduced cell viability by more than 80% and two compounds reduced cell viability by less than 50%.

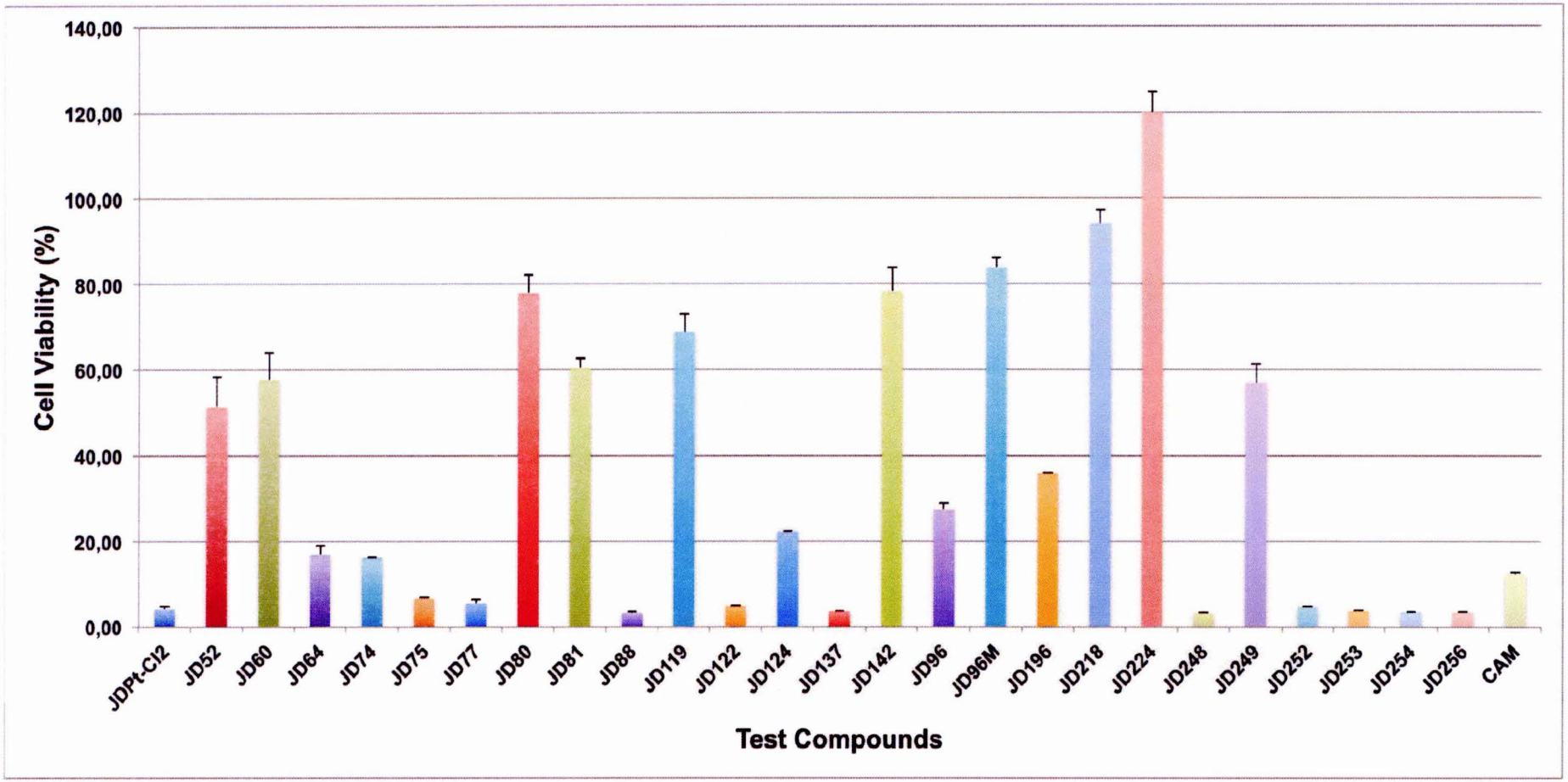


Figure 3.2 The effect of test compound on cell viability of MDA-MB-231 cells after 48 hours exposure at 100 µM Each column represents the mean of at least three independent experiments. The bars represent the standard error of the mean for each mean value. A total of 11 test compounds reduced cell viability by more than 90% and 10 of the test compounds reduced cell viability by less than 50%.

3.2.1 MCF-7 IC_{50} values of active compounds

When the test compounds were evaluated against MCF-7 cells, seven of them, JD52, JD60, JD74, JD77, JD80, JD119 and JD137, had IC_{50} values greater than 30 µM, two of them, JD75 and JD122, had IC_{50} values between 10 and 20 µM, and three compounds had IC_{50} values lower than 10 µM. The three compounds with the lowest IC_{50} values were JD88, JD253 and JD256 and their IC_{50} values were 0.62±0.03 µM, 3.66±0.49 µM and 2.23±0.10 µM respectively. The IC_{50} value for the positive control camptothecin was 0.32±0.01 µM (**Figure 3.3**).

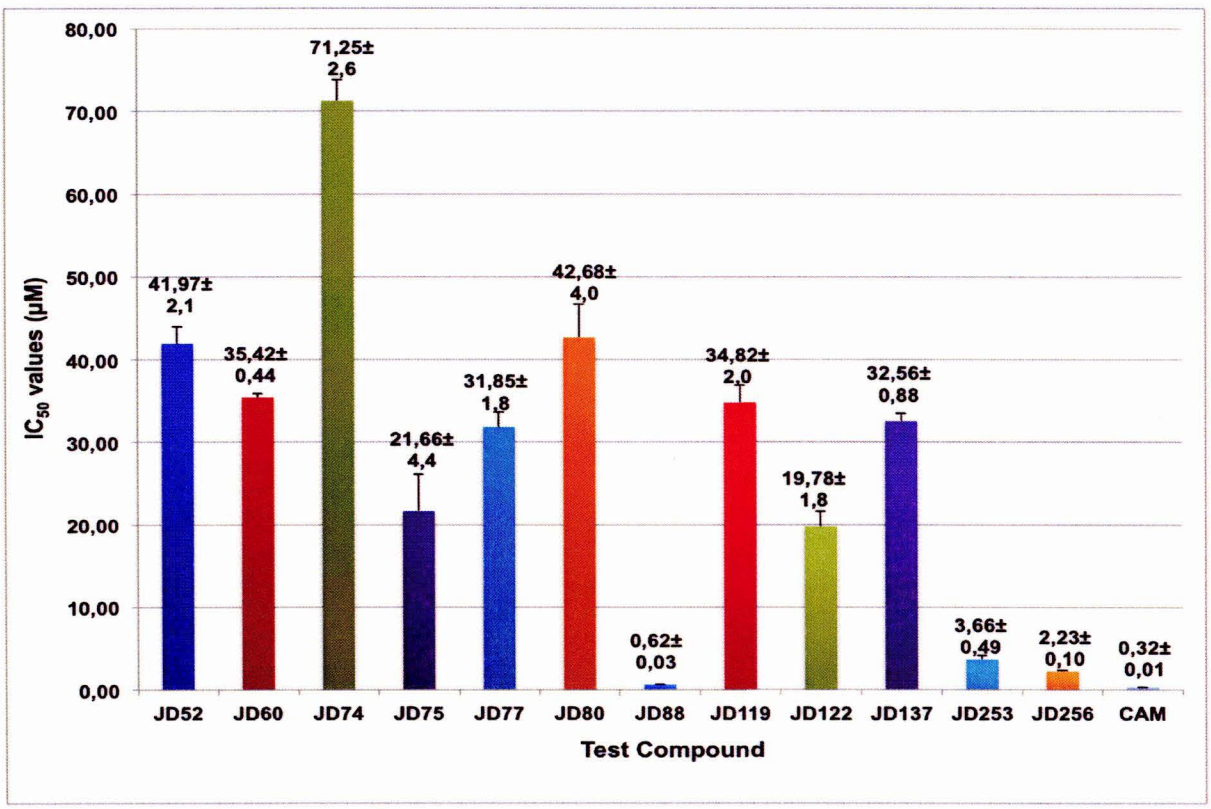


Figure 3.3 Summary of IC_{50} values of MCF-7 cells exposed to active test compounds for 48 hours The bar graph shows the IC_{50} values of 12 active imidazo[1,2-a]pyridine amine derivatives and the positive control camptothecin (CAM). Each column represents the mean of at least three independent experiments. The bars represent the standard error of the mean for each IC_{50} value

3.2.2 MDA-MD-231 IC_{50} values of active compounds

Three test compounds JD75, JD248 and JD258 had IC_{50} values higher 40 µM, another three; Pt-c12, JD77 and JD254 have IC_{50} values between 30 and 40 µM and four test compounds had IC_{50} values than lower than 30 µM. These four test compounds with IC_{50} values lower than 30 µM were JD88, JD122, JD253 and JD256 with IC_{50} values of 27.88±2.12 µM, 29.47±2.34 µM, 29.76±1.72 µM and 28.82±1.35 µM respectively. The positive control camptothecin had an IC_{50} value of 0.33±0.04 µM (**Figure 3.4**)

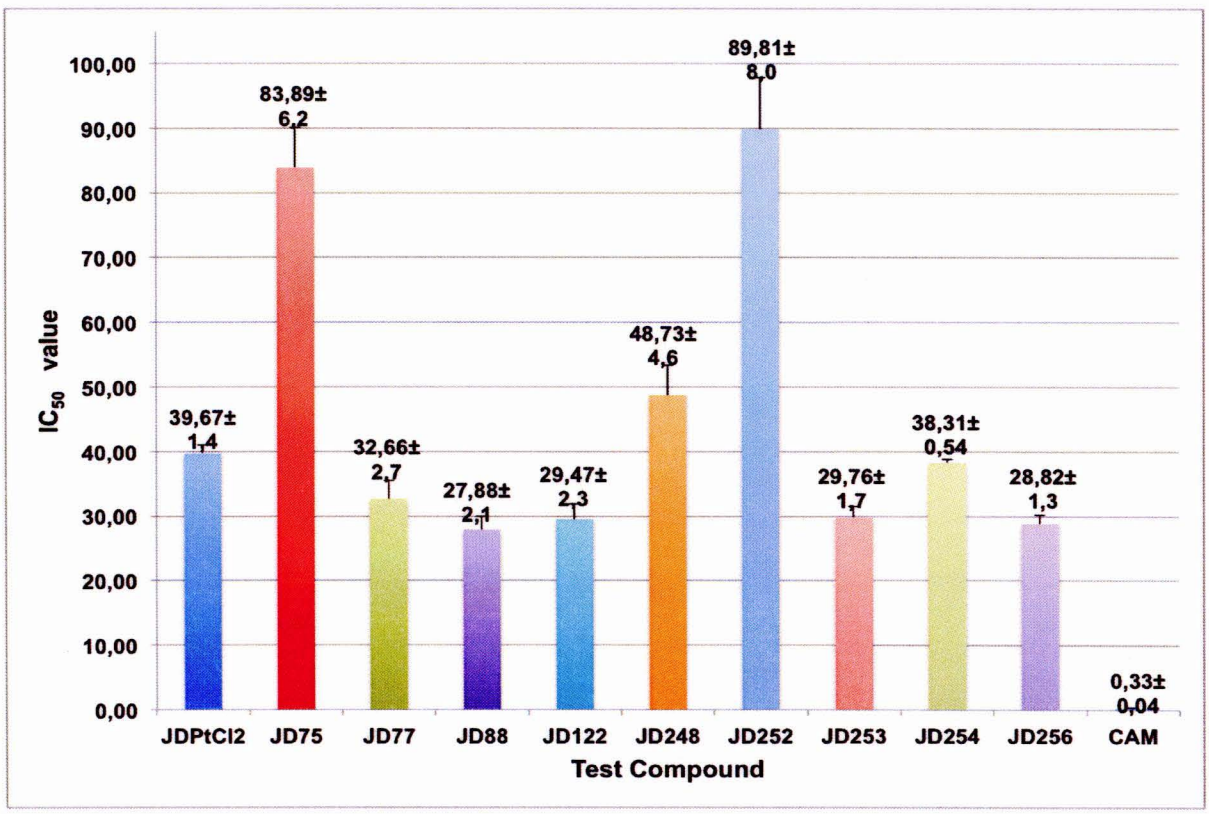
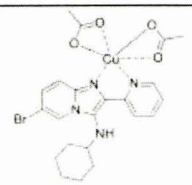
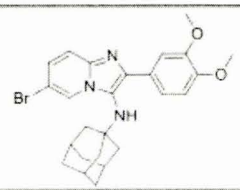
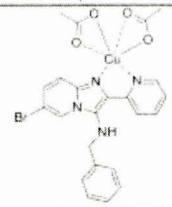
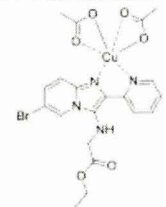


Figure 3.4 Summary of IC_{50} values of MDA-MB-231 cells exposed to active test compounds for 48 hours The bar graph shows the IC_{50} values of the 10 most active imidazopyridines and the positive control camptothecin (CAM). Each column represents the mean of at least three independent experiments. The bars represent the standard error of the mean for each IC_{50} value

Table 3.1, a summary of IC_{50} values and active test compound structures, shows a comparison of the IC_{50} values of JD88, JD122, JD253 and JD256 in both MCF-7 and MDA-MB-231 cells. The structures for each test compound are shown with their respective IC_{50} values.

Table 3.1 Summary of structures and IC_{50} values of active test compounds

	Structure	IC_{50} Value (μM) MCF-7	IC_{50} Value (μM) MDA-MB-231
JD88		0.62±0.03	27.88±2.12
JD122		19.78±1.80	29.47±2.34
JD253		3.66±0.49	29.76±1.72
JD256		2.23±0.10	28.82±1.35

3.2.3 Dose response curves for MCF-7 and MDA-MB-231 cells

Data obtained from the MTT assay was used to construct sigmoidal dose response curves to determine the IC_{50} values of active test compounds against MCF-7 and MDA-MB-231 cells. Cells were exposed to a concentration range (0.001 μM – 100 μM) of compounds in a 96 well plate. Each data point was obtained in quadruplicate and each experiment was repeated at least 5 times. The GraphPad Prism® v.5 software package was used to analyse the data and to construct sigmoidal dose response curves. Representative dose response curves for both cell lines are shown in **Figure 3.5**

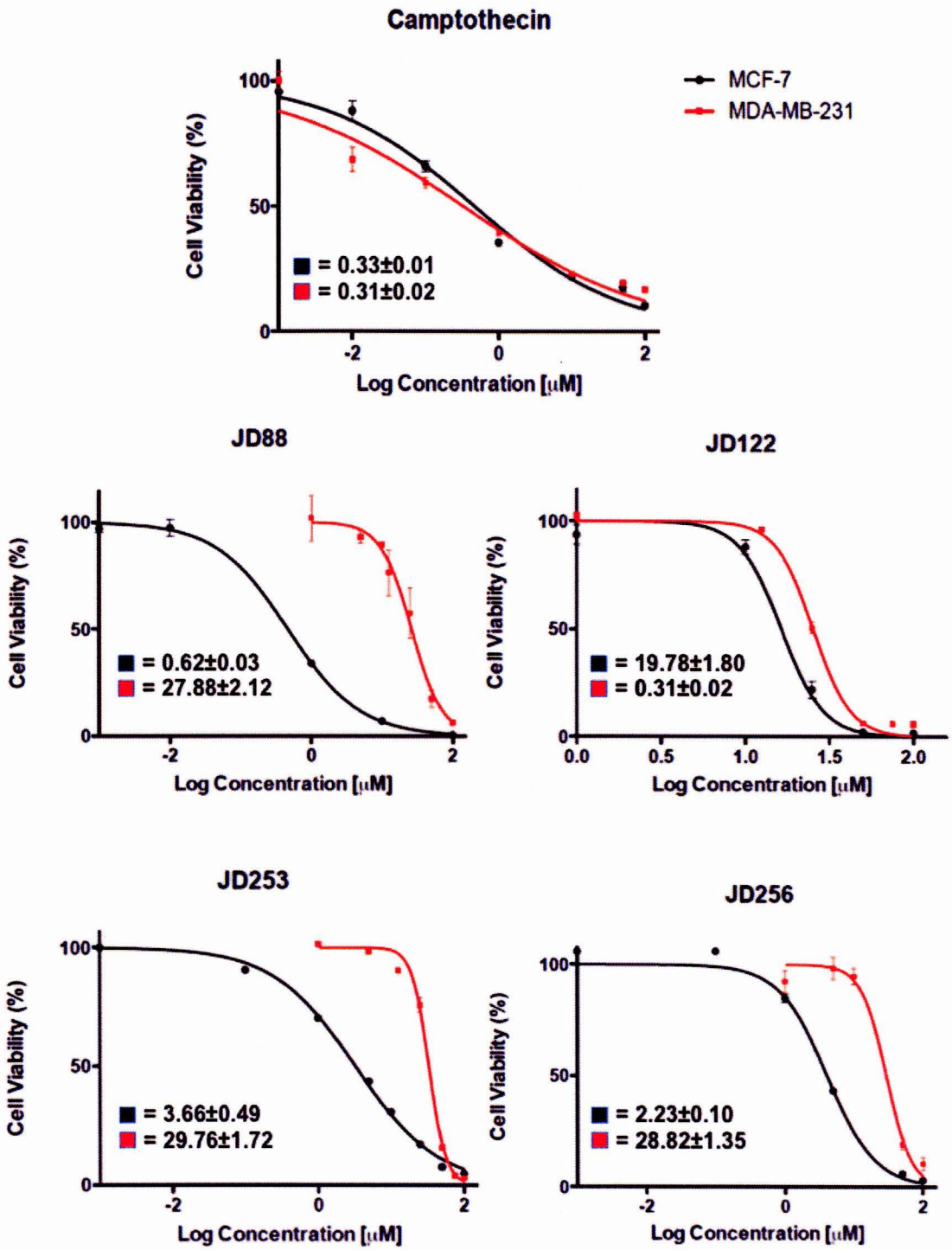


Figure 3.5 Representative dose response curves of test compounds and camptothecin (CAM) for MCF-7 and MDA-MB-231 cells The dose response curves are representative of at least three independent experiments for JD88, JD122, JD253 and JD256. Cells were exposed to a concentration range between 0.001 μM and 100 μM. The data points represent the mean cell viability at each concentration and the error bars indicate the standard error of the mean.

3.2.4 Effect of test compounds on leukocyte viability

Leukocytes isolated from whole blood were exposed to JD88, JD253 and JD256 at concentrations of 15 and 25 µM for 24 hours (**Figure 3.6**). JD256 was significantly less toxic to leukocytes than the positive control camptothecin at both 15 and 25 µM ($p = 0.0149$ and 0.0041 respectively). JD253 at 25 µM was the most toxic to the leukocytes but this was not significantly different from camptothecin ($p = 0.0742$). The cell viability (%) of leukocytes exposed to JD88, JD253, JD256 and camptothecin at 15 µM were 51.19±1.9, 48.75±2.9, 60.99±3.3 and 46.50±2.8 respectively. Leukocytes exposed to 25 µM of JD88, JD253, JD256 and camptothecin had cell viabilities (%) of 41.45±1.7, 34.92±1.5, 52.66±1.4 and 41.34±1.4 respectively (**Figure 3.6**).

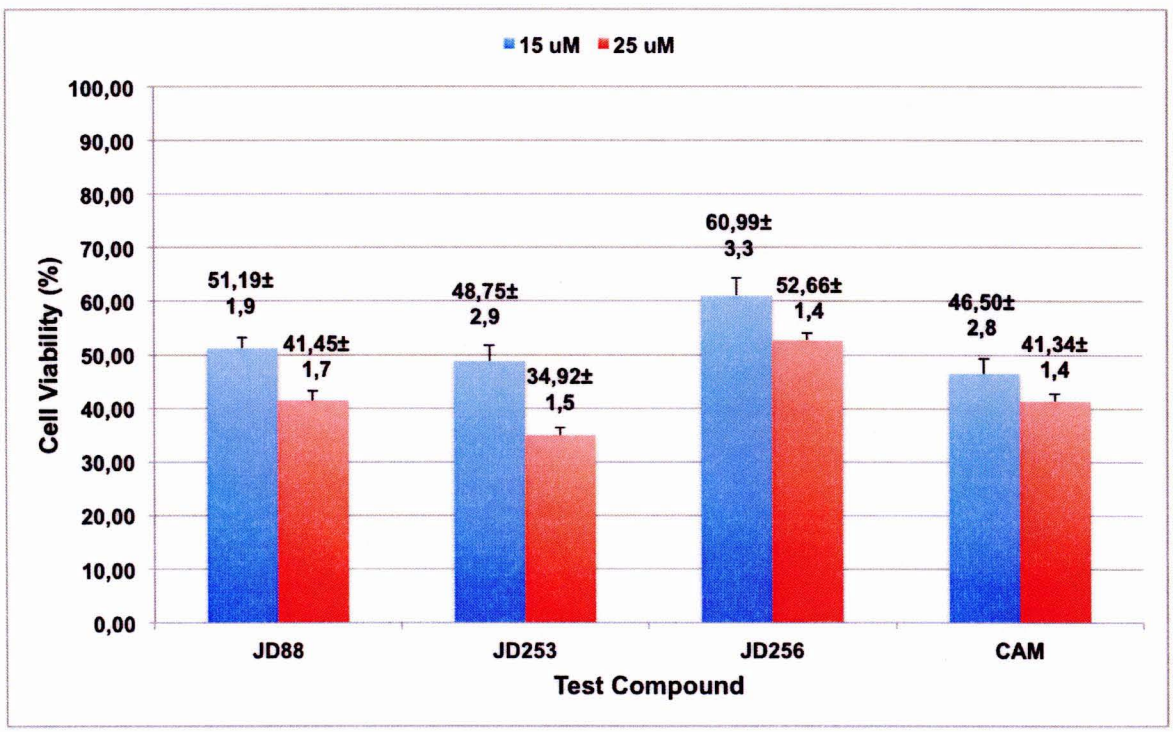


Figure 3.6 Effect of test compounds on leukocyte cell viability at 15 and 25 µM after 48 hours Leukocytes were exposed to test compounds JD88, JD253, JD256 and camptothecin at 15 and 25 µM. The bars for each compound represent the mean cell viability of at least three independent experiments and the error bars indicate the standard error of the mean (SEM).

3.2.5 Statistical analysis of cell viability

IC_{50} values for the active test compounds JD88, JD253, JD256 and the positive control camptothecin were compared to determine if there were any significant differences. A student-t test was used to compare paired IC_{50} values assuming unequal variances. The IC_{50} value of camptothecin was significantly different to all

three of the active test compounds in both MCF-7 and MDA-MB-231 cells (**Table 3.2**).

JD88 had an IC_{50} value that was significantly lower than JD253 and JD256 in MCF-7 cells while the IC_{50} values of JD253 and JD256 in MCF-7 cells were not significantly different from each other. In MDA-MB-231 there was no significant difference between the IC_{50} values of the three compounds JD88, JD253 and JD256 (**Table 3.2**). When IC_{50} values were compared between the two cell lines for JD88, JD253 and JD256 the IC_{50} values for MCF-7 cells were significantly lower than the IC_{50} values in MDA-MB-231 cells. Camptothecin IC_{50} values between the two cell lines were not significantly different.

Table 3.2 Statistical comparisons of IC_{50} values of test compounds and positive control camptothecin (CAM)

Common Variable	Test Variables	p-value	Significance (p<0,05)
MCF-7	CAM vs JD88	0.0007	Significant
	CAM vs JD253	0.0028	Significant
	CAM vs JD256	0.0004	Significant
	JD88 vs JD253	0.0037	Significant
	JD88 vs JD256	0.0007	Significant
	JD253 vs JD256	0.107	Non-significant
MDA-MB-231	CAM vs JD88	0.0021	Significant
	CAM vs JD253	0.0003	Significant
	CAM vs JD256	0.0001	Significant
	JD88 vs JD253	0.71	Non-significant
	JD88 vs JD256	0.9633	Non-significant
	JD253 vs JD256	0.645	Non-significant
Comparison of IC50 values between MCF-7 and MDA-MB-231 cells			
JD88	MCF-7 vs MDA-MB-231	0.0022	Significant
JD253	MCF-7 vs MDA-MB-231	0.0006	Significant
JD256	MCF-7 vs MDA-MB-231	0.0001	Significant
CAM	MCF-7 vs MDA-MB-231	0.8764	Non-significant

3.3 Morphology of cells exposed to test compounds

3.3.1 Effect of test compounds on MCF-7 cell morphology

3.3.1.1 Effect of test compounds on MCF-7 morphology at concentrations equal to their IC_{50} values

MCF-7 cells were treated with JD88, JD253 and JD256, and the positive control camptothecin. Cells were observed by phase contrast microscopy for morphological changes up to 48 hours of exposure to concentrations of these test compounds equal to their IC_{50} values (0,60 µM, 4 µM, 2,5 µM and 0,30 µM for JD88, JD253, JD256 and camptothecin respectively) and at 25 µM for MCF-7 cells.

There were no significant changes observed in any on the treated cells before 18 hours (**Appendix Figure C7.8**). After 24 hours of exposure to JD88, MCF-7 cells lost their normal cell shape and appeared larger than untreated cells (**Figure 3.7**). After 24 hours of exposure, cells exposed to JD253 had extensive perinuclear vacuole formation (block arrows), which persisted up to 30 hours of exposure (**Figure 3.7**). Untreated cells did not have any perinuclear vacuoles and the cell density after 48 hours was greater than that of cells treated with JD253 (**Figure 3.7**). Cells treated with JD256 displayed a granular appearance at 24 hours of exposure. These cells also had perinuclear vacuoles (block arrows) at 24 and 30 hours of exposure and cells lost normal cell shape after 24 hours of exposure (**Figure 3.7**). Cells treated with the positive control camptothecin surprisingly did not appear affected. The cells did however appear larger than untreated cells (**Figure 3.7**).

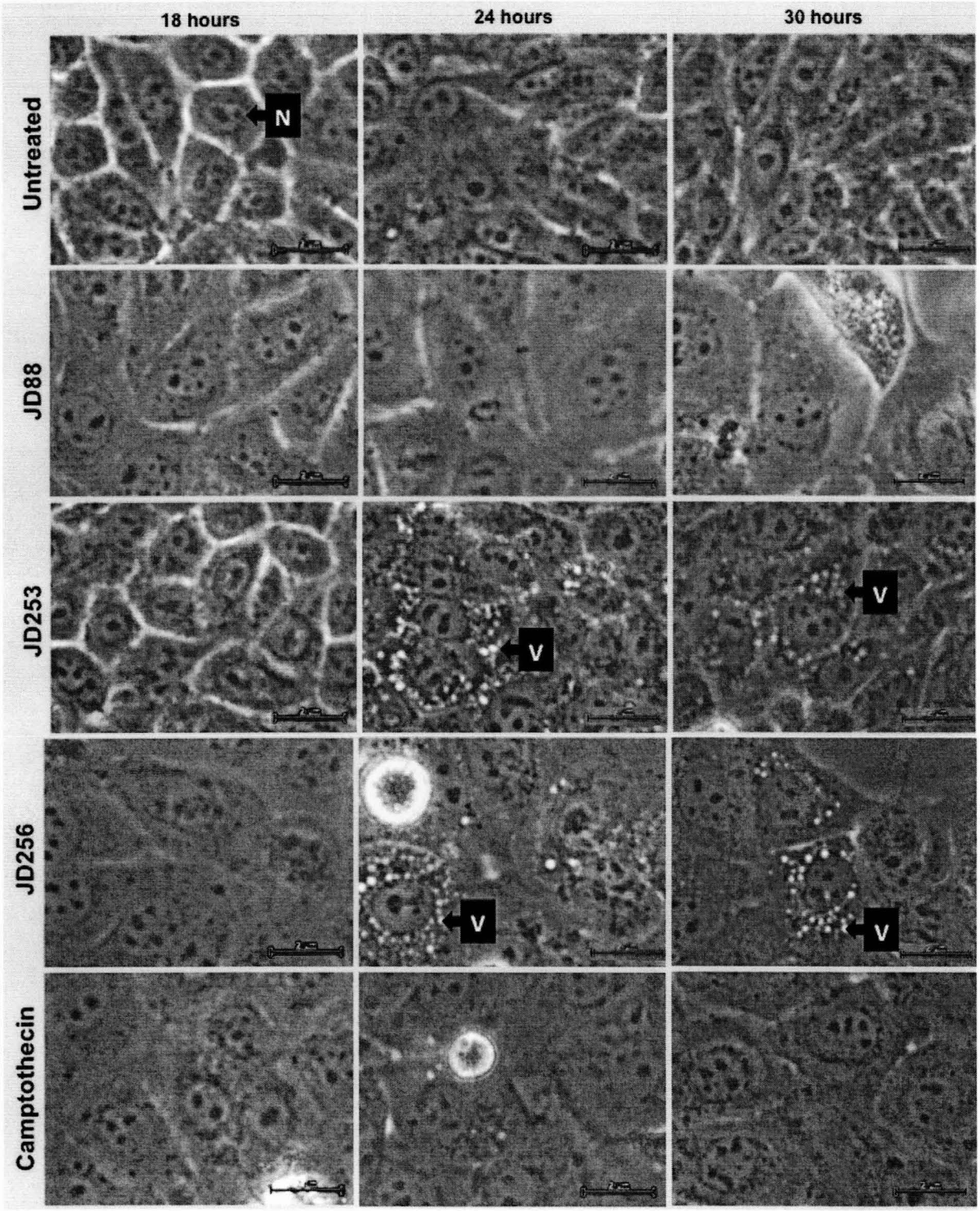


Figure 3.7 Effect of test compounds on MCF-7 cell morphology at IC_{50} values

Untreated cells and cells exposed to 0,60 µM of JD88, cells, 4 µM of JD253, 2.5 µM of JD256 and cells exposed to 0.30 µM of camptothecin. The photographs were taken at 200X magnification and the scale bars represent 50 µM. A Nikon Optiphot light microscope was used. **Key**| N: –Nucleus, V: –Vacuoles

3.3.1.2 Effect of test compounds on MCF-7 morphology at 25 µM

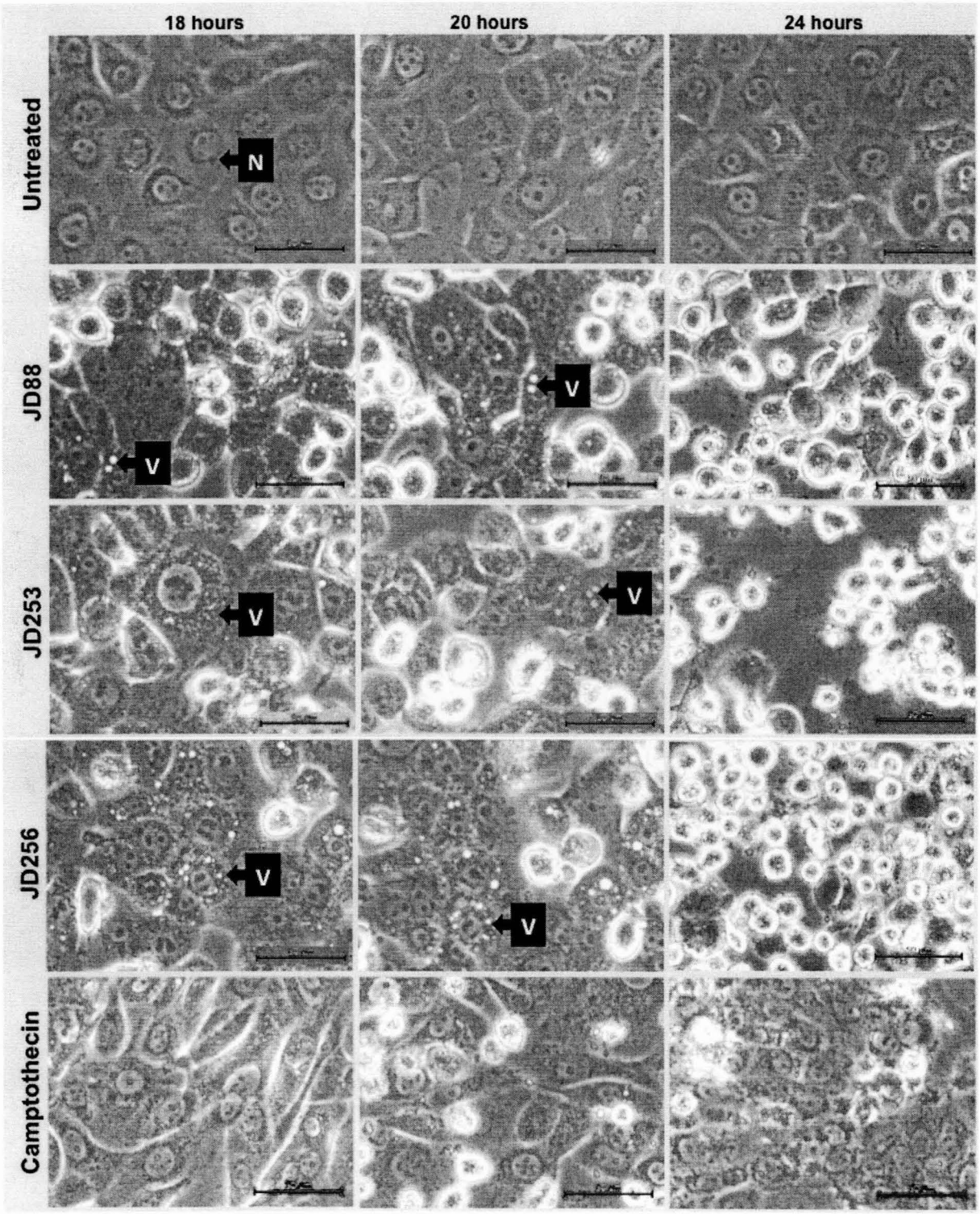


Figure 3.8 Effect of test compounds on MCF-7 cell morphology at 25 µM Untreated cells and cells treated with 25 µM of JD88, JD253, JD256 and the positive control camptothecin. The photographs were taken at 200X magnification and the scale bars represent 50 µM. A Nikon Optiphot light microscope was used. **Key**| N: – Nucleus, V: – Vacuoles

MCF-7 cells exposed to 25 µM of JD88, JD256 and camptothecin did not show any significant changes in morphology until 18 hours of exposure. However, cells exposed to JD256 began to detach from the growth surface and changing shape to become rounded as early as 6 hours after exposure (**Appendix Figure C7.9**).

Cells treated with JD88 changed shape to become rounded 18 hours after exposure while untreated cells did not show any change in shape. These cells also began retracting from the growth surface and formed perinuclear vacuoles after 18 hours of exposure, which persisted until 24 hours of exposure **(Figure 3.8)**.

Cells treated with JD253 and JD256 also showed extensive perinuclear vacuole formation at 18 hours of exposure and this persisted until 20 hours of exposure (block arrows). Cells treated with camptothecin showed a mixture of spindle shaped and round cells at 20 hours of exposure. At 24 hours of exposure, the cells appeared granulated and did not appear to have distinct cell wall boundaries. There was no formation of perinuclear vacuoles but the cells appeared smaller than untreated cells (**Figure 3.8**).

3.3.2 Effect of test compounds on MDA-MB-231 cell morphology

MDA-MB-231 cells were exposed to three test compounds JD88, JD253 and JD256 that had the lowest IC_{50} values and the positive control camptothecin. These cells were exposed to concentrations equal to the IC_{50} values (27 µM, 30 µM, 29 µM and 0,30 µM for JD88, JD253, JD256 and camptothecin respectively) for time periods between 2 hours and 48 hours.

Effects on cell morphology were only visible after 18 hours of exposure to test compounds (**Appendix Figure C7.10**). Cell morphology in cells exposed to JD88 began to change after 18 hours of exposure when cells became amorphous losing their normal spindle shaped appearance. A rounding of the cells at 24 hours of exposure followed this change and cell aggregation was evident from 30 and onwards (**Figure 3.9**). This was in contrast to untreated cells that maintained their normal spindle-like shape and with a few detached cells within the field of view (**Figure 3.9**).

At 24 hours of exposure, JD253 treated cells assumed a round shape and started to adhere to each other, which persisted until 30 hours of exposure (**Figure 3.9**). A significant amount of cellular debris was visible after 48 hours of exposure (block arrows) (**Figure 3.9**). Cells exposed to JD256 did not have normal spindle shape after 18 hours of exposure and did not aggregate like those treated with JD88 and JD253 (**Figure 3.9**). In comparison to the untreated cells exposed to JD256 detached from the growth surface after 24 hours of exposure and cell density was visibly reduced (**Figure 3.9**).

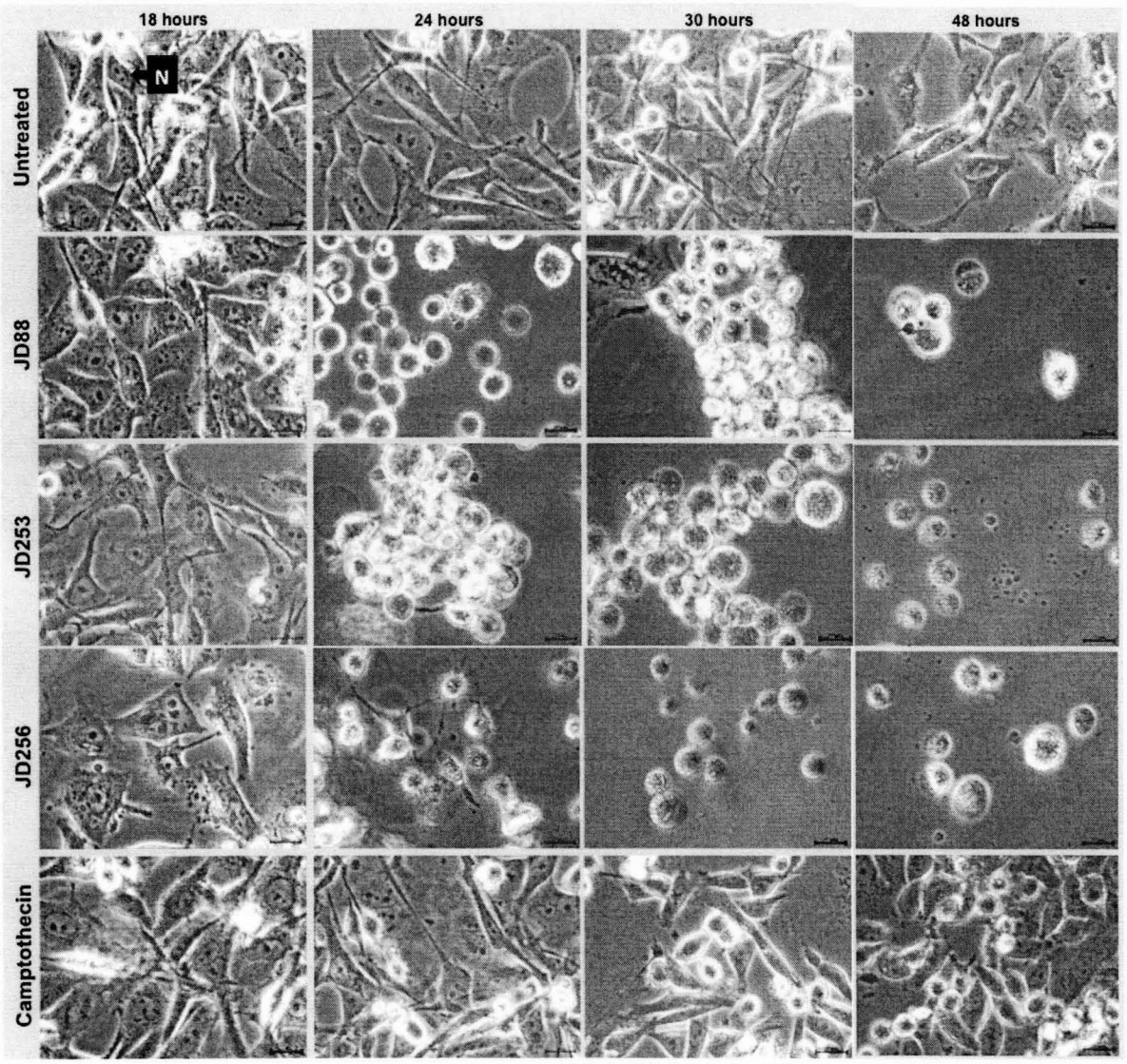


Figure 3.9 Effect of test compounds on MDA-MB-231 cell morphology at IC_{50} values

(A) Untreated cells, (B) cells treated with 27 µM of JD88, (C) cells treated with 30 µM of JD253, (D) cells treated with 29 µM of JD256 and (E) cells treated with 0,30 µM of camptothecin. The photographs were taken at 200X magnification and the scale bars represent 50 µM. A Nikon Optiphot light microscope was used.

Key| N – Nucleus

Cells treated with camptothecin had a similar spindle shaped appearance consistent with untreated cells until 30 hours. However at 48 hrs, they appeared to lose this shape and assumed a round detached morphology. Camptothecin treated cells maintained their normal morphology until 48 hrs of exposure (**Figure 3.9**).

3.3.3 Effect of test compounds on cell and nuclear morphology

A combination of three dyes, acridine orange (AO), ethidium bromide (EB) and Hoechst 33342 (HO) were used to identify specific morphological changes in cells exposed to JD88, JD253, JD256 and the positive control camptothecin. HO stains the nucleus, AO stains both living and dead cells, and EB only stains cells that have lost their cell membrane integrity (Mpoke *et al.*, 1997). The three test compounds JD88, JD253 and JD256 had the lowest IC_{50} values in both MCF-7 and MDA-MB-231 cells and were therefore considered the most active.

3.3.3.1 Effect of test compounds on MCF-7 cell and nuclear morphology

MCF-7 cells exposed to concentrations equal to the IC_{75} values of JD88, JD253 and JD256 as shown in **Figure 3.10** showed changes to nuclear morphology and cell membrane integrity when compared to untreated cells. The main difference observed in cells treated with JD88, JD253 and JD256 compared to untreated cells for 24 hours was an increase in fluorescence intensity of HO dye combined with fragmented nuclei which is indicative of apoptosis.

Cells exposed to JD88, JD253 and JD256 had a higher apoptotic index when compared to untreated cells as shown in **Table 3.3**. The average size of the nuclei of cells exposed to test compounds was smaller than untreated cells while nuclei of cells exposed to camptothecin were larger than those exposed to test compounds (**Table 3.3**). Cells exposed to JD88 were green-yellow in colour when stained with AO-EB and showed fragmented nuclei that fluoresced bright blue when stained with HO. In contrast to the untreated cells, JD88 treated cells began to detach from the growth surface (**Figure 3.10 E-G**). The nuclei of untreated cells also stained blue with HO and green with AO-EB without any associated chromatin condensation (**Figure 3.10 A-C**)

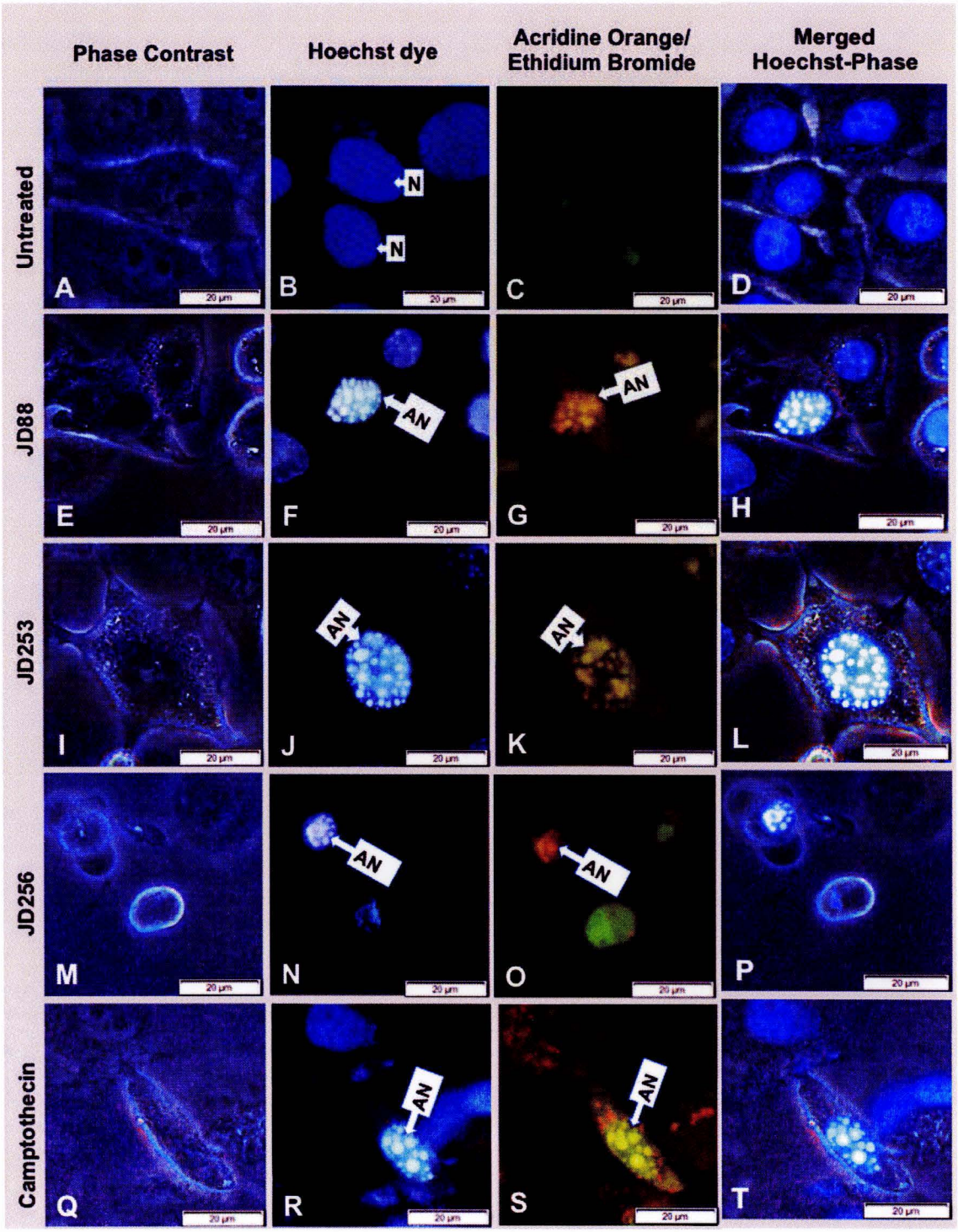


Figure 3.10 Effect of test compounds on cell and nuclear morphology of MCF-7 cells after 24 hours at 400x magnification (A-D) Untreated cells, (E-H) cells treated with JD88 at a concentration of 1.5 µM. (I-L) Cells exposed to 10 µM of JD253, (M-P) 9 µM of JD256 and (Q-T) 0.30 µM of camptothecin. Images are a representative portion of a larger image (**Appendix Figure C7.11**). An Olympus BX41 microscope was used.

Key| N: – nucleus, AN: – apoptotic nucleus

Cells treated with JD253 had the highest apoptotic index of all treated cells as shown in **Table 3.3**. The nuclei of these cells were bright blue and had fragmented nuclei visible when they were stained with HO. The nucleoli of these cells changed to yellow when stained with AO indicating apoptotic changes and these cells were sparsely populated and larger compared to the untreated cells (**Figure 3.10 I-L**, **Figure B7.11**). Untreated cells were densely populated throughout the growth area (**Figure B7.11**).

Cells treated with JD256 began to detach from the growth surface and were round in shape. The nuclei of these cells were fragmented fluorescing bright purple and blue when stained with HO and orange when stained with AO-EB (**Figure 3.10**, **M-P**).

Table 3.3 Effect of test compounds on MCF-7 cell nuclear length and induction of apoptosis and necrosis

	Nuclear size (µm)*					
	0-10	10-15	15-20	>20	Apoptotic Index (Ratio)**	Necrotic Index (Ratio)**
	Number of cells					
Untreated	1	26	23	0	0.02	0.04
JD88	2	23	18	7	0.29	0.03
JD253	1	34	14	1	0.42	0.05
JD256	21	29	0	0	0.30	0.15
Camptothecin	1	7	32	10	0.30	0.08

* Nuclear size is expressed as the length of the nucleus on its longest axis

** The apoptotic/necrotic index is a ratio of apoptotic/necrotic cells against the total number of cells in the field of view

Cells exposed to camptothecin showed signs of cellular stress and extensive nuclear fragmentation, which include extensive granulation and loss of adherence to the growth surface. HO and AO-EB staining revealed fragments within the nuclei that fluoresced bright blue and green respectively (**Figure 3.10**, **R-T**). Cell nuclei were much larger in cells treated with camptothecin (15 – 20 µM) than untreated cells (10 – 15 µM) (**Table 3.3**)

3.3.3.2 Effects on MDA-MB-231 cell and nuclear morphology

MDA-MB-231 cells treated with test compounds JD88, JD253 and JD256 at concentrations equal to their IC_{75} values (44 µM, 37 µM, 37 µM, 9 µM for JD88,

JD253, JD256 and camptothecin respectively) showed differences in cell morphology when compared to untreated cells after 24 hours of exposure.

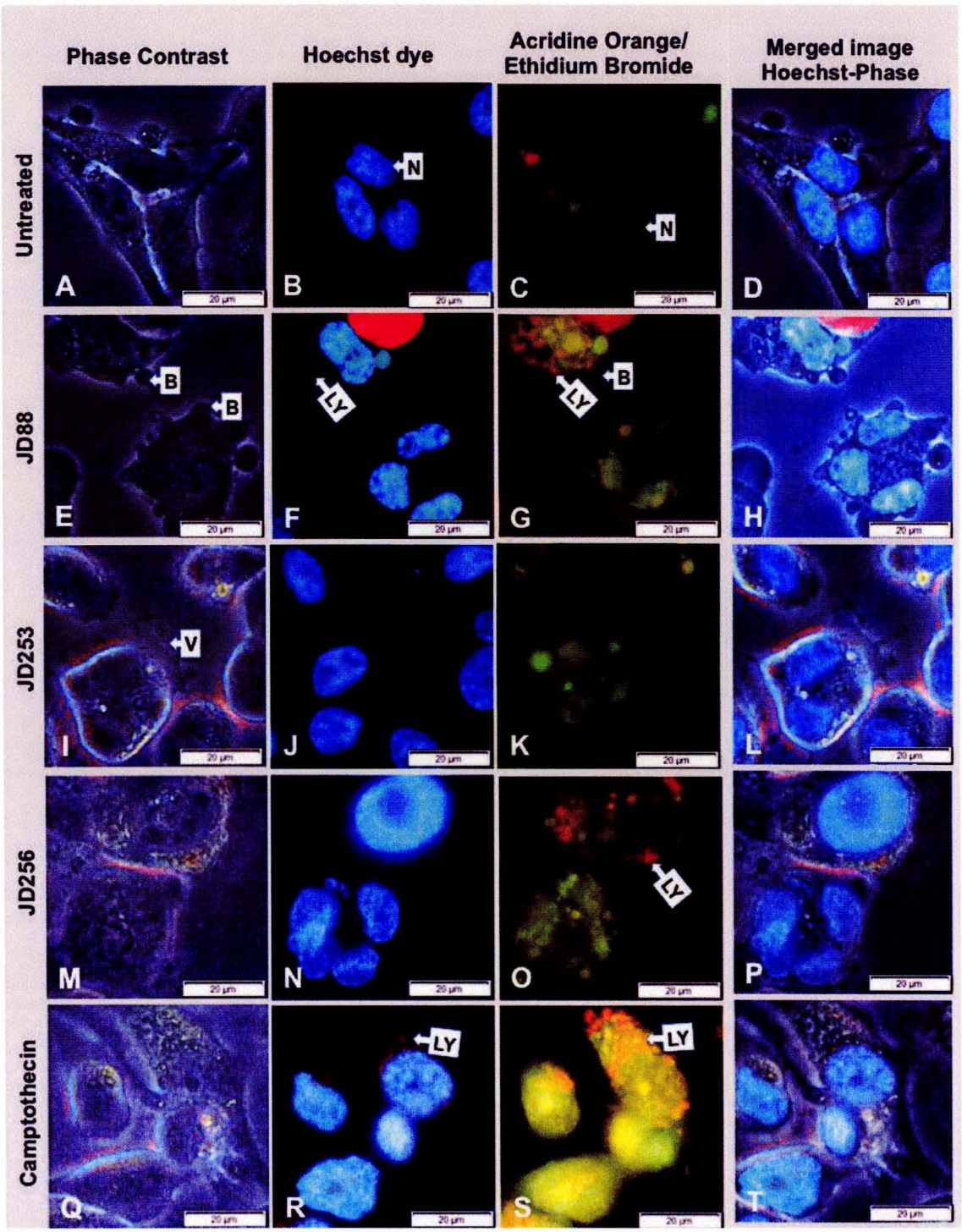


Figure 3.11 Effect of test compounds on cell and nuclear morphology of MDA-MB-231 cells after 24 hours at 400x magnification (A-D) Untreated cells, (E-H) cells exposed to 44 µM of JD88, (I-L) 37 µM of JD253, (M-P) 37 µM of JD256 and (Q-T) 9 µM of camptothecin. Images are a representative portion of a larger image (**Figure B7.12**). An Olympus BX41 microscope was used

Key| N – nucleus, B – blebs, LY – lysosomes, V – vacuoles

Cells exposed to JD88 for 24 hours lost their normal cell shape appearance with no distinct nucleus visible under phase contrast mode. Cells showed multiple irregularly shaped nuclei and membrane blebbing (**Figure 3.11 E**). A large number of counted cells had larger nuclei when compared to nuclei of untreated cells (**Table 3.4**). Cells also had a large number of lysosomes around the nuclei that fluoresced red-orange when stained with AO (**Figure 3.11 E, G**).

There was also the appearance of multiple nuclei in some of the cells and some cells showed signs of nuclei budding (**Figure 3.11 F, H**). In contrast to MCF-7 cells, JD88 induced loss of cell membrane integrity in some MDA-MB-231 cells (**Figure 3.11 F**) a sign of necrosis. This was also observed in counted cells with a necrotic index of 0.27 (**Table 3.4**).

Table 3.4 Effect of test compounds on MDA-MB-231 cell nuclear length and induction of apoptosis and necrosis

	Nuclear size (µM)*					
	0-10	**10-15**	**15-20**	**>20**	**Apoptotic Index (Ratio)****	**Necrotic Index (Ratio)****
	Number of cells					
Untreated	0	29	16	5	0	0.04
JD88	0	11	23	15	0.04	0.27
JD253	0	19	22	8	0	0.14
JD256	0	14	29	6	0	0.16
Camptothecin	1	7	27	14	0	0.02

* Nuclear size is expressed as the length of the nucleus on its longest axis

** The apoptotic/necrotic index is a ratio of apoptotic/necrotic cells against the total number of cells in the field of view

Cells exposed to JD253 had larger nuclei (15 – 20 µM) compared to untreated cells (10 – 15 µM) (**Table 3.4**). Phase contrast images of these cells show vacuole formation on the edge of the cell membrane in some of the cells (**Figure 3.11 I**). These cells were also oval in shape while untreated cells had a normal spindle shape (**Figure 3.11 I, K**). When stained with HO, JD253 treated cells had enlarged nuclei and the nuclei were green when stained with AO-EB. Lysosomes were visible and appeared red-orange when stained with AO (**Figure 3.11 L**).). Despite the difference

in size of the nuclei, cells treated with JD253 did not show any obvious apoptotic features had a necrotic index of 0,14 (**Table 3.4**).

Nuclei of cells treated with JD256 were also much larger than nuclei of untreated cells (**Table 3.4**). The cells also showed perinuclear aggregation of lysosomes that fluoresced red-orange with AO staining. Nuclei fluoresced bright blue when stained with HO (**Figure 3.11 N**, **O**). Some of the cells contained multiple irregularly shaped blue nuclei (**Figure 3.11 F**, **N**) as seen with HO staining. This was confirmed by the merged image, which clearly showed multiple nuclei in within the same cell. JD256 also did not induce any visible apoptotic features in MDA-MB-231 cells.

Cells exposed to camptothecin showed extensive lysosomal aggregation, which appeared red-orange when the cells were stained with AO. Nuclei appeared amorphous as observed with HO staining (**Figure 3.11 R**, **S**). Nuclei of cells treated with camptothecin were larger than untreated cells and no visible features related to apoptosis or necrosis (**Table 3.4**). Most of the cells exposed to camptothecin still had the normal spindle shape and no blebs were observed on their cell surface.

3.4 Identity of vacuoles formed in MCF-7 cells treated with test compounds

Vacuoles were formed as shown in section 3.4.1 when MCF-7 cells were exposed to active test compounds. These cells were therefore exposed to JD88, JD253, JD256 and camptothecin and exposed to monodansylcadaverine (MDC) a non-specific dye that stains autophagic vacuoles fluorescing green. Therefore, untreated and treated cells were exposed to MDC to determine if vacuoles formed were autophagic in nature, a feature of autophagic cell death. The cells were also exposed chloroquine, a known inducer of autophagy, as a positive control for autophagic vacuole formation. Untreated cells did not show formation of vacuoles in phase-contrast images and exposure to MDC showed MDC accumulation around the nuclei of these cells but no vesicles as indicated by the formation of fluorescent clusters. Cells treated with JD88 showed similar morphological features observed in section 3.4.1, which include detachment and the cells assuming a spherical form.

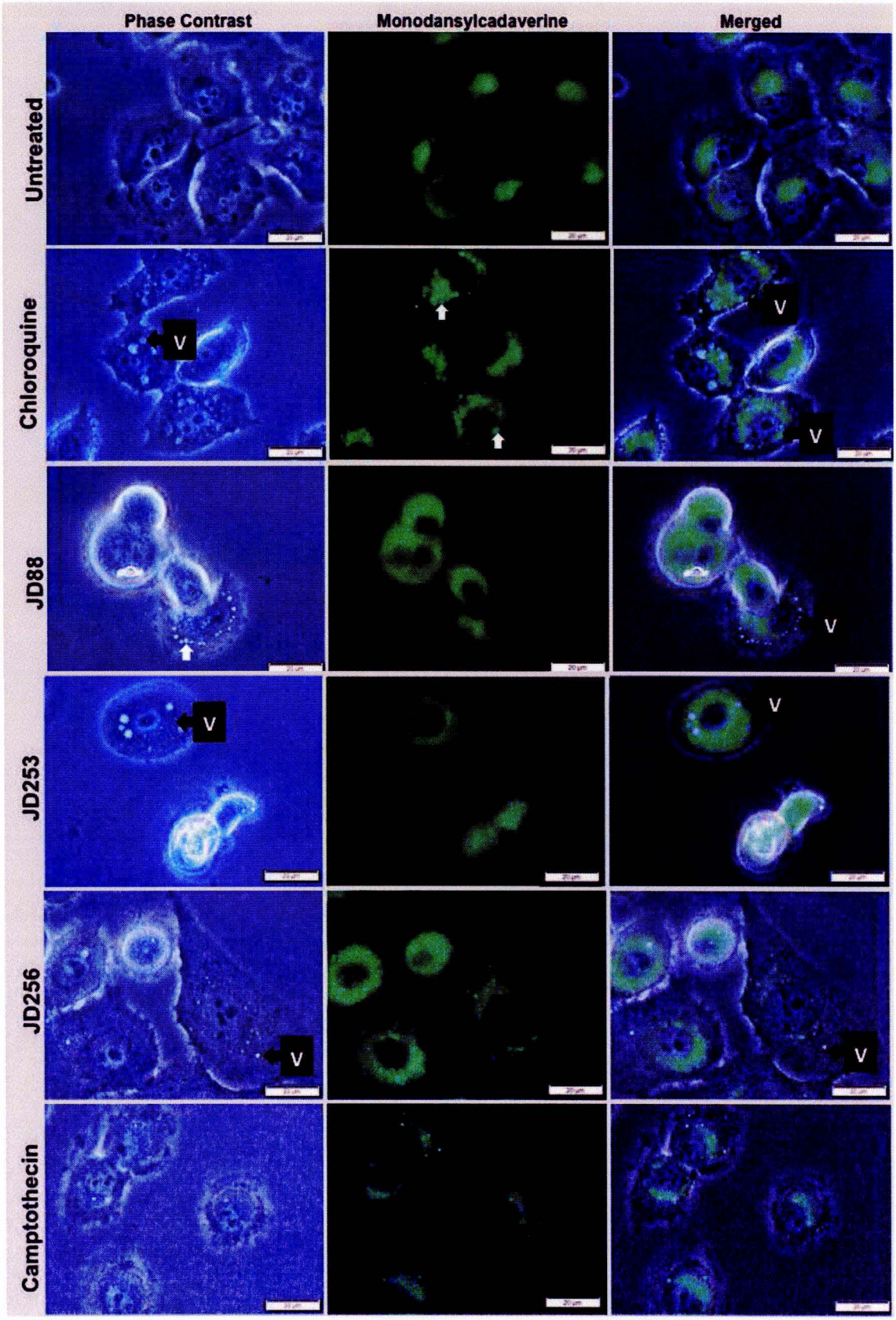


Figure 3.12 Monodansylcadaverine fluorescent clustering in MCF-7 cells treated with test compounds for 20 hours Cells treated with 25 μM of JD88, JD253, JD256 and camptothecin, and 50 μM of chloroquine were compared to untreated cells. Cells were then exposed to with monodansylcadaverine (MDC) and viewed at 400X magnification. Scale bar is equal to 20 μm. An Olympus BX41 microscope was used.

Key| V: - vacuole

These cells showed vacuolation in phase contrast images. These vacuoles did not co-localise with MDC fluorescent clusters as these vacuoles formed dark spots with MDC staining and the merged images confirm this with no green fluorescence within these vacuoles (black arrow) (**Figure 3.12**). JD253 induced perinuclear vacuolation in MCF-7 cells that were located around the nuclei of cells. These vacuoles also appeared as dark spots when stained with MDC and viewed under UV illumination. These vacuoles did not co-localise with MDC fluorescent clusters that were spread around the nucleus of these cells (white arrows). Cells exposed to JD256 also had vacuole formation within the cytoplasm and these vacuoles did not co-localise with MDC fluorescent clusters forming dark patches (white arrows) (**Figure 3.12**).

Camptothecin did not show any formation of vacuoles in phase contrast images and MDC staining did not show any autophagic vacuole formation in these cells. Chloroquine induced formation of vacuoles within the cytoplasm that could be observed under phase-contrast imaging. These vacuoles however formed dark spots when stained with MDC and did not co-localise with MDC staining when images merged (white arrows). However chloroquine induced the formation of vesicle-like fluorescent clusters that fluoresced after exposure to MDC and these clusters did not co-localise with vacuoles observed in phase-contrast images (white arrows) (**Figure 3.12**).

3.5 Effect on test compounds on biochemical markers

3.5.1 Effect of test compounds on caspase-3/7 activity

3.5.1.1 Caspase-3/7 activity in MCF-7 cells

MCF-7 cells were exposed to JD88, JD253 and JD256, the three most active test compounds according to their IC_{50} values, and the positive control camptothecin. The cells were exposed to the test compounds at concentrations equal to their IC_{75} values of 1.5 µM, 10 µM, 9 µM and 9 µM for JD88, JD253, JD256 and camptothecin respectively over a range of time periods between 2 and 30 hours. The protein content of each lysate as measured by the Bradford protein assay was used to determine the specific caspase-3/7 activity per microgram of protein.

Cells that were exposed to JD88 showed peak caspase-3/7 activity after two hours of exposure. Caspase-3/7 activity thereafter decreased to levels observed in untreated

cells (**Figure 3.13**). Caspase-3/7 activity of cells treated with the positive control camptothecin also peaked after two hours of exposure. The peak activity for cells exposed to camptothecin was marginally higher than peak activity observed in cells treated with JD88. Cells treated with JD253 and JD256 did show caspase-3/7 activity comparable to that of untreated cells (**Figure 3.13**).

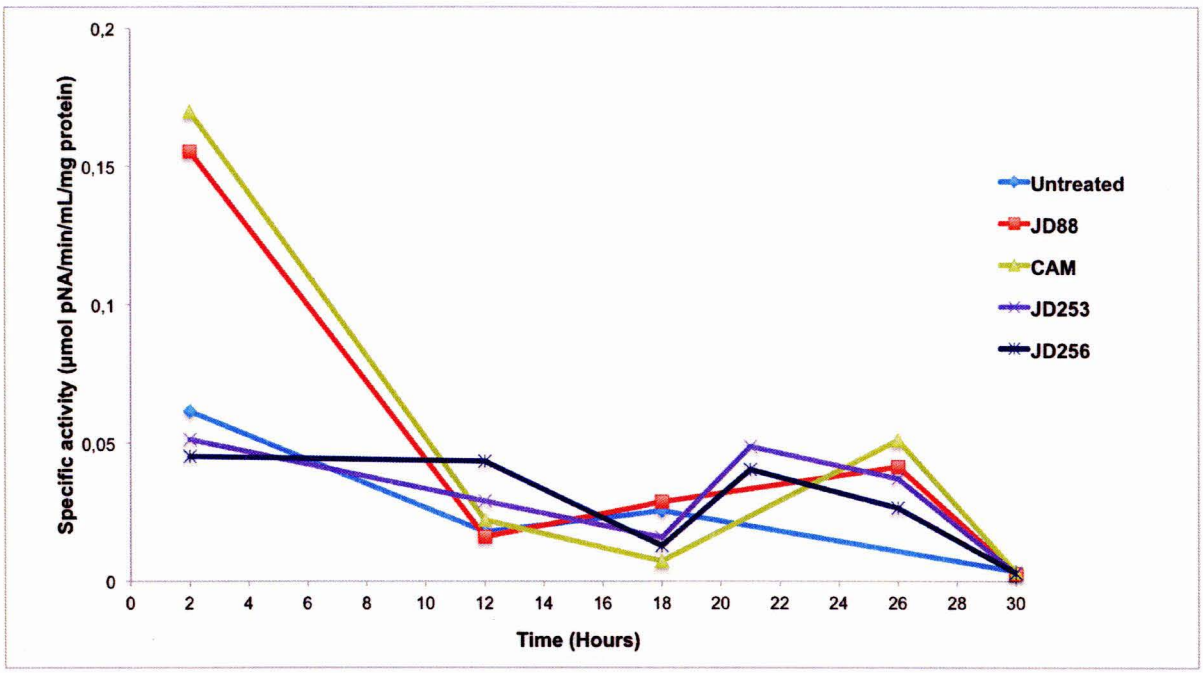


Figure 3.13 The effect of test compounds on caspase-3/7 activity in MCF-7 cells at various exposure times Each data point represents the specific caspase activity at that time point. Cells were exposed to concentrations of 1.5 µM, 10 µM, 9 µM and 9 µM of JD88, JD253, JD256 and camptothecin (CAM) respectively. Cells were exposed for up to 30 hours.

3.5.1.2 Caspase-3/7 activity in MDA-MB-231 cells

MDA-MB-231 cells were exposed to JD88 and the positive control camptothecin, as they were the most active compounds according to their IC_{50} values. Cells were exposed to these compounds at 44 µM and 9 µM for JD88 and camptothecin (CAM) respectively, for various time periods between 2 hours and 30 hours (**Figure 3.14**). The protein concentration of each lysate was determined by the Bradford assay and used to calculate the specific caspase-3/7 activity per microgram of protein.

Cells exposed to JD88 and camptothecin showed an increase in caspase activity at 2 hours after exposure compared to the control, which then declined to levels similar to the control cells at 6 hours (**Figure 3.14**). Although the pattern of caspase-3/7 activity

in JD88 and camptothecin mirrored each other, JD88 induced less activity of caspase-3/7 in MDA-MB-231 cells than camptothecin after two hours.

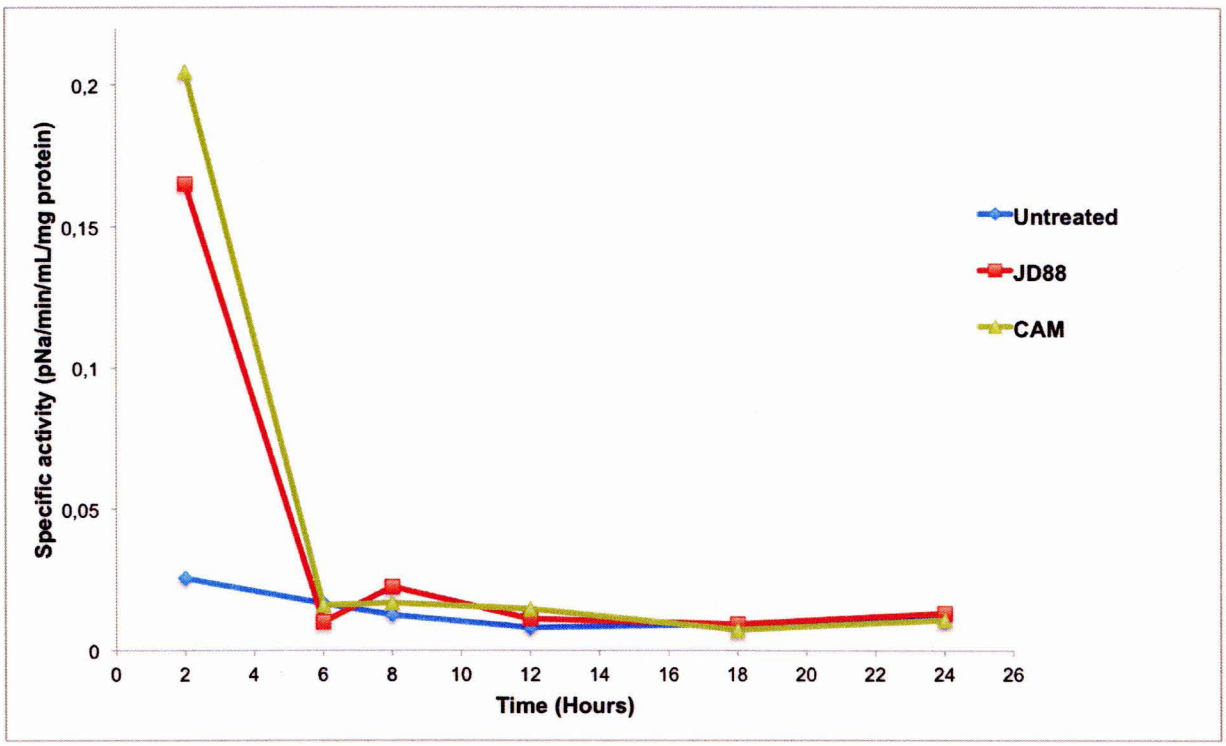


Figure 3.14 The effect of test compounds on caspase-3/7 activity in MDA-MB231 cells at various exposure times Each data point represents the specific caspase activity at that time point. Cells were exposed to concentrations of 44 µM and 9 µM of JD88 and camptothecin (CAM) respectively for up to 24 hours.

3.5.2 Exposure of phosphatidylserine on the surface of the cell membrane

Breast cancer cells grown on coverslips were exposed to test compounds JD88, JD253 and JD256 at concentrations equal to their IC_{75} value for 24 hours. These cells were exposed to fluorescein isothiocyanate (FITC) conjugated to Annexin-V. The exposure of phosphatidyl serine on the cell membrane is an early apoptotic feature. FITC conjugated to Annexin V binds to phosphatidylserine and bound FITC-Annexin V stains the cell membrane green. Cells exposed to active test compounds were counter stained with propidium iodide (PI), and PI stains nuclei of cell that have lost their cell membrane integrity red-orange (Galluzzi *et al.*, 2012; Kerr *et al.*, 1972). These experiments were conducted at least three times.

3.5.2.1 Exposure of phosphatidylserine on the cell membrane of MCF-7 cells

Some of the cells exposed to active test compounds JD256 and JD253 for 24 hours fluoresced green while cells treated with the positive control camptothecin and JD88

fluoresced green after 18 hours of exposure. This was indicative of exposure of phosphatidylserine to the surface of the cell membrane a feature of apoptosis.

Cells treated with JD88 were round in shape and sparsely populated on the growth surface when compared to untreated cells. Annexin-V conjugated with FITC was able to bind to the surface of these cells and fluoresced green in the 90.9% of cells (**Table 3.5**). The location of the Annexin-V FITC on the surface of the cell membrane was confirmed by a merged image of the phase contrast and fluorescent image (**Figure 3.15**). Green fluorescence on the surface of the cell membrane was observed in a small population of cells treated with JD253 (**Table 3.5**) after 24 hours and these cells were sparsely populated (**Figure 3.15**). Cells treated with JD256 for 24 hours were round in shape compared to untreated cells and 4.8% of the cells had Annexin-V FITC green fluorescence on the surface of the cell membrane (**Table 3.5**) (**Figure 3.15**). Cells exposed to camptothecin for 18 hours showed similar results to those exposed to JD253 and JD256. The cells were sparsely populated and only one cell fluoresced green on the surface of the cell membrane. However, the cells had a similar cell shape to untreated cells (**Figure 3.15**).

Table 3.5 The effect of test compounds on phosphatidylserine exposure in MCF-7 cells (IC_{75} value)

	% FITC-PS Positive Cells*	% PI Positive Cells*
Untreated	0	0
JD88	90.9	0
JD253	9.1	0
JD256	4.8	0
Camptothecin	21.4	0

* The percentage is the ratio of the cells fluorescing positive for FITC-PS or PI against the total cell population in the field of view

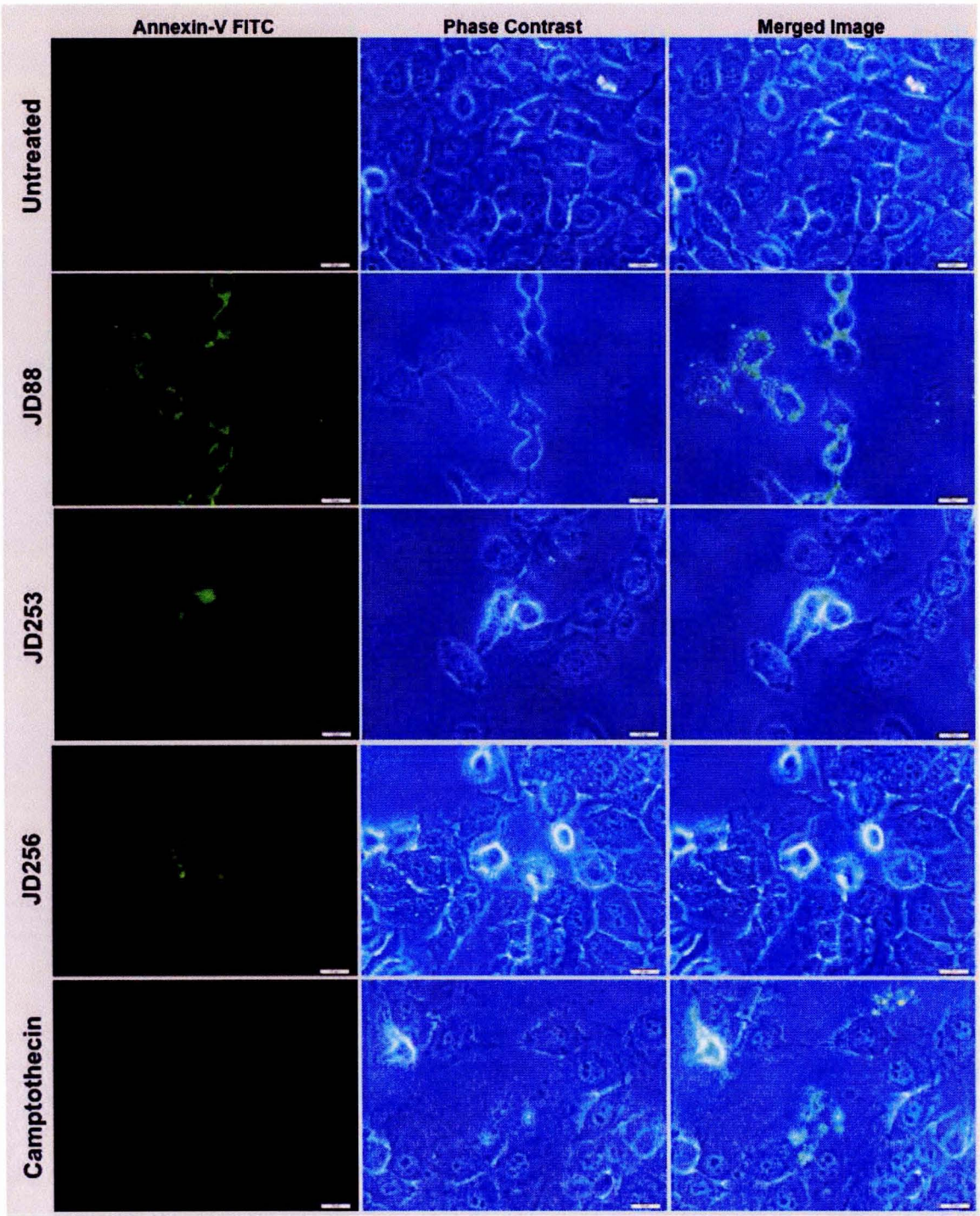


Figure 3.15 The effect of test compounds on phosphatidylserine exposure in MCF-7 cells at 400X magnification Untreated cells and cells exposed to 1.5 µM JD88 for 18 hours, 10 µM of JD253 for 24 hours, 9 µM of JD256 for 24 hours and 9 µM of the positive control camptothecin for 18 hours. The scale bar represents 20 µm. An Olympus BX41 microscope was used.

3.5.2.2 Exposure of phosphatidylserine on the cell membrane of MDA-MB-231 cells

Cells exposed for 27 hours showed varied responses to active test compounds. Cells treated with JD88 fluoresced green when due to the binding of FITC conjugated

Annexin V. This fluorescence was also observed in cells treated with JD253, JD256 and the positive control camptothecin (**Table 3.6**).

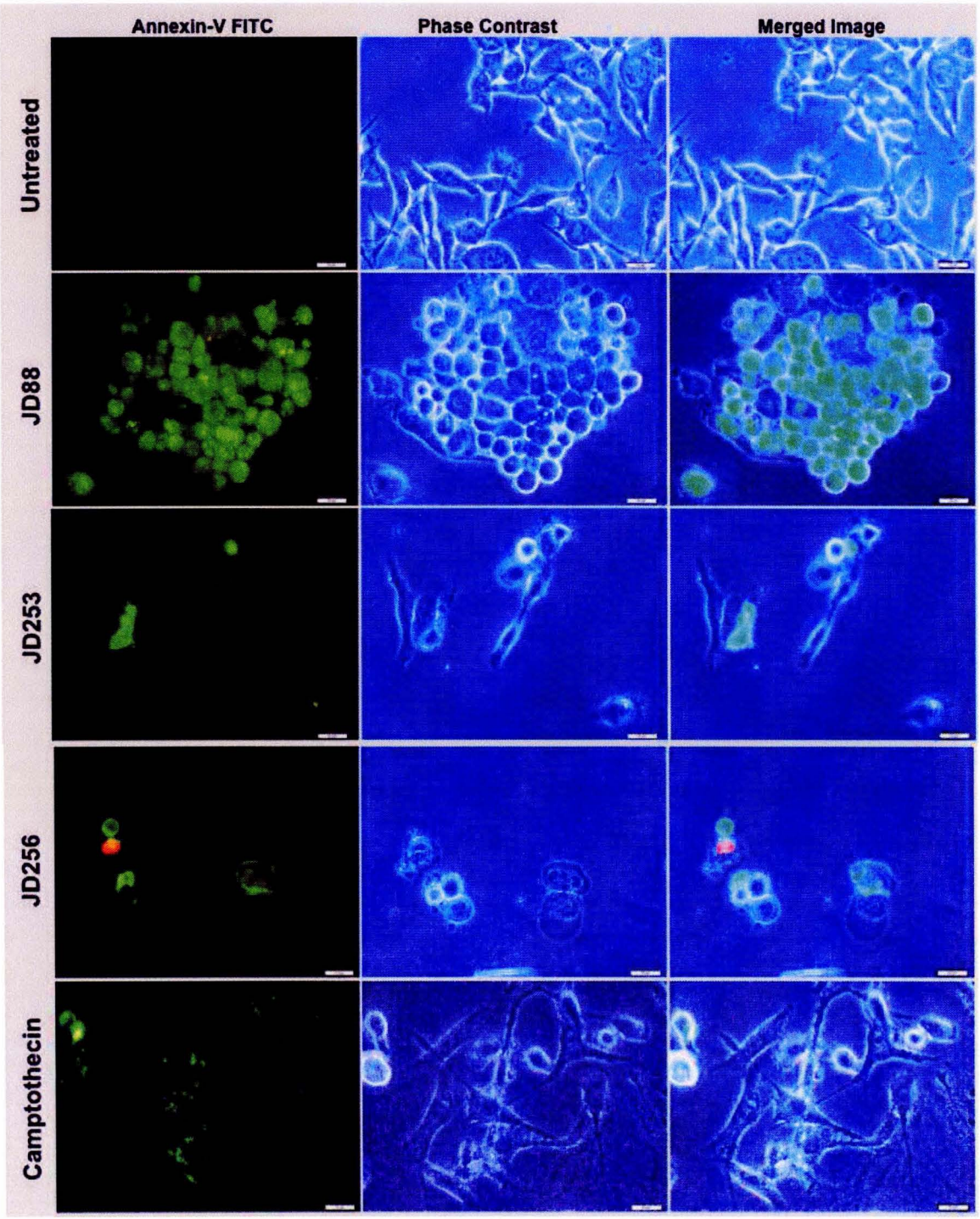


Figure 3.16 The effect of test compounds on phosphatidylserine exposure in MDA-MB-231 cells at 400X magnification Untreated cells, cells treated with 44 µM of JD88, 37 µM of JD253, 37 µM of JD256 and 9 µM of the positive control camptothecin. An Olympus BX41 microscope was used.

Cells treated with JD88 also showed some blebbing and a granular appearance on the surface of the cells. This granular appearance was also observed on the surface of cells treated with JD253 and JD256. The nuclei of cells that were exposed to JD256 fluoresced orange showing the entry of PI through the cell membrane an indication of late apoptosis or necrosis (**Figure 3.16**).

Table 3.6 The effect of test compounds on phosphatidylserine exposure in MDA-MB-231 cells (IC_{75} value)

	% FITC-PS Positive Cells*	% PI Positive Cells*
Untreated	0	0
JD88	88.3	17,4
JD253	40,5	0
JD256	33,3	16,7
Camptothecin	50,6	0

* The percentage is the ratio of the cells fluorescing positive for FITC-PS or PI against the total cell population in the field of view

3.5.3 Effect of active test compounds on the cytoskeleton of MCF-7 cells

MCF-7 and MDA-MB-231 cells exposed to 1.5 µM of JD88, 9 µM of JD253 and JD256, and camptothecin respectively were stained with phalloidin conjugated with FITC and viewed under a fluorescent microscope. Phalloidin binds to the cytoskeletal protein F-actin of cells and when conjugated to FITC is used to visualize the cytoskeleton. The cells were also counter stained with Hoechst, in order to visualize the nucleus.

Untreated MCF-7 cells fluoresced green and blue, highlighting their nucleus and cytoskeleton. F-actin fibres of untreated cells showed connections to neighbouring cells forming a dense green cell-cell junction. When cells were treated with JD88 there was increased fluorescence showing condensation of the actin because the cells became round and began to lose attachment to the growth surface (white arrows). The cells also had a dense population of F-actin fibres on the surface of the cell. Some cells had retracted from other cells and these had F-actin fibres densely populated around the cell surface (white arrows). There was an increase in fluorescence as the cells began to detach from the growth surface (**Figure 3.17**).

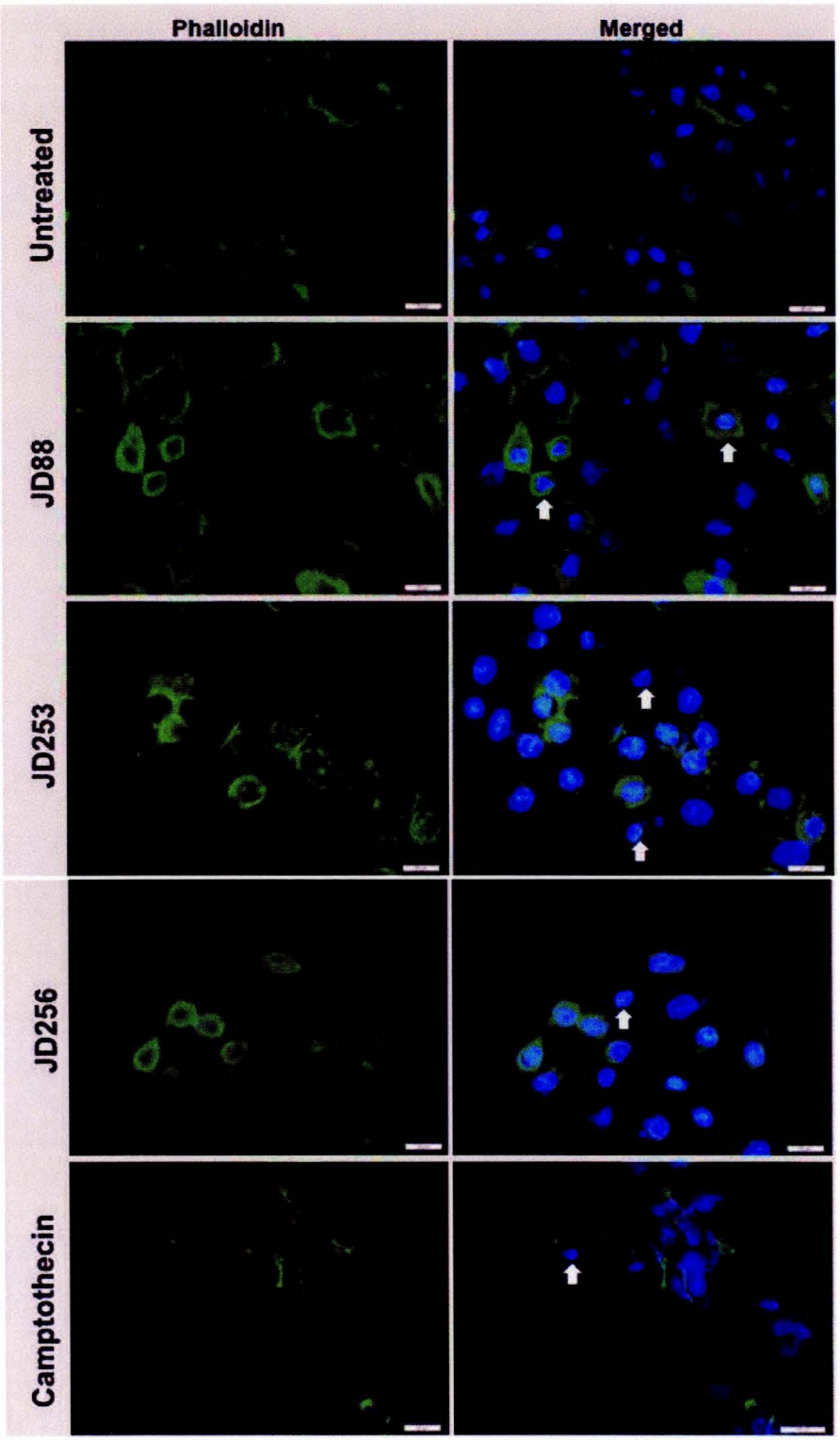


Figure 3.17 Effect of test compounds on the cytoskeleton of MCF-7 cells at 24 hours of exposure Cells were treated with 1.5 µM of JD88, 9 µM of JD253, JD256 and camptothecin and compared to an untreated control. The cytoskeleton was visualized with FITC conjugated phalloidin and the nuclei counterstained with Hoechst 33342. The images were taken at 400X magnification and the scale bar represents 20 µm. An Olympus BX41 microscope was used.

Cells exposed to JD253 also became round and had shortened cytoskeletal fibres. Only one cell that had fragmented nuclei did not show any F-actin fibres in their cytoskeleton, as it did not have any green fluorescence (white arrows). Cells that were treated with JD256 had almost no visible intercellular connections. These cells also had shortened cytoskeletal fibres that were densely populated around the nucleus. Cells with fragmented nuclei did not fluoresce green indicating a loss of F-actin (white arrow) (**Figure 3.17**).

Cells treated with camptothecin formed clusters and also had shortened cytoskeletal fibres similar to those observed in cell treated with JD253. Cells with fragmented nuclei did not show any F-actin (white arrow). The cytoskeleton was not densely packed around the nucleus (**Figure 3.17**).

3.5.4 Effect of test compounds on mitochondrial integrity in MCF-7 cells

MCF-7 cells were treated to three active test compounds JD88, JD253 and JD256 at concentrations equal to their IC_{75} values (1.5 µM, 9 µM and 9 µM respectively) for 24 hours. The cells were also treated to the positive control camptothecin for 24 hours at a concentration of 9 µM (IC_{75} value). A loss of mitochondrial membrane integrity during the process of apoptosis through the mitochondrial pathway results in the release of cytochrome c (Ouyang *et al.*, 2012). Therefore by measuring the amount of cytochrome c in the cytoplasm and mitochondria, it can be determined if cytochrome c is released into the cytoplasm. The concentration of cytochrome c was presented as a proportion of the protein content. The MCF-7 cell line was chosen because it showed greater sensitivity to these three active test compounds than MDA-MB-231 cells.

MCF-7 cells treated with 1,5 µM of JD88 showed cytochrome c in the mitochondria and an undetectable amount in the cytoplasm. This pattern was also seen in the other two active compounds JD253 (10 µM) and JD256 (9 µM). The positive control camptothecin didn't show any release of cytochrome c in the cytoplasm and untreated cells did not show any release of cytochrome c in the cytoplasm (**Figure 3.18**).

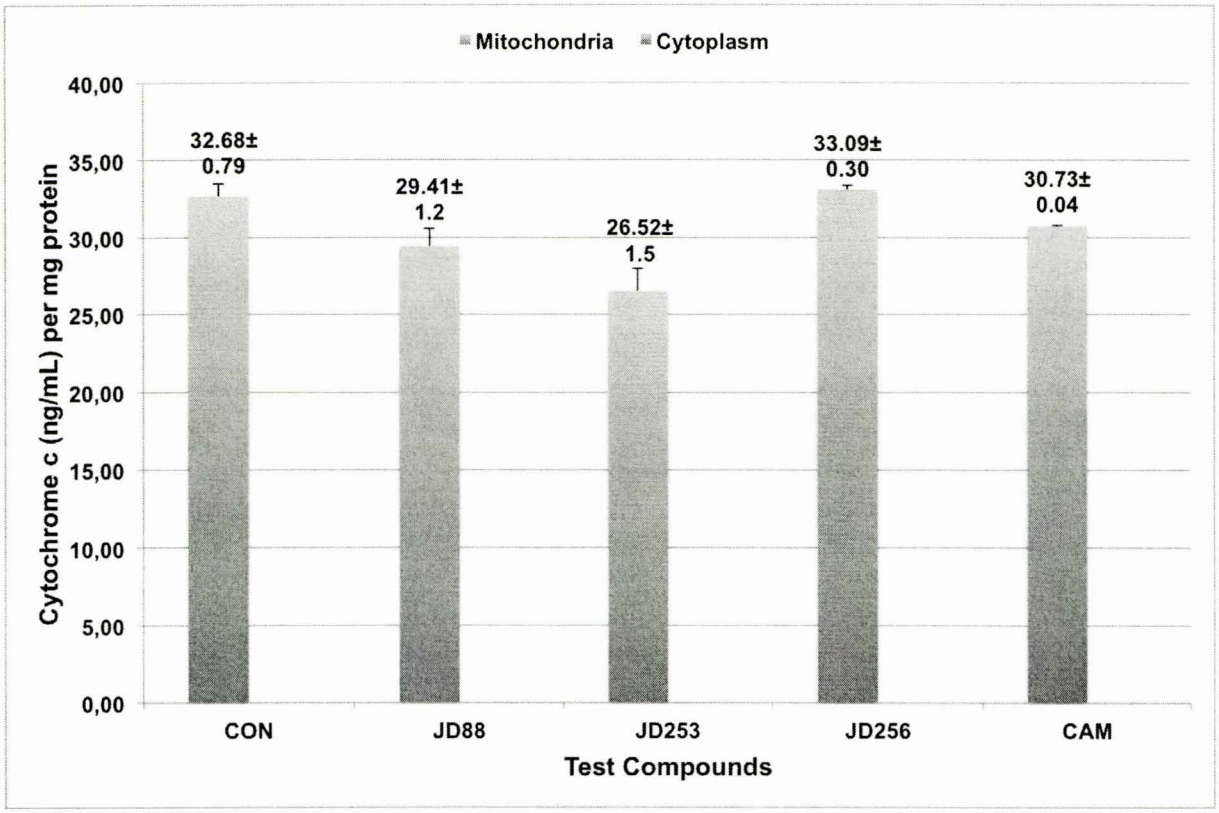


Figure 3.18 The effect of test compounds on the translocation of cytochrome c to the cytoplasm in MCF-7 cells Cell were treated with 1.5 µM of JD88, 9 µM of JD253, 9 µM of JD256 and 9 µM of camptothecin (CAM). CON is representative of untreated cells. Each bar represents the mean of at most three independent experiments and each error bar represents the standard error of the mean (SEM)

3.6 Effect of copper containing imidazo[1,2-a]pyridine analogues on MCF-7 and MDA-MB-231 cells

3.6.1 Effect of copper containing imidazo[1,2-a]pyridine amine analogues on cell viability

Towards the end of this study, additional compounds based on the structure of JD88 became available for evaluation on cell growth. These new copper containing compounds were tested against MCF-7 and MDA-MB-231 cells to evaluate their effect on cell viability using the MTT assay. IC_{50} values were determined for most of the active test compounds. These were the only tests conducted using these additional compounds as the compounds were only developed at the later stages of this study. The results are included in this dissertation in order to conduct a qualitative structure activity analysis.

A total of 10 compounds were assessed on MCF-7 and MDA-MB-231 cells at a concentration of 100 µM and of these, seven reduced cell growth by over 95%. These seven compounds were then tested to determine their IC_{50} values against MCF-7 and MDA-MB-231 cells as shown in **Figure 3.19** and **Figure 3.20**.

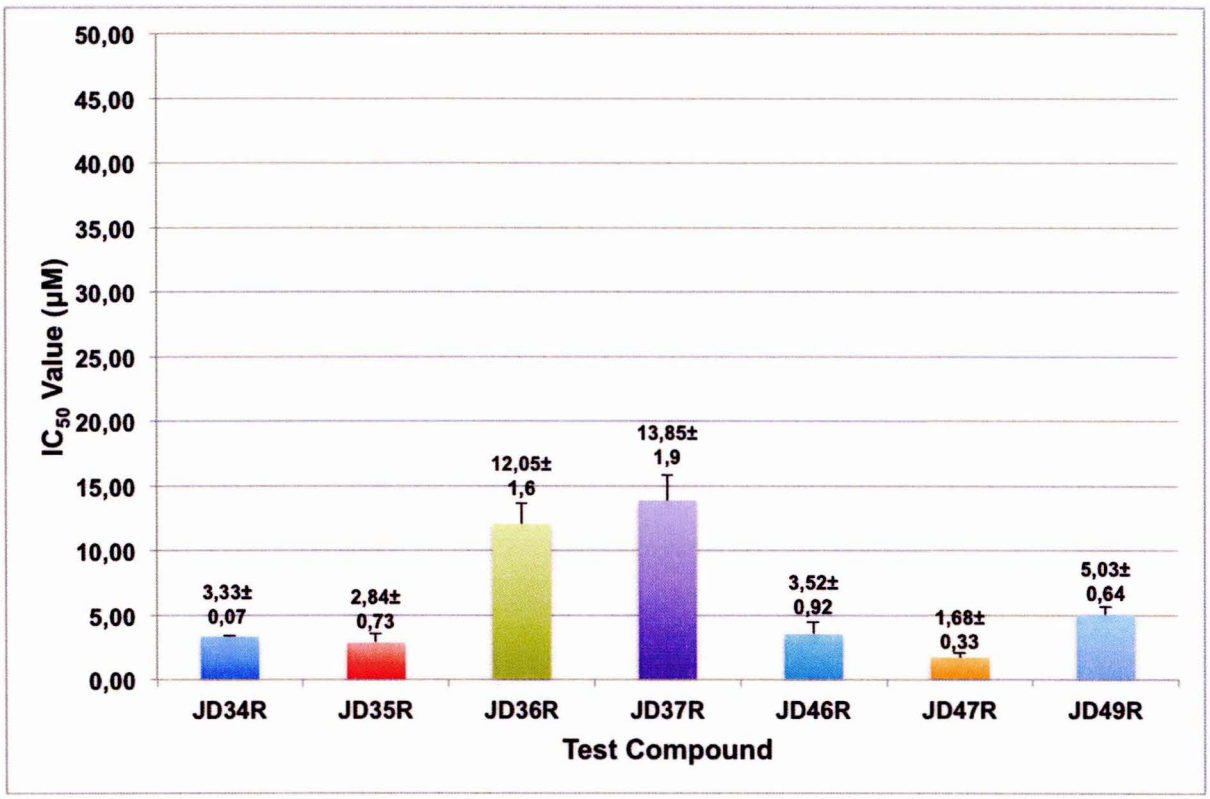


Figure 3.19 Summary of IC_{50} values of copper containing compounds against MCF-7 Cells were treated over a range of concentrations (0.001 µM – 100 µM) for 48 hours. Each bar represents the mean of at least three independent experiments and the error bars represent the standard error of the mean

The IC_{50} values of JD34R, JD35R, JD46R and JD47R against MCF-7 cells were lower than 5.5 µM of 3.33±0.07 µM, 2.84±0.73 µM, 3.52±0.92 µM, 1.68±0.33 µM and 5.03±0.64 µM respectively. JD37R had the highest IC50 value of 13.85±1.98 µM while JD36R and JD49R had IC_{50} values of 12.05±1.62 µM.

Seven test compounds were identified as active against MDA-MB-231 cells. The active test compounds were JD34R, JD35R, JD36R, JD46R, JD47R and JD49R. JD47R had the lowest IC_{50} value against MDA-MB-231 cells at 2.35±0.12 µM. JD46R was the other test compound that had an IC_{50} values lower than 5 µM of 3.40±0.94 µM. JD34R, JD35R and JD36R had IC_{50} values lower than 15 µM at 13.04±1.82 µM,

18.85±0.90 μM and 14.61±1.23 μM respectively. JD37R had the highest IC_{50} value against MDA-MB-231 cells at 32.81±1.15 μM (**Figure 3.20**).

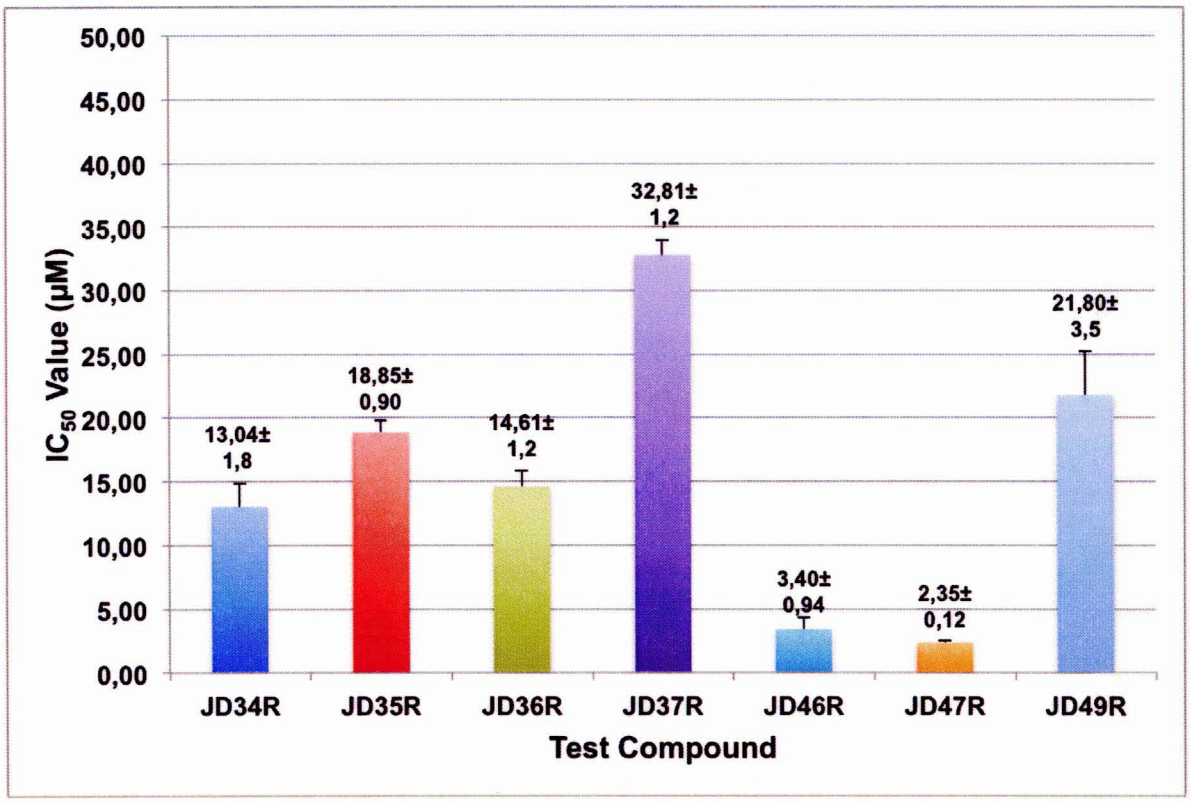


Figure 3.20 IC_{50} values of copper containing compounds against MDA-MB-231 Cells were treated over a range of concentrations (0.001 μM – 100 μM) for 48 hours. Each bar represents the mean of at least three independent experiments and the error bars represent the standard error of the mean

Table 3.7 Statistical significance of effect of imidazo[1,2-a]pyridine amine analogues in MCF-7 cells

Common Variable	Test Variables	p-value	Significance (p<0,05)
MCF-7	CAM vs JD34R	<0.0001	Significant
	CAM vs JD35R	0.0053	Significant
	CAM vs JD36R	0.0017	Significant
	CAM vs JD37R	<0.0001	Significant
	CAM vs JD46R	0.0038	Significant
	CAM vs JD47R	0.0066	Significant
	CAM vs JD49R	0.0002	Significant

Statistical analysis between the effect of analogues of imidazo[1,2-a]pyridine amines and camptothecin showed that camptothecin was significantly more active in MCF-7 and MDA-MB-231 cells than the analogues (**Table 3.7** and **Table 3.8**). Analogues of imidazo[1,2-a]pyridine amines were significantly active against MCF-7 cells than in MDA-MB-231 cells apart from JD36R, JD46R and 47R which showed no significantly different activity between the two cell lines.

Table 3.8 Statistical significance of effect of imidazo[1,2-a]pyridine amine analogues in MDA-MB-231 cells

MDA-MB-231	CAM vs JD34R	<0.0001	Significant
	CAM vs JD35R	<0.0001	Significant
	CAM vs JD36R	<0.0001	Significant
	CAM vs JD37R	<0.0001	Significant
	CAM vs JD46R	0.0016	Significant
	CAM vs JD47R	0.0002	Significant
	CAM vs JD49R	0.0008	Significant
Comparison of IC_{50} values between MCF-7 and MDA-MB-231 cells			
JD34R	MCF-7 vs MDA-MB-231	<0.0001	Significant
JD35R	MCF-7 vs MDA-MB-231	0.0001	Significant
JD36R	MCF-7 vs MDA-MB-231	0.1867	Non-significant
JD37R	MCF-7 vs MDA-MB-231	<0.0001	Significant
JD46R	MCF-7 vs MDA-MB-231	0.4899	Non-significant
JD47R	MCF-7 vs MDA-MB-231	0.1773	Non-significant
JD49R	MCF-7 vs MDA-MB-231	0.0030	Significant

3.6.2 Structural activity relationships (SARs) of imidazo[1,2-a]pyridine amines

The test compounds were based was an imidazo[1,2-a] pyridine amine scaffold and various substituent groups were added to this scaffold in order to generate the different test compounds. To assess the effect of the substituents on biological activity, a qualitative structure activity analysis was conducted comparing both active and inactive compounds with similar structures. Results and observations are outlined in **Table 3.7** and **Table 3.8**. The test compounds were compared according to their basic scaffold and similar substitution points.

Table 3.9 Comparison of base structure and structures containing transition metal complexes

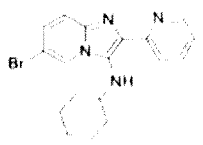
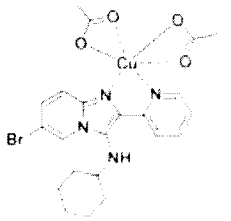
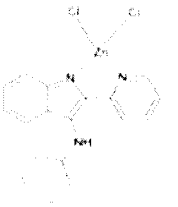
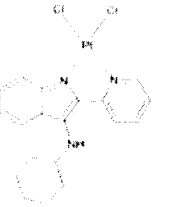
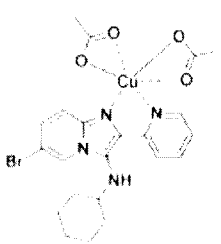
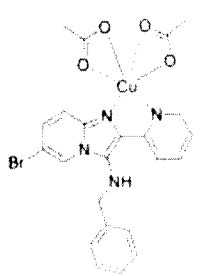
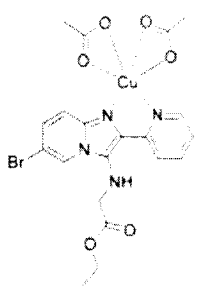
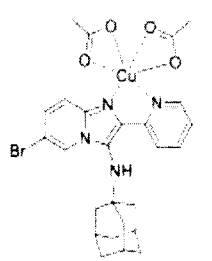
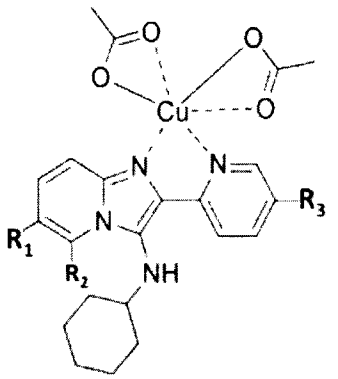
	JD60	**JD88**	**JD142**	**JDPtCl$_2$**
				
MCF-7	35.42±0.44 μM	0.62±0.03 μM	inactive	inactive
MDA-MB-231	inactive	27.88±2.12 μM		39.67±1.37 μM
Comments	• Addition of a copper complex increases activity against not MCF-7 and MDA-MB-231. • Addition of a platinum complex reduces activity against MCF-7 cells but increases activity against MDA-MB-231 cells. • The imidazo[1,2-a]pyridine amine base structure is inactive against MDA-MB-231 cells. • Addition of a zinc chloride complex reduces activity against both MCF-7 and MDA-MB-231 cells.			

Table 3.10 Comparison of copper containing structures and substitutions on the amidogen group

	JD88	**JD253**	**JD256**	**JD258**
				
MCF-7	0.62±0.03 μM	3.66±0.49 μM	2.23±0.10 μM	insoluble
MDA-MB-231	27.88±2.12 μM	29.76±1.72 μM	28.82±1.35 μM	
Comments	• Addition of a cyclohexane to the amidogen group significantly increase activity against MCF-7 cells but has not significant difference against MDA-MB-231 cells. • Addition of an amantadine group to the amidogen group makes the compounds insoluble in aqueous solution.			

Several analogues that contain copper complexes were synthesised and an analysis was performed to determine the effect on activity of different substitutions when compared to our active compounds JD88, JD253 and JD256.

Table 3.11 Structure activity relationships of imidazo[1,2-a]pyridine amines and analogues



	R_1	R_2	R_3	MCF-7 IC_{50} value (μM)	MDA-MB-231 IC_{50} value (μM)
JD88	Br	—	—	0.62±0.03	27.88±2.12
JD36R	—	—	Cl	12.05±1.57	14.61±1.23
JD37R	—	—	Br	13.85±1.97	32.81±1.15
JD46R	—	—	—	3.52±0.92	3.40±0.94
JD47R	—	Br	—	1.68±0.33	2.35±0.12
JD49R	Cl	—	—	5.03±0.64	21.80±3.45

The relationship between structure and activity of JD88, the most active test compounds and its analogues is outlined in **Table 3.9**. JD88 and its analogues contained copper dioxygen complexes and a cyclohexane added to the amidogen group (**Table 3.9**). In MCF-7 cells, the addition of bromine at R_1 increased the activity

of JD88 against MCF-7 cells while a substitution of chlorine at the same position increased the activity of JD49R against MDA-MB-231 cells but reduced activity against MCF-7 cells. A substitution at only R_2 with bromine in JD47R increases its activity against MCF-7 cells and significantly increases the activity of the test compounds in MDA-MB-231. The substitution with chlorine at R_3 in JD36R reduces the activity of test compounds in MCF-7 cells but increases it against MDA-MB-231 cells (**Table 3.9**). If there are no substitutions at R_1, R_2 or R_3 as in JD46R, there is improved effectiveness against MDA-MB-231 cells and reduced activity in MCF-7 cells.

In summary, the following structural features are important:

- Copper containing complex coordinated to the nitrogens on the pyridine and imidazole rings.
- The addition of a cyclohexane to the amidogen group.
- The absence of a substitution on R_1 and R_3.

Chapter 4 – Discussion

In this study, the potential for novel imidazo[1,2-a]pyridine amines as anti-cancer agents was evaluated. Out of a total of 27 compounds, three novel imidazo[1,2-a]pyridine amines, JD88, JD253 and JD256, were most active against MCF-7 and MDA-MB-231 breast cancer cells. These three compounds had the lowest IC_{50} values in MCF-7 and MDA-MB-231 cells (< 5 μM in MCF-7 cells and < 30 μM in MDA-MB-231 cells). MCF-7 cells were more sensitive to these three test compounds than the MDA-MB-231 cells but the difference in sensitivity of the cells to the test compounds within each cell line was small. JD88, JD253 and JD256 induced apoptosis in MCF-7 cells, but the mitochondrial pathway did not appear to be involved. In MDA-MB-231 cells JD88, JD253 and JD256 induced non-apoptotic cell death, which display features of mitotic catastrophe.

4.1 Effect of imidazo[1,2-a]pyridine amines on cell viability of MCF-7, MDA-MB-231 cells and leukocytes

Cell viability studies showed that 12 imidazo[1,2-a]pyridine amines reduced cell viability in MCF-7 cells and MDA-MB-231 cells. Previous studies have confirmed the reliability of the MTT assay as a bulk screening assay for screening of compounds and have shown correlation between in vitro and clinical studies (Alley *et al.*, 1988; Kaspers *et al.*, 2005). IC_{50} values reported in section 3.1 identified JD88, JD253 and JD256 as the most active compounds against both MCF-7 and MDA-MB-231 cells according to the selection criteria (<5 μM in MCF-7 cells, <30 μM in MDA-MB-231). Dose response curves of these three compounds showed that these compounds decreased cell viability in a dose dependent manner.

The difference in IC_{50} values between the two tested cell lines could be indicative of selective toxicity of the active test compounds for MCF-7 cells compared to MDA-MB-231 cells. The differences in sensitivity to test compounds between the cells lines could also be attributed to the characteristics of the type of tumours each cell line was derived. The two cells lines chosen in this study differ in terms of their molecular characteristics. MCF-7 cells are considered a model for hormone receptor positive tumours (Lacroix *et al.*, 2004; Levenson *et al.*, 1997) which are Luminal A type breast tumours which have been shown to be responsive to chemotherapy and have a good prognostic outcome (Sørlie *et al.*, 2001; Sørlie *et al.*, 2003). MDA-MB-231 cells

model triple-negative breast cancer tumour cells (Holliday *et al.*, 2011; Lacroix *et al.*, 2004), which are known to be aggressive in nature, refractory to chemotherapy and contain mutations in p53 (Dumay *et al.*, 2013; Prat *et al.*, 2010; Sørlie *et al.*, 2001). A study carried out against eight breast cancer cell lines using camptothecin and 7-hydroxystaurosporine found that MDA-MB-231 cells have mutated p53 in addition to overexpressing antiapoptotic proteins Bcl-2 and Bcl-X_L, which could explain the resistance to cytotoxicity in MDA-MB-231 cells when compared to MCF-7 cells (Nieves-Neira *et al.*, 1999). This is supported by data in this study that showed little induction of apoptosis in these cells.

p53 is a sequence specific transcription factor at the centre of many cell death and differentiation signalling networks. It has many functions and is regarded the master guardian and regulator of these pathways. One of its functions is the induction of the mitochondrial pathway of apoptosis but has been observed to enhance surface levels of the Fas ligand and activate DR5, both of which are involved in the death receptor pathway (Amaral *et al.*, 2010; Estaquier *et al.*, 2012; Kracikova *et al.*, 2013; Vaseva *et al.*, 2012). Therefore given the crucial nature of p53 in cell death and effects of its mutation in cancer pathogenesis and resistance to chemotherapy, it affords an explanation as to why the MDA-MB-231 cells were more resistant to test compounds than MCF-7 cells (Amaral *et al.*, 2010; Jackson *et al.*, 2012; Kracikova *et al.*, 2013; Nik-Zainal *et al.*, 2012).

Neutropenia is the most common adverse effect observed in treatment of metastatic breast cancer with cytotoxic therapies like anthracyclines and taxanes, especially when they are administered in combination (Carrick *et al.*, 2004; Carrick *et al.*, 2009; Dear *et al.*, 2013; Ghersi *et al.*, 2015; Mayer *et al.*, 2007). Therefore, effective compounds that are able to selectively induce cell death or inhibit cell growth in cancer cells, while exhibiting sparing toxicity to leukocytes are beneficial. In this study leukocytes were exposed to two concentrations, 15 µM and 25µM of the test compounds. When compared to the camptothecin, JD256 was significantly less toxic to the leukocytes. This is important considering the complications of neutropenia in breast cancer therapy. Furthermore, at these concentrations, which were considerably higher than its IC_{75} value, JD256 did not cause more than 50% cell death. This may be indicative of selective toxicity of the JD256 for MCF-7 cells

compared to leukocytes. Selective toxicity is a desired feature in potential chemotherapeutic compounds (Minotti *et al.*, 2004; Moreno-Aspitia *et al.*, 2009).

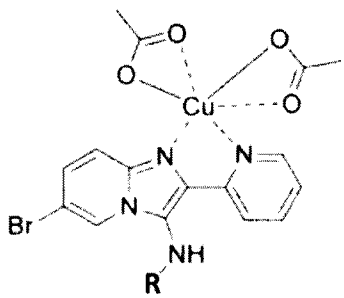
The positive control camptothecin was more active in both MCF-7 and MDA-MB-231 cells than the test compounds as shown by the lower IC_{50} values when compared to the active test compounds. IC_{50} values observed for camptothecin were consistent with those observed in previous studies in these cell lines highlighting its potency in breast cancer cell lines (Acevedo-Morantes *et al.*, 2013; Jones *et al.*, 1997). However, the IC_{50} value for camptothecin was inconsistent with the observation on cell morphology at this concentration. This puts into question the reliability of camptothecin IC_{50} values. Haibe-Kains *et al.* (2013) have identified inconsistencies in the IC50 value of many anticancer drugs including camptothecin. They found out 252 cell lines tested in two different locations using identical protocols the Spearman's coefficient was less than 0.6 for camptothecin IC_{50} values (Haibe-Kains *et al.*, 2013). Therefore the value of the IC_{50} value reported in MDA-MB-231 and MCF-7 may not be reflective of the actual IC_{50} value. Camptothecin is also a highly toxic compound, last used in clinical settings three decades ago, that is known to cause severe adverse effects most notably myelotoxicity (Erickson-Miller *et al.*, 1997; Gottlieb *et al.*, 1970; Muggia *et al.*, 1972; Uday Bhanu *et al.*, 2010).

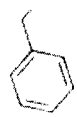
Therefore the evidence discussed above shows that JD88, JD253, JD256 are cytotoxic against both breast cancer cell lines with IC_{50} values below the NCI-60 screen recommendation and differential toxicity between MCF-7 and MDA-MB-231. JD256 shows further differential toxicity against leukocytes, however this was not determined in JD88 and JD253. Although camptothecin was significantly more active than the test compounds, it did not show differential activity to one breast cancer cell line and it was more toxic to leukocytes than JD256. The active test compounds JD88, JD253 and JD256 were then analysed to determine the mode of cell death that they induced in MCF-7 and MDA-MB-231 cells. Programmed cell death is a desired end point for cancer chemotherapy, unlike necrosis, programmed cell death particularly apoptosis has well documented pathways and does not have any associated inflammation when cells die (Galluzzi *et al.*, 2012; Henry *et al.*, 2013; Kerr *et al.*, 1972; Kroemer *et al.*, 2009; Saraste *et al.*, 2000).

4.2 Effect of active test compounds on programmed cell death in MCF-7 cells

Markers for apoptosis, which include specific changes in cellular morphology, caspase-7 activity, phosphatidylserine exposure and cytochrome c translocation from the mitochondria, were evaluated to determine the ability of active test compounds to induce apoptosis in MCF-7 cells. MCF-7 cells do not express caspase-3 an executioner caspase associated with apoptosis (Jänicke *et al.*, 1998). A summary of the effects of active test compounds on the programmed cell death is displayed in **Table 4.1**.

Table 4.1 Summary of effect of active test compounds on MCF-7 programmed cell death



	R-group	IC_{50} Value (μM)	Nuclear & Cell Morphology	Caspase activity	Phosphatidyl serine exposure
JD88		0.62±0.03	Nuclear fragmentation, perinuclear vacuolation, cell rounding	present	present
JD253		3.66±0.49		minimal	minimal
JD256		2.23±0.10		minimal	minimal

4.2.1 Effect of active test compounds on cell morphology of MCF-7 cells

Cell and nuclear morphology changes are considered common features of apoptotic cell death. These changes include membrane blebbing, formation of apoptotic bodies, condensation of chromatin, and fragmentation of the nucleus (Galluzzi *et al.*, 2012; Kerr *et al.*, 1972; Kroemer *et al.*, 2009). Microscopy remains an important

method to confirm apoptosis in target cells by test compounds (Darzynkiewicz *et al.*, 1997; Henry *et al.*, 2013; Vanden Berghe *et al.*, 2013) and the use of fluorescent stains in microscopy help distinguish apoptotic, necrotic and viable cells (Mpoke *et al.*, 1997; Ribble *et al.*, 2005).

At lower test concentrations (equal to IC_{50} values) JD88, JD253 and JD256 did not show any significant changes in cell morphology until 48 hours of exposure. Perinuclear vacuole formation was observed in cells treated with JD253 and JD256 after 24 hours of exposure. At higher test compound concentrations (25 μM) cells exposed to JD88, JD253 and JD256 also showed perinuclear vacuole formation. There are no reports that perinuclear vacuole formation is an apoptotic marker but it has been shown to occur in conjunction with apoptosis (Harmse *et al.*, 2015). Vacuole formation is associated with autophagy, a process that leads to mass degradation of cellular protein and organelles in order to provide energy to the cell in response to chemotherapy, nutrient deprivation and hypoxia (Childs, 2004; Meijer *et al.*, 2009).

Whether or not the vacuoles were autophagic in nature was tested with the use of MDC. The results indicate that the vacuoles were not autophagic in nature as MDC accumulates in late endosomes associated with autophagy. The vacuoles observed in MCF-7 cells exposed to test compounds did not co-localise with MDC fluorescent clusters indicating their non-autophagic nature. Furthermore, the vacuoles appear not to have membranes and are filled with fluid. MDC does cause non-specific staining of lysosomal structures around the nucleus but staining is generally diffuse and not punctate as is the case with chloroquine (Klionsky et al., 2012). Chloroquine is known to induce formation of autophagic vacuoles (Fedorko *et al.*, 1968; Geng *et al.*, 2010; Kimura *et al.*, 2013) and these were observed in MCF-7 cells treated with chloroquine and stained with MDC. There were no MDC fluorescent structures observed in MCF-7 cells exposed to JD88, JD253 and JD256 therefore providing evidence that the perinuclear vacuoles observed by phase contrast microscopy were not autophagic in nature.

4.2.2 Effect of active test compounds on nuclear morphology of MCF-7 cells

When apoptosis is induced in cells, changes in nuclear morphology such as chromatin condensation and nuclear fragmentation are considered hallmarks of this process (Galluzzi *et al.*, 2012; Kerr *et al.*, 1972; Kroemer *et al.*, 2009). Hoechst 33342, acridine orange and ethidium bromide were used to distinguish apoptotic and non-apoptotic cells due to their ability to differentially stain the nucleus of apoptotic, necrotic and living cells (Kamal *et al.*, 2014; Kamal *et al.*, 2013; Mpoke *et al.*, 1997; Ribble *et al.*, 2005).

Nuclear fragmentation was observed in MCF-7 cells treated with JD88, JD253 and JD256 when the cells were stained with Hoechst 33342 (**Figure 3.10**). These fragments were confirmed when the same cells were stained with acridine-orange and the nuclear fragments fluoresced green-yellow. Cells treated with JD88 and JD253 were considered to be in an early apoptotic state, since the cell membrane maintained integrity as evidenced by the lack of entry ethidium bromide. However, cells treated with JD256 were considered late apoptotic showing loss of cell membrane integrity in the late stages of apoptosis (Mpoke *et al.*, 1997; Ribble *et al.*, 2005).

As observed in **Figure 3.12**, cells treated with the positive control camptothecin, a known inducer of apoptosis, showed similar nuclear morphology to cells treated with active test compounds. The cells showed nuclear fragmentation both with Hoechst 33342 and acridine orange staining. These cells were also considered as early apoptotic due to the lack of entry of ethidium bromide showing that cell membranes were still intact.

4.2.3 Effect of active test compound on caspase-7 activity and phosphatidylserine exposure in MCF-7 cells

Caspase-3 activity has been established in many different cell lines but has been found to be absent in MCF-7 cells due to a deletion on exon 3 of the *CASP3* gene (Jänicke *et al.*, 1998). However caspase-7 is present in MCF-7 cells and has the ability to function as an executioner caspase in apoptosis (Brentnall *et al.*, 2013; Slee *et al.*, 2001; Twiddy *et al.*, 2006; Wolf *et al.*, 1999). Caspase-7 is protease that primarily cleaves Poly(ADP-ribose) polymerase-1 (PARP-1) during the execution

phase of apoptosis (Ame *et al.*, 2004; Earnshaw *et al.*, 1999). Caspase-7 cleaves the same synthetic peptide as caspase-3 with the sequence DEVD (Earnshaw *et al.*, 1999) and therefore colorimetric assays that make use of this peptide as a substrate can be used to detect both caspase-3 and -7. The activity of caspase-7 is a biomarker that indicates the induction of apoptosis in cells undergoing cell death.

An increase in caspase-7 activity was observed in MCF-7 cells treated with JD88 and camptothecin shortly after the addition of the compounds. JD253 and JD256 did not induce an increase in caspase-7 activity when compared to untreated cells. Cleavage of PARP-1 by caspase-7 leads the increase in synthesis of Poly(ADP-ribose) (PAR) and associated chromatin condensation (Ame *et al.*, 2004; Chaitanya *et al.*, 2010; Soldani *et al.*, 2001; Soldani *et al.*, 2002). This is supported by observed nuclear fragmentation and chromatin condensation discussed in section 4.2.2. Another function executioner caspases perform during apoptosis is to facilitate the exposure of phosphatidylserine on the outer leaflet of cell membrane (Marino *et al.*, 2013; Segawa *et al.*, 2014; Vanags *et al.*, 1996). MCF-7 cells exposed to JD88 and camptothecin showed extensive exposure of phosphatidylserine on the cell surface while cells exposed to JD253 and JD256 showed lower levels of phosphatidylserine exposure. This correlated to the lack of caspase-7 activity discussed above and supports the hypothesis that phosphatidylserine exposure is caspase dependent.

Although caspase-7 can perform different roles to caspase-3, one of the roles that they share is the activation of caspase-2 (Cullen *et al.*, 2009). One of the functions of caspase-2 is the degradation of the cytoskeleton during apoptosis (Kong *et al.*, 2004; Vakifahmetoglu-Norberg *et al.*, 2013). Several studies have shown an association between apoptotic cell death and cytoskeletal degradation in various cancer cell lines. These studies have correlated the loss of F-actin, a component of the cytoskeleton, to nuclear fragmentation and other features associated with apoptosis *in vitro* (Bursch *et al.*, 2000; Song *et al.*, 1997; Vakifahmetoglu-Norberg *et al.*, 2013). Cells treated with JD256, JD253 and camptothecin had condensed chromatin associated with detachment of cells from their growth surface. Although there were cells that showed degradation of F-actin, they were too few to support a firm conclusion.

4.2.4 Effect of active test compounds on cytochrome c translocation in MCF-7 cells

The translocation of cytochrome c from the mitochondria to the cytoplasm is a key process in the intrinsic pathway of apoptosis. The proapoptotic protein Bax plays a crucial role in changing the permeability of the mitochondria allowing for the release of cytochrome c to the cytoplasm (Wei *et al.*, 2001). MCF-7 cells are known to overexpress Bcl-2, an inhibitor of Bax, and studies have shown that MCF-7 cells treated with Bcl-2 inhibitors are sensitised to chemotherapy (Binder *et al.*, 1996; Juin *et al.*, 2013; Martin *et al.*, 2013; Nieves-Neira *et al.*, 1999; Sharifi *et al.*, 2014).

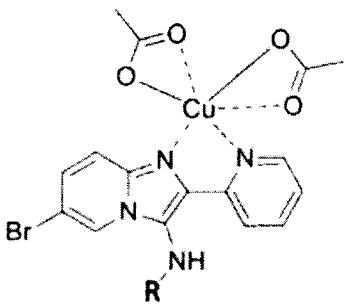
Cells treated with JD88, JD253 and JD256 did not show translocation of cytochrome c into the cytoplasm. The same was observed for camptothecin at the dose tested (9 µM). Previous studies with camptothecin indicated a cytochrome c translocation to the cytoplasm in different cell lines and at a much higher dose (Dahan-Farkas *et al.*, 2011; Sanchez-Alcazar *et al.*, 2000). It is therefore plausible that camptothecin is not able to induce cytochrome c translocation at the doses tested. This indicates that the intrinsic apoptotic pathway is not activated in these cells. Numerous studies on breast cancer tumours show that upregulation of Bcl-2 and downregulation of Bax leads to a decreased intrinsic apoptotic pathway response (Estaquier *et al.*, 2012; Krajewski *et al.*, 1995; Sharifi *et al.*, 2014; Zapata *et al.*, 1998).

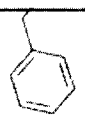
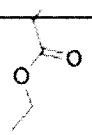
Data obtained in this study suggests that the intrinsic apoptotic pathway is not activated in MCF-7 cells treated with JD88, JD253 and JD256. However changes in nuclear and cell morphology, and caspase-7 activation suggest strongly that apoptosis is still induced particularly in JD88 indicating activation of the extrinsic apoptotic pathway. This study shows that JD253 and JdD56 showed strong evidence of apoptotic induction according to morphology data but very little evidence in terms of caspase activation and phosphatidylserine exposure. Thus it can be postulated that apoptosis is induced via the extrinsic pathway. Additional tests like measuring activity of caspase-8 or caspase-2 will provide additional information to this effect (Dickens *et al.*, 2012; Ouyang *et al.*, 2012).

4.3 Effect of active test compounds on programmed cell death in MDA-MB-231 cells

As discussed in section 4.1, three of the test compounds JD88, JD253 and JD256 were the most active against MDA-MB-231. The compounds were less active against MDA-MB-231 cells than MCF-7 cells. MDA-MB-231 cells exposed to active test compounds showed signs of mitotic catastrophe, necrosis and apoptosis. **Table 4.2** below provides a summary of the outcomes from the different methods used to evaluate the mechanism of cell death.

Table 4.2 Summary of effect of active test compounds on MDA-MB-231 programmed cell death



	R-group	IC_{50} Value (μM)	Nuclear & Cell Morphology	Caspase activity	Phosphatidyl serine exposure
JD88		27.88±2.12	- cell rounding - decondensed nuclei - multiple nucleated cells - cell blebbing - lysosomal activation	present	present
JD253		29.76±1.72	- cell rounding - decondensed nuclei - large nuclei	absent	present
JD256		28.82±1.35	- cell rounding - decondensed nuclei - multiple nucleated cells - cell blebbing - lysosomal activation	absent	minimal

4.3.1 Effect of active test compounds on cell morphology of MDA-MB-231 cells

When MDA-MB-231 cells were exposed to JD88, JD253 and JD256, cells became round, detached from the growth surface and showed a decrease in cell density compared to untreated cells. Cells treated with JD88, JD253, JD256 displayed a high level of cell-cell adherence, a feature not observed in untreated cells. The detachment and subsequent clustering of cells occurred earlier in cells treated with JD253 than those treated with JD88 and JD256. In her review on apoptosis, Elmore (2007) argued that rounding of cells was a feature of apoptosis. It is suspected that the change in cell shape may be due to the action of caspases on focal adhesion and structural proteins although downstream processes may be responsible for degradation of these proteins (Häcker, 2000; Lu *et al.*, 2012; Marushige *et al.*, 1998). Cells treated with camptothecin showed some detachment and rounded cells during the exposure period but largely retained cell growth surface attachments and the normal spindle-like MDA-MB-231 cell shape as observed in untreated cells.

4.3.2 Effect of active test compounds on nuclear morphology of MDA-MB-231 cells

One of the main features observed in cells treated with JD88, JD256 and camptothecin was the presence of red/orange coloured granules/vesicles around the nuclei. The presence of these structures was also closely correlated with cells undergoing cell death (Lovelace *et al.*, 2007; Mpoke *et al.*, 1997; Robbins *et al.*, 1964; Zelenin, 1966).

Cells treated with JD88 showed blebbing on the surface of the cell membrane, a feature of apoptosis (Kerr *et al.*, 1972; Kroemer *et al.*, 2009). Cells treated with JD253 and JD256 were stained green, which indicated that the cell membrane was intact. Cells treated with camptothecin displayed yellow-green nucleus surrounded by red/orange lysosome granules. These cells did not however show blebbing of the cell membrane or any other features associated with apoptosis. MDA-MB-231 cells, treated with JD88, JD253 and JD256, stained with Hoechst 33342 did not show chromatin condensation, a prominent feature associated with apoptosis. Cells treated with JD88 and JD256 contained multiple decondensed nuclei while cells treated with JD253 showed enlarged nuclei. A decondensed nucleus is one that contains chromatin that appears loosened in texture. The presence of multiple nuclei and

decondensed chromatin are considered markers of a form of programmed cell death known as mitotic catastrophe (Castedo *et al.*, 2004; Galluzzi *et al.*, 2012; Kroemer *et al.*, 2009).

Mitotic catastrophe is characterised by large multinucleated cells with decondensed nuclei as observed in MDA-MB-231 cells treated with JD88, JD253 and JD256 (Castedo *et al.*, 2004; Galluzzi *et al.*, 2012; Jordan *et al.*, 1996; Kroemer *et al.*, 2009). Studies using low concentrations of the taxane paclitaxel in HeLa cells showed that the drug induced formation of an interphase-like state. This was characterised by reformation of nuclear membrane around decondensed chromatin and multiple nuclei. Upon removal of paclitaxel in these cells, apoptotic cell death was induced (Jordan *et al.*, 1996). Roninson *et al.* (2001) have argued that many anticancer drugs like taxol, cisplatin or bleomycin exhibit cell death consistent with mitotic catastrophe and although mitotic catastrophe sometimes precedes apoptosis, cell death has been observed to occur independent of apoptosis (Parton *et al.*, 2001). It is therefore conceivable that cell death observed in MDA-MB-231 cells induced by active compounds is due to mitotic catastrophe.

4.3.3 Effect of active test compound on caspase-3/7 activity and phosphatidylserine exposure in MDA-MB-231 cells

An increase in caspase-3/7 activity in MDA-MB-231 cells treated with JD88 and camptothecin occurring as early as 2 hours after exposure to the test compounds. This was similar to the activity of MCF-7 cells when they were treated with JD88 and camptothecin. However caspase-3/7 activation in MCF-7 cells was consistent with apoptotic features like chromatin condensation, which is not present in MDA-MB-231 cells treated with JD88 and JD253. In their reviews on cell death and mitotic catastrophe, Galluzzi *et al.* (2012) and Castedo *et al.* (2004) have shown that caspase activation and death by mitotic catastrophe are not mutually exclusive. Portugal *et al.* (2010) have also found that an aberrant p53 protein promotes death of tumour cells by mitotic catastrophe and this has been observed in other studies as well (Ianzini *et al.*, 2006). MDA-MB-231 cells are known to have a mutated p53 protein (Nieves-Neira *et al.*, 1999) and therefore are more likely to undergo mitotic catastrophe.

MDA-MB-231 cells treated with JD88 showed a large body of clumped cells that stained positive with Annexin-V-FITC showing phosphatidylserine exposure. As mentioned in section 4.2.3 phosphatidylserine exposure on the surface of the cell membrane is related to the activity of effector caspases apart from caspase-3 (Marino *et al.*, 2013; Segawa *et al.*, 2014; Woo *et al.*, 1998). Some studies have shown the presence of phosphatidylserine exposure in cells undergoing mitotic catastrophe (Eom *et al.*, 2005) therefore it is possible that MDA-MB-231 cells treated with test compounds undergo mitotic catastrophe.

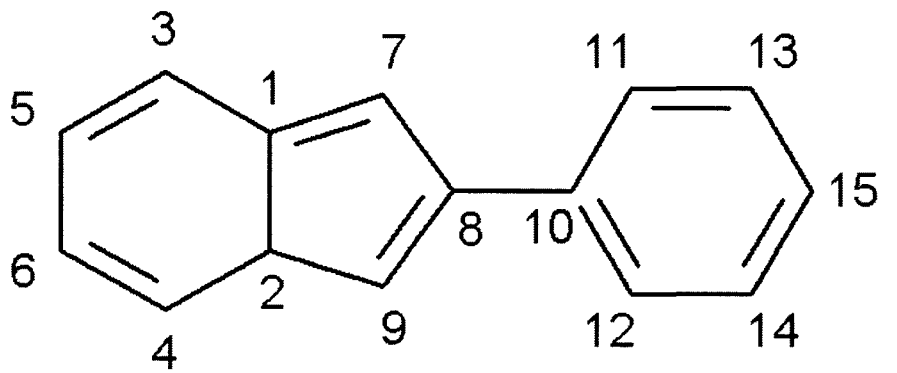
Data from this study suggests that mitotic catastrophe is activated in cells treated to active test compounds. This evidence is largely morphological as there are currently no available biomarkers that are strongly linked to mitotic catastrophe (Galluzzi *et al.*, 2012). In MDA-MB-231 cells, JD88 showed some features of apoptotic cell death like membrane blebbing, caspase activation and phosphatidylserine exposure. JD253 and JD256 did not show biochemical features consistent with apoptosis but microscopy data showed a significant amount of necrosis occurring in these cells. Therefore data from this study suggest mitotic catastrophe is not the only cell death pathway activated when MDA-MB-231 cells were exposed to test compounds.

Active test compounds JD88, JD253 and JD256 showed cytotoxic activity against both MCF-7 and MDA-MB-231 cells lines. In MCF-7 cells, apoptotic cell death was the main mode of cell death although the intrinsic apoptotic pathway did not appear to be activated. In MDA-MB-231 features of apoptosis, necrosis and mitotic catastrophe were observed when cells were exposed to JD88, JD253 and JD256. The data also suggests that MCF-7 cells are more sensitive to the active test compounds than MDA-MB-231 cells and MCF-7 cells are more sensitive to JD256 than leukocytes.

4.4 Structure activity relationships of active test compounds

Structure activity relationships of imidazo[1,2-a]pyridine amines show that coordination of copper to the scaffold increases its activity significantly. Several studies have shown increase in cytotoxicity in cancer cell lines of pyridine containing structures coordinated with transition metal complexes (Fernandes *et al.*, 2012; Martinez-Bulit *et al.*, 2015). Substitution of position-6 with bromine increased activity of imidazo[1,2-a]pyridine amines containing a copper dioxygen complex in MCF-7

cells. In MDA-MB-231 cells, the substitution with bromine at position-4 instead of position-6 or the removal of a substitution at position-6 greatly increases the activity of the imidazo[1,2-a]pyridine amines in these cells without a minor loss of activity in MCF-7 cells.



The initial study results gave rise to the synthesis of a panel of new copper containing compounds with improved efficacy against both MCF-7 and MDA-MB-231 cells. These new compounds have the potential to exhibit favourable anticancer activity and therefore evaluation of their mode of cell death and breast cancer animal models are important for future consideration.

Chapter 5 – Conclusion

The current treatment of breast cancer is not always successful and the development of resistance is a continuous threat to patient survival. In this study a panel of novel imidazo[1,2-a]pyridine amines was synthesized by the School of Chemistry, Wits University and evaluated against two breast cancer cell lines in order to identify new lead compounds with potential anticancer effects. Furthermore, this study aimed to identify the mechanism of cell death, induced by these test compounds.

The results of this study have shown that imidazo[1,2-a]pyridine amines were active against both MCF-7 and MDA-MB-231 cells. The estrogen receptor positive MCF-7 cells were more sensitive to inhibition by the compounds than the MDA-MD-231 cells as shown by the lower IC_{50} values obtained by testing MCF-7 cells. Three compounds, JD88, JD253 and JD256 showed the most activity in MCF-7 and MDA-MB-231 cells. An investigation into toxicity towards non-tumorigenic cells using peripheral leukocytes indicated that one of the compounds, JD256, was significantly less toxic to white blood cells than the positive control camptothecin.

This study has shown that in MCF-7 cells, the three compounds, JD88, JD256 and JD253 were able to induce apoptosis, an important cell death pathway for potential chemotherapeutic agents. This was supported by specific morphological changes, which show chromatin condensation and nuclear fragmentation in cells exposed to these compounds. Imidazo[1,2-a]pyridine amines, induced the formation of perinuclear vacuoles which were determined to be non-autophagic using MDC as an indicator. The evaluation of caspase-3/7 activity showed an increase in activity at two hours after exposure to JD88 started. This, together with exposure of phosphatidylserine on the cell surface of MCF-7 cells suggests that JD88 induces apoptosis in a caspase dependent manner. There was however no increase in caspase-3/7 activity in cells exposed to JD253 and JD256 suggesting that there is no significant apoptotic induction by these two compounds. The imidazo[1,2-a]pyridine amines did not appear to induce the translocation of cytochrome c from the mitochondria to the cytoplasm, which suggests that the intrinsic apoptotic pathway was not active in MCF-7 cells.

In MDA-MB-231 cells, the active imidazo[1,2-a]pyridine amines appeared to induce mitotic catastrophe alongside apoptosis and necrosis. Mitotic catastrophe is supported by morphological observations that show the formation of large multinucleated cells with decondensed chromatin. Necrosis is also supported by morphological data as cell exposed to these compounds showed a loss of cell membrane integrity without any visible chromatin condensation. Morphological data also suggests that in both cell lines, JD88 caused cell membrane blebbing. This together with increased activity of caspase-3/-7 shortly after exposure and the exposure of phosphatidylserine on the cell surface of MDA-MB-231 cells indicated that JD88 is able to induce apoptosis. The other two test compounds JD253 and JD256 showed minimal exposure of phosphatidylserine to the surface of the cell membrane and this suggests that apoptosis may not be the primary mode of cell death induced by these compounds in MDA-MB-231 cells.

The development of analogues to imidazo[1,2-a]pyridine amines similar in structure to the most active compounds show that structure plays a crucial role in the cytotoxic activity of these compounds. The addition of a copper dioxygen group to JD60 to form JD88 significantly increased of activity imidazo[1,2-a]pyridine amines in MCF-7 cells and MDA-MB-231 cells. Copper complexes in JD253 and JD256 increased activity in these compounds compared to zinc and platinum containing complexes. The copper complexes were also more soluble in aqueous solution than their platinum counterparts, an important property for the bio-evaluation of compounds. The addition of a cyclohexane group to the amidogen of the imidazo[1,2-a]pyridine amine scaffold is particularly important in increasing activity against MCF-7 cells. Not adding a substituent to carbon-6 or adding bromine or chlorine to carbon-4 further increases activity of these compounds in MDA-MB-231 cells.

Imidazo[1,2-a]pyridine amines are cytotoxic compounds against breast cancer cells with promising cytotoxic properties. Manipulation of the base structure of these compounds has given rise to new copper containing configurations with improved efficacy against both MCF-7 and MDA-MB-231 cells. These new copper containing compounds require further testing to evaluate their mode of cell death and should be evaluated in animal models of breast cancer to determine their efficacy.

Chapter 6 – References

Aapro M, Finek J (2012). Oral vinorelbine in metastatic breast cancer: A review of current clinical trial results. *Cancer Treatment Reviews* **38**(2): 120-126.

Abal M, Andreu JM, Barasoain I (2003). Taxanes: microtubule and centrosome targets, and cell cycle dependent mechanisms of action. *Current cancer drug targets* **3**(3): 193-203.

Acevedo-Morantes CY, Acevedo-Morantes MT, Suleiman-Rosado D, Ramírez-Vick JE (2013). Evaluation of the cytotoxic effect of camptothecin solid lipid nanoparticles on MCF7 cells. *Drug Delivery* **20**(8): 338-348.

Alberts B, Johnson A, Lewis J, Raff M, Roberts K, Walter P (2007a). Apoptosis. In: *Molecular Biology of the Cell*, 5th edn. New York: Garland Science: 1115 - 1129.

Alberts B, Johnson A, Lewis J, Raff M, Roberts K, Walter P (2007b). Cancer. In: *Molecular Biology of the Cell*, 5th edn. New York: Garland Science: 1205 - 1265.

Alberts B, Johnson A, Lewis J, Raff M, Roberts K, Walter P (2007c). The Cell cycle. In: *Molecular Biology of the Cell*, 5th edn. New York: Garland Science: 1053-1114.

Alley MC, Scudiero DA, Monks A, Hursey ML, Czerwinski MJ, Fine DL, *et al.* (1988). Feasibility of Drug Screening with Panels of Human Tumor Cell Lines Using a Microculture Tetrazolium Assay. *Cancer Research* **48**(3): 589-601.

Allred DC, Wu Y, Mao S, Nagtegaal ID, Lee S, Perou CM, *et al.* (2008). Ductal Carcinoma In situ and the Emergence of Diversity during Breast Cancer Evolution. *Clinical Cancer Research* **14**(2): 370-378.

Amaral JD, Xavier JM, Steer CJ, Rodrigues CM (2010). The role of p53 in apoptosis. *Discovery medicine* **9**(45): 145-152.

Ame JC, Spenlehauer C, de Murcia G (2004). The PARP superfamily. *BioEssays : news and reviews in molecular, cellular and developmental biology* **26**(8): 882-893.

American Joint Committee on Cancer (2012). Breast. In: *AJCC Cancer Staging Atlas: A Companion to the Seventh Editions of the AJCC Cancer Staging Manual and Handbook*, 2nd edn. New York: Springer: 419 - 440.

Arndt-Jovin DJ, Jovin TM (1977). Analysis and sorting of living cells according to deoxyribonucleic acid content. *Journal of Histochemistry & Cytochemistry* **25**(7): 585-589.

Bachelot T, Romieu G, Campone M, DiÈras V, Cropet C, Dalenc F, *et al.* (2013). Lapatinib plus capecitabine in patients with previously untreated brain metastases from HER2-positive metastatic breast cancer (LANDSCAPE): a single-group phase 2 study. *The Lancet Oncology* **14**(1): 64-71.

Balduzzi S, Mantarro S, Guarneri V, Tagliabue L, Pistotti V, Moja L, *et al.* (2014). Trastuzumab-containing regimens for metastatic breast cancer. *The Cochrane database of systematic reviews* **6:** CD006242.

Balmaña J, Díez O, Rubio IT, Cardoso F, Group ObotEGW (2011). BRCA in breast cancer: ESMO Clinical Practice Guidelines. *Annals of Oncology* **22**(suppl 6)**:** vi31-vi34.

Benson JR (2012). Long-term outcome of breast conserving therapy. *The Lancet Oncology* **13**(4)**:** 331-333.

Bertos NR, Park M (2011). Breast cancer — one term, many entities? *The Journal of Clinical Investigation* **121**(10)**:** 3789-3796.

Beslija S, Bonneterre J, Burstein HJ, Cocquyt V, Gnant M, Heinemann V, *et al.* (2009). Third consensus on medical treatment of metastatic breast cancer. *Annals of Oncology* **20**(11)**:** 1771-1785.

Binaschi M, Bigioni M, Cipollone A, Rossi C, Goso C, Maggi CA, *et al.* (2001). Anthracyclines: selected new developments. *Current medicinal chemistry. Anti-cancer agents* **1**(2)**:** 113-130.

Binder C, Marx D, Binder L, Schauer A, Hiddemann W (1996). Expression of Bax in relation to Bcl-2 and other predictive parameters in breast cancer. *Annals of Oncology* **7**(2)**:** 129-133.

Binder C, Marx D, Overhoff R, Binder L, Schauer A, Hiddemann W (1995). Bcl-2 protein expression in breast cancer in relation to established prognostic factors and other clinicopathological variables. *Annals of Oncology* **6**(10)**:** 1005-1010.

Blumberg N, Triulzi DJ, Heal JM (1990). Transfusion-Induced Immunomodulation and Its Clinical Consequences. *Transfusion Medicine Reviews* **4**(4)**:** 24-35.

Boyd M (1997). The NCI In Vitro Anticancer Drug Discovery Screen. In: *Anticancer Drug Development Guide*: Humana Press: 23-42.

Boyum A (1976). Isolation of Lymphocytes, Granulocytes and Macrophages. *Scandinavian Journal of Immunology* **5**(s5)**:** 9-15.

Bradford MM (1976). A rapid and sensitive method for the quantitation of microgram quantities of protein utilizing the principle of protein-dye binding. *Anal Biochem* **72:** 248-254.

Brentnall M, Rodriguez-Menocal L, De Guevara RL, Cepero E, Boise LH (2013). Caspase-9, caspase-3 and caspase-7 have distinct roles during intrinsic apoptosis. *BMC cell biology* **14:** 32.

Brooks SC, Locke ER, Soule HD (1973). Estrogen Receptor in a Human Cell Line (MCF-7) from Breast Carcinoma. *Journal of Biological Chemistry* **248**(17)**:** 6251-6253.

Bursch W, Hochegger K, Torok L, Marian B, Ellinger A, Hermann RS (2000). Autophagic and apoptotic types of programmed cell death exhibit different fates of cytoskeletal filaments. *Journal of Cell Science* **113**(7): 1189-1198.

Cardoso F, Costa A, Norton L, Senkus E, Aapro M, André F, *et al.* (2014). ESO-ESMO 2nd international consensus guidelines for advanced breast cancer (ABC2). *Annals of Oncology*. **25**(10): 1871-1888.

Carrick S, Ghersi D, Wilcken N, Simes J (2004). Platinum containing regimens for metastatic breast cancer. *The Cochrane Database of Systematic Reviews* (2): CD003374.

Carrick S, Parker S, Thornton CE, Ghersi D, Simes J, Wilcken N (2009). Single agent versus combination chemotherapy for metastatic breast cancer. *The Cochrane Database of Systematic Reviews* (2): CD003372.

Castedo M, Perfettini JL, Roumier T, Andreau K, Medema R, Kroemer G (2004). Cell death by mitotic catastrophe: a molecular definition. *Oncogene* **23**(16): 2825-2837.

Chaitanya G, Alexander J, Babu P (2010). PARP-1 cleavage fragments: signatures of cell-death proteases in neurodegeneration. *Cell Communication and Signaling* **8**(1): 31.

Childs O (2004). Pathways of apoptotic and non-apoptotic death in tumour cells. *Nature Reviews Cancer* **4**(8): 592-603.

Coop A, Ellis MJ (2003). The Nature and development of cancer. In: *Oxford Textbook of Medicine*, 4 edn: 219-228.

Cubasch H, Joffe M, Hanisch R, Schuz J, Neugut A, Karstaedt A, *et al.* (2013). Breast cancer characteristics and HIV among 1,092 women in Soweto, South Africa. *Breast Cancer Res Treat* **140**(1): 177-186.

Cullen SP, Martin SJ (2009). Caspase activation pathways: some recent progress. *Cell Death Differ* **16**(7): 935-938.

Czajka-Oraniec I, Simpson ER (2010). Aromatase research and its clinical significance. *Endokrynologia Polska* **61**(1): 126-134.

Dahan-Farkas N, Langley C, Rousseau AL, Yadav DB, Davids H, de Koning CB (2011). 6-Substituted imidazo[1,2-a]pyridines: synthesis and biological activity against colon cancer cell lines HT-29 and Caco-2. *European Journal of Medicinal Chemistry* **46**(9): 4573-4583.

Dallavalle F, Gaccioli F, Franchi-Gazzola R, Lanfranchi M, Marchio L, Pellinghelli MA, *et al.* (2002). Synthesis, molecular structure, solution equilibrium, and antiproliferative activity of thioxotriazoline and thioxotriazole complexes of copper II and palladium II. *Journal of Inorganic Biochemistry* **92**(2): 95-104.

Darzynkiewicz Z, Juan G, Li X, Gorczyca W, Murakami T, Traganos F (1997). Cytometry in cell necrobiology: Analysis of apoptosis and accidental cell death (necrosis). *Cytometry* **27**(1): 1-20.

Dear RF, McGeechan K, Jenkins MC, Barratt A, Tattersall MH, Wilcken N (2013). Combination versus sequential single agent chemotherapy for metastatic breast cancer. *The Cochrane Database of Systematic Reviews* **12:** CD008792.
Degardin M, Bonneterre J, Hecquet B, Pion J-M, Adeins A, Horner D, *et al.* (1994). Vinorelbine (Navelbine) as a salvage treatment for advanced breast cancer. *Annals of Oncology* **5**(5)**:** 423-426.

Dickens LS, Powley IR, Hughes MA, MacFarlane M (2012). The 'complexities' of life and death: Death receptor signalling platforms. *Experimental Cell Research* **318**(11)**:** 1269-1277.

Dumay A, Feugeas JP, Wittmer E, Lehmann-Che J, Bertheau P, Espie M, *et al.* (2013). Distinct tumor protein p53 mutants in breast cancer subgroups. *International Journal of Cancer.* **132**(5)**:** 1227-1231.

Earnshaw WC, Martins LM, Kaufmann SH (1999). MAMMALIAN CASPASES: Structure, Activation, Substrates, and Functions During Apoptosis. *Annual Review of Biochemistry* **68**(1)**:** 383-424.

Elledge SJ (1996). Cell cycle checkpoints: preventing an identity crisis. *Science* **274**(5293)**:** 1664-1672.

Ellis IO, Elston CW (2006). Chapter 19 - Histologic Grade. In: *Breast Pathology*: Churchill Livingstone: 225-233.

Ellis IO, Galea M, Broughton N, Locker A, Blamey RW, Elston CW (1992). Pathological prognostic factors in breast cancer. II. Histological type. Relationship with survival in a large study with long-term follow-up. *Histopathology* **20**(6)**:** 479-489.

Elmore S (2007). Apoptosis: A Review of Programmed Cell Death. *Toxicologic Pathology* **35**(4)**:** 495-516.

Elston CW, Ellis IO (1991). pathological prognostic factors in breast cancer. I. The value of histological grade in breast cancer: experience from a large study with long-term follow-up. *Histopathology* **19**(5)**:** 403-410.

Endresen PC, Prytz PS, Aarbakke J (1995). A new flow cytometric method for discrimination of apoptotic cells and detection of their cell cycle specificity through staining of F-actin and DNA. *Cytometry* **20**(2)**:** 162-171.

Eom Y-W, Kim MA, Park SS, Goo MJ, Kwon HJ, Sohn S, *et al.* (2005). Two distinct modes of cell death induced by doxorubicin: apoptosis and cell death through mitotic catastrophe accompanied by senescence-like phenotype. *Oncogene* **24**(30)**:** 4765-4777.

Erickson-Miller CL, May RD, Tomaszewski J, Osborn B, Murphy MJ, Page JG, *et al.* (1997). Differential toxicity of camptothecin, topotecan and 9-aminocamptothecin to human, canine, and murine myeloid progenitors (CFU-GM) in vitro. *Cancer Chemotherapy and Pharmacology* **39**(5)**:** 467-472.

Estaquier J, Vallette F, Vayssiere J-L, Mignotte B (2012). The Mitochondrial Pathways of Apoptosis. In: Scatena R, Bottoni P, Giardina B (ed). *Advances in Mitochondrial Medicine*. **942**, Springer Netherlands:157-183.

Evan GI, Vousden KH (2001). Proliferation, cell cycle and apoptosis in cancer. *Nature* **411**(6835): 342-348.

Fedorko ME, Hirsch JG, Cohn ZA (1968). AUTOPHAGIC VACUOLES PRODUCED IN VITRO: I. Studies on Cultured Macrophages Exposed to Chloroquine. *The Journal of Cell Biology* **38**(2): 377-391.

Feinberg AP, Ohlsson R, Henikoff S (2006). The epigenetic progenitor origin of human cancer. *Nature Reviews Genetics* **7**(1): 21-33.

Ferlay J, Soerjomataram I, Dikshit R, Eser S, Mathers C, Rebelo M, *et al.* (2015). Cancer incidence and mortality worldwide: sources, methods and major patterns in GLOBOCAN 2012. *International Journal of Cancer* **136**(5): E359-386.

Ferlay J, Soerjomataram I, Dikshit R, Eser S, Mathers C, Rebelo M, *et al.* (2013). GLOBOCAN 2012 v1.0, Cancer Incidence and Mortality Worldwide: IARC CancerBase No. 11. Lyon, France: International Agency for Research on Cancer.

Fernandes AS, Costa J, Gaspar J, Rueff J, Cabral MF, Cipriano M, *et al.* (2012). Development of pyridine-containing macrocyclic copper(II) complexes: potential role in the redox modulation of oxaliplatin toxicity in human breast cells. *Free Radical Research* **46**(9): 1157-1166.

Festjens N, Vanden Berghe T, Cornelis S, Vandenabeele P (2007). RIP1, a kinase on the crossroads of a cell's decision to live or die. *Cell Death Differ* **14**(3): 400-410.

Freshney RI (2006). Basic Principles of Cell Culture. In: *Culture of Cells for Tissue Engineering*, John Wiley & Sons, Inc: 1-22.

Freshney RI (2010). Defined Media and Supplements. In: *Culture of Animal Cells*, John Wiley & Sons, Inc: 99-114.

Galluzzi L, Vitale I, Abrams JM, Alnemri ES, Baehrecke EH, Blagosklonny MV, *et al.* (2012). Molecular definitions of cell death subroutines: recommendations of the Nomenclature Committee on Cell Death 2012. *Cell Death & Differentiation* **19**(1): 107-120.

Gandhi A, Holland PA, Knox WF, Potten CS, Bundred NJ (1998). Evidence of significant apoptosis in poorly differentiated ductal carcinoma in situ of the breast. *British Journal of Cancer* **78**(6): 788-794.

Geng Y, Kohli L, Klocke BJ, Roth KA (2010). Chloroquine-induced autophagic vacuole accumulation and cell death in glioma cells is p53 independent. *Neuro-Oncology* **12**(5): 473-481.

Ghersi D, Wilcken N, Simes RJ (2005). A systematic review of taxane-containing regimens for metastatic breast cancer. *British Journal of Cancer* **93**(3): 293-301.

Ghersi D, Willson ML, Chan MM, Simes J, Donoghue E, Wilcken N (2015). Taxane-containing regimens for metastatic breast cancer. *The Cochrane Database of Systematic Reviews* **6:** CD003366.

Gibson L, Lawrence D, Dawson C, Bliss J (2009). Aromatase inhibitors for treatment of advanced breast cancer in postmenopausal women. *The Cochrane Database of Systematic Reviews*(4)**:** CD003370.

Goldhirsch A, Winer EP, Coates AS, Gelber RD, Piccart-Gebhart M, Thürlimann B*, et al.* (2013). Personalizing the treatment of women with early breast cancer: highlights of the St Gallen International Expert Consensus on the Primary Therapy of Early Breast Cancer 2013. *Annals of Oncology* **24**(9)**:** 2206-2223.

Goodwin A, Parker S, Ghersi D, Wilcken N (2009). Post-operative radiotherapy for ductal carcinoma in situ of the breast. *The Cochrane Database of Systematic Reviews* (4)**:** CD000563.

Gottlieb JA, Guarino AM, Call JB, Oliverio VT, Block JB (1970). Preliminary pharmacologic and clinical evaluation of camptothecin sodium (NSC-100880). *Cancer Chemotherapy Reports. Part 1* **54**(6)**:** 461-470.

Häcker G (2000). The morphology of apoptosis. *Cell and Tissue Research* **301**(1)**:** 5-17.

Haibe-Kains B, El-Hachem N, Birkbak NJ, Jin AC, Beck AH, Aerts HJWL*, et al.* (2013). Inconsistency in large pharmacogenomic studies. *Nature* **504**(7480)**:** 389-393.

Hangen E, Blomgren K, Bénit P, Kroemer G, Modjtahedi N (2010). Life with or without AIF. *Trends in Biochemical Sciences* **35**(5)**:** 278-287.

Harmse L, Dahan-Farkas N, Panayides J-L, van Otterlo W, Penny C (2015). Aberrant Apoptotic Response of Colorectal Cancer Cells to Novel Nucleoside Analogues. *PLoS ONE* **10**(9)**:** e0138607.

Henry CM, Hollville E, Martin SJ (2013). Measuring apoptosis by microscopy and flow cytometry. *Methods* **61**(2)**:** 90-97.

Higa GM, Abraham J (2007). Lapatinib in the treatment of breast cancer. *Expert Review of Anticancer Therapy* **7**(9)**:** 1183-1192.

Holliday D, Speirs V (2011). Choosing the right cell line for breast cancer research. *Breast Cancer Research* **13**(4)**:** 215.

Horwitz KB, Costlow ME, McGuire WL (1975). MCF-7: A human breast cancer cell line with estrogen, androgen, progesterone, and glucocorticoid receptors. *Steroids* **26**(6)**:** 785-795.

Ianzini F, Bertoldo A, Kosmacek E, Phillips S, Mackey M (2006). Lack of p53 function promotes radiation-induced mitotic catastrophe in mouse embryonic fibroblast cells. *Cancer Cell International* **6**(1)**:** 11.

International Union Against Cancer (1959). Clinical Stage Classification. Malignant Tumours of the Breast 1960–1964. *British Journal of Radiology* **32**(384): 824-826.

Jackson James G, Pant V, Li Q, Chang Leslie L, Quintás-Cardama A, Garza D, *et al.* (2012). p53-Mediated Senescence Impairs the Apoptotic Response to Chemotherapy and Clinical Outcome in Breast Cancer. *Cancer Cell* **21**(6): 793-806.

Jänicke RU, Sprengart ML, Wati MR, Porter AG (1998). Caspase-3 Is Required for DNA Fragmentation and Morphological Changes Associated with Apoptosis. *Journal of Biological Chemistry* **273**(16): 9357-9360.

Jemal A, Bray F, Center MM, Ferlay J, Ward E, Forman D (2011). Global cancer statistics. *CA Cancer Journal for Clinicians* **61**(2): 69-90.

Jones CB, Clements MK, Wasi S, Daoud SS (1997). Sensitivity to camptothecin of human breast carcinoma and normal endothelial cells. *Cancer Chemotherapy and Pharmacology* **40**(6): 475-483.

Jones SE (2008). Metastatic Breast Cancer: The Treatment Challenge. *Clinical Breast Cancer* **8**(3): 224-233.

Jordan MA, Wendell K, Gardiner S, Brent Derry W, Copp H, Wilson L (1996). Mitotic Block Induced in HeLa Cells by Low Concentrations of Paclitaxel (Taxol) Results in Abnormal Mitotic Exit and Apoptotic Cell Death. *Cancer Research* **56**(4): 816-825.

Juin P, Geneste O, Gautier F, Depil S, Campone M (2013). Decoding and unlocking the BCL-2 dependency of cancer cells. *Nature Reviews Cancer* **13**(7): 455-465.

Kalogerakos K, Sofoudis C, Baltayiannis N (2008). Early breast cancer: A review. *Cancer Therapy* **6**: 463-473.

Kamal A, Rao AV, Nayak VL, Reddy NV, Swapna K, Ramakrishna G, *et al.* (2014). Synthesis and biological evaluation of imidazo[1,5-a]pyridine-benzimidazole hybrids as inhibitors of both tubulin polymerization and PI3K/Akt pathway. *Organic & Biomolecular Chemistry* **12**(48): 9864-9880.

Kamal A, Reddy VS, Karnewar S, Chourasiya SS, Shaik AB, Kumar GB, *et al.* (2013). Synthesis and Biological Evaluation of Imidazopyridine–Oxindole Conjugates as Microtubule-Targeting Agents. *ChemMedChem* **8**(12): 2015-2025.

Kaspers GJL, Wijnands JJM, Hartmann R, Huismans L, Loonen AH, Stackelberg A, *et al.* (2005). Immunophenotypic cell lineage and in vitro cellular drug resistance in childhood relapsed acute lymphoblastic leukaemia. *European Journal of Cancer* **41**(9): 1300-1303.

Kerr JF, Wyllie AH, Currie AR (1972). Apoptosis: a basic biological phenomenon with wide-ranging implications in tissue kinetics. *British Journal of Cancer* **26**(4): 239-257.

Kim R, Tanabe K, Uchida Y, Emi M, Inoue H, Toge T (2002). Current status of the molecular mechanisms of anticancer drug-induced apoptosis. *Cancer Chemotherapy and Pharmacology* **50**(5): 343-352.

Kimura T, Takabatake Y, Takahashi A, Isaka Y (2013). Chloroquine in Cancer Therapy: A Double-Edged Sword of Autophagy. *Cancer Research* **73**(1): 3-7.

King M-C, Marks JH, Mandell JB (2003). Breast and Ovarian Cancer Risks Due to Inherited Mutations in BRCA1 and BRCA2. *Science* **302**(5645): 643-646.

Kinzler KW, Vogelstein B (1997). Cancer-susceptibility genes. Gatekeepers and caretakers. *Nature* **386**(6627): 761, 763.

Klionsky DJ, Abdalla FC, Abeliovich H, Abraham RT, Acevedo-Arozena A, Adeli K, *et al.* (2012). Guidelines for the use and interpretation of assays for monitoring autophagy. *Autophagy* **8**(4): 445-544.

Kong JY, Rabkin SW (2004). Cytoskeletal actin degradation induced by lovastatin in cardiomyocytes is mediated through caspase-2. *Cell Biology International* **28**(11): 781-790.

Kotz J (2012). Phenotypic screening, take two. *SciBX: Science-Business eXchange* **5**(15).

Kracikova M, Akiri G, George A, Sachidanandam R, Aaronson SA (2013). A threshold mechanism mediates p53 cell fate decision between growth arrest and apoptosis. *Cell Death & Differentiation* **20**(4): 576-588.

Krajewski S, Blomqvist C, Franssila K, Krajewska M, Wasenius V-M, Niskanen E, *et al.* (1995). Reduced Expression of Proapoptotic Gene BAX Is Associated with Poor Response Rates to Combination Chemotherapy and Shorter Survival in Women with Metastatic Breast Adenocarcinoma. *Cancer Research* **55**(19): 4471-4478.

Kroemer G, Galluzzi L, Vandenabeele P, Abrams J, Alnemri ES, Baehrecke EH, *et al.* (2009). Classification of cell death: recommendations of the Nomenclature Committee on Cell Death 2009. *Cell Death & Differentiation* **16**(1): 3-11.

Kumar R, Vadlamudi RK, Adam L (2000). Apoptosis in mammary gland and cancer. *Endocrine-Related Cancer* **7**(4): 257-269.

Kunkel TA (2004). DNA Replication Fidelity. *Journal of Biological Chemistry* **279**(17): 16895-16898.

Lacroix M, Leclercq G (2004). Relevance of breast cancer cell lines as models for breast tumours: an update. *Breast Cancer Research and Treatment* **83**(3): 249-289.

Laurent G, Jaffrézou J-P (2001). Signaling pathways activated by daunorubicin. *Blood* **98**(4): 913-924.

Lepecq JB, Paoletti C (1967). A fluorescent complex between ethidium bromide and nucleic acids. *Journal of Molecular Biology* **27**(1): 87-106.

Lester SC, Bose S, Chen YY, Connolly JL, de Baca ME, Fitzgibbons PL, *et al.* (2009). Protocol for the examination of specimens from patients with invasive carcinoma of the breast. *Archives of Pathology & Laboratory Medicine* **133**(10): 1515-1538.

Levenson AS, Jordan VC (1997). MCF-7: The First Hormone-responsive Breast Cancer Cell Line. *Cancer Research* **57**(15): 3071-3078.

Levitt NC, Hickson ID (2002). Caretaker tumour suppressor genes that defend genome integrity. *Trends in Molecular Medicine* **8**(4): 179-186.

Li Y, Karlin A, Loike JD, Silverstein SC (2002). A critical concentration of neutrophils is required for effective bacterial killing in suspension. *Proceedings of the National Academy of Sciences* **99**(12): 8289-8294.

Lindsay MA (2003). Innovation: Target discovery. *Nature Reviews Drug Discovery* **2**(10): 831.

Litière S, Werutsky G, Fentiman IS, Rutgers E, Christiaens M-R, Van Limbergen E, *et al.* (2012). Breast conserving therapy versus mastectomy for stage I–II breast cancer: 20 year follow-up of the EORTC 10801 phase 3 randomised trial. *The Lancet Oncology* **13**(4): 412-419.

Loubser F, Edge, J., Fieggen, K. (2008). Epidemiology, risk factors and genetics in breast cancer. *Continuing Medical Education* **26**(10): 497-500

Lovelace MD, Cahill DM (2007). A rapid cell counting method utilising acridine orange as a novel discriminating marker for both cultured astrocytes and microglia. *Journal of Neuroscience Methods* **165**(2): 223-229.

Lowe SW, Lin AW (2000). Apoptosis in cancer. *Carcinogenesis* **21**(3): 485-495.

Lowery A, Kell M, Glynn R, Kerin M, Sweeney K (2012). Locoregional recurrence after breast cancer surgery: a systematic review by receptor phenotype. *Breast Cancer Research & Treatment* **133**(3): 831-841.

Lozano R, Naghavi M, Foreman K, Lim S, Shibuya K, Aboyans V, *et al.* (2012). Global and regional mortality from 235 causes of death for 20 age groups in 1990 and 2010: a systematic analysis for the Global Burden of Disease Study 2010. *The Lancet* **380**(9859): 2095-2128.

Lu Q, Rounds S (2012). Focal adhesion kinase and endothelial cell apoptosis. *Microvascular Research* **83**(1): 56-63.

Majno G, Joris I (1995). Apoptosis, oncosis, and necrosis. An overview of cell death. *The American Journal of Pathology* **146**(1): 3-15.

Makin G, Hickman JA (2000). Apoptosis and cancer chemotherapy. *Cell and Tissue Research* **301**(1): 143-152.

Malhotra GK, Zhao X, Band H, Band V (2010). Histological, molecular and functional subtypes of breast cancers. *Cancer Biology & Therapy* **10**(10): 955-960.

Mansilla S, Priebe W, Portugal J (2005). Mitotic Catastrophe Results in Cell Death by Caspase-Dependentand Caspase-Independent Mechanisms. *Cell Cycle* **5**(1): 53-60.

Marino G, Kroemer G (2013). Mechanisms of apoptotic phosphatidylserine exposure. *Cell Research* **23**(11): 1247-1248.

Martin L-A, Dowsett M BCL-2: A New Therapeutic Target in Estrogen Receptor-Positive Breast Cancer? *Cancer Cell* **24**(1): 7-9.

Martin L-A, Dowsett M (2013). BCL-2: A New Therapeutic Target in Estrogen Receptor-Positive Breast Cancer? *Cancer Cell* **24**(1): 7-9.

Martinez-Bulit P, Garza-Ortíz A, Mijangos E, Barrón-Sosa L, Sánchez-Bartéz F, Gracia-Mora I, *et al.* (2015). 2,6-Bis(2,6-diethylphenyliminomethyl)pyridine coordination compounds with cobalt(II), nickel(II), copper(II), and zinc(II): synthesis, spectroscopic characterization, X-ray study and in vitro cytotoxicity. *Journal of Inorganic Biochemistry* **142**: 1-7.

Martínez-Urbina MA, Zentella A, Vilchis-Reyes MA, Guzmán Á, Vargas O, Ramírez Apan MT, *et al.* (2010). 6-Substituted 2-(N-trifluoroacetylamino)imidazopyridines induce cell cycle arrest and apoptosis in SK-LU-1 human cancer cell line. *European Journal of Medicinal Chemistry* **45**(3): 1211-1219.

Marushige Y, Marushige K (1998). Alterations in focal adhesion and cytoskeletal proteins during apoptosis. *Anticancer research* **18**(1A): 301-307.

Mayer EL, Burstein HJ (2007). Chemotherapy for Metastatic Breast Cancer. *Hematology/Oncology Clinics of North America* **21**(2): 257-272.

McCormack VA, Joffe M, van den Berg E, Broeze N, Silva Idos S, Romieu I, *et al.* (2013). Breast cancer receptor status and stage at diagnosis in over 1,200 consecutive public hospital patients in Soweto, South Africa: a case series. *Breast Cancer Research* **15**(5): R84.

McMaster GK, Carmichael GG (1977). Analysis of single- and double-stranded nucleic acids on polyacrylamide and agarose gels by using glyoxal and acridine orange. *Proceedings of the National Academy of Sciences* **74**(11): 4835-4838.

Meijer AJ, Codogno P (2009). Autophagy: regulation and role in disease. *Critical Reviews in Clinical Laboratory Sciences* **46**(4): 210-240.

Minotti G, Menna P, Salvatorelli E, Cairo G, Gianni L (2004). Anthracyclines: Molecular Advances and Pharmacologic Developments in Antitumor Activity and Cardiotoxicity. *Pharmacological Reviews* **56**(2): 185-229.

Mommers E, van Diest P, Leonhart A, Meijer C, Baak J (1999). Balance of cell proliferation and apoptosis in breast carcinogenesis. *Breast Cancer Research & Treatment* **58**(2): 163-169.

Monks A, Scudiero D, Skehan P, Shoemaker R, Paull K, Vistica D, *et al.* (1991). Feasibility of a High-Flux Anticancer Drug Screen Using a Diverse Panel of Cultured Human Tumor Cell Lines. *Journal of the National Cancer Institute* **83**(11): 757-766.

Montemurro F, Redana S, Nole F, Donadio M, Jacomuzzzi M, Valabrega G, *et al.* (2008). Vinorelbine-based salvage therapy in HER2-positive metastatic breast cancer

patients progressing during trastuzumab-containing regimens: a retrospective study. *BMC Cancer* **8**(1): 209.

Moreno-Aspitia A, Perez EA (2009). Treatment Options for Breast Cancer Resistant to Anthracycline and Taxane. *Mayo Clinic proceedings. Mayo Clinic* **84**(6): 533-545.

Mosmann T (1983). Rapid colorimetric assay for cellular growth and survival: Application to proliferation and cytotoxicity assays. *Journal of Immunological Methods* **65**(1–2): 55-63.

Moy B, Goss PE (2007). Lapatinib-Associated Toxicity and Practical Management Recommendations. *The Oncologist* **12**(7): 756-765.

Mpoke SS, Wolfe J (1997). Differential Staining of Apoptotic Nuclei in Living Cells: Application to Macronuclear Elimination in Tetrahymena. *Journal of Histochemistry & Cytochemistry* **45**(5): 675-683.

Muggia FM, Creaven PJ, Hansen HH, Cohen MH, Selawry OS (1972). Phase I clinical trial of weekly and daily treatment with camptothecin (NSC-100880): correlation with preclinical studies. *Cancer Chemotherapy Reports. Part 1* **56**(4): 515-521.

Nabholtz JM, Reese D, Lindsay MA, Riva A (2002). Evidence for the use of chemotherapy in breast cancer. *International Journal of Clinical Oncology* **7**(4): 254-264.

National Cancer Institute (2013). Breast Cancer Treatment. In: *National Cancer Institute*, Institute NC (ed) Vol. 2013.

National Health Laboratory Services (2010). Cancer in South Africa Full Reports: 2000 - 2010. http://www.nioh.ac.za/?page=national_cancer_registry&id=41 [accessed 23 June 2015]

Nieves-Neira W, Pommier Y (1999). Apoptotic response to camptothecin and 7-hydroxystaurosporine (UCN-01) in the 8 human breast cancer cell lines of the NCI Anticancer Drug Screen: multifactorial relationships with topoisomerase I, protein kinase C, Bcl-2, p53, MDM-2 and caspase pathways. *International Journal of Cancer* **82**(3): 396-404.

Nik-Zainal S, Alexandrov Ludmil B, Wedge David C, Van Loo P, Greenman Christopher D, Raine K, *et al.* (2012). Mutational Processes Molding the Genomes of 21 Breast Cancers. *Cell* **149**(5): 979-993.

O'Shaughnessy J (2005). Extending Survival with Chemotherapy in Metastatic Breast Cancer. *The Oncologist* **10**(s3): 20-29.

Oakes SR, Vaillant F, Lim E, Lee L, Breslin K, Feleppa F, *et al.* (2012). Sensitization of BCL-2–expressing breast tumors to chemotherapy by the BH3 mimetic ABT-737. *Proceedings of the National Academy of Sciences* **109**(8): 2766-2771.

Outhoff K (2011). The art of prescribing trastuzumab for HER2-positive breast cancer. *South African Journal of Gynaecology and Oncology* **3**(1): 16-26.

Ouyang L, Shi Z, Zhao S, Wang FT, Zhou TT, Liu B, *et al.* (2012). Programmed cell death pathways in cancer: a review of apoptosis, autophagy and programmed necrosis. *Cell Proliferation* **45**(6): 487-498.

Pagani O, Senkus E, Wood W, Colleoni M, Cufer T, Kyriakides S, *et al.* (2010). International Guidelines for Management of Metastatic Breast Cancer: Can Metastatic Breast Cancer Be Cured? *Journal of the National Cancer Institute* **102**(7): 456-463.

Parton M, Dowsett M, Smith I (2001). Studies of apoptosis in breast cancer. *BMJ* **322**(7301): 1528-1532

Perou CM (2011). Molecular Stratification of Triple-Negative Breast Cancers. *The Oncologist* **16**(s1): 61-70.

Perou CM, Sorlie T, Eisen MB, van de Rijn M, Jeffrey SS, Rees CA, *et al.* (2000). Molecular portraits of human breast tumours. *Nature* **406**(6797): 747-752.

Pizzo PA (1993). Management of Fever in Patients with Cancer and Treatment-Induced Neutropenia. *New England Journal of Medicine* **328**(18): 1323-1332.

Portier BP, Taglialatela G (2006). Bcl-2 localized at the nuclear compartment induces apoptosis after transient overexpression. *The Journal of Biological Chemistry* **281**(52): 40493-40502.

Portugal J, Mansilla S, Bataller M (2010). Mechanisms of drug-induced mitotic catastrophe in cancer cells. *Current Pharmaceutical Design* **16**(1): 69-78.

Prat A, Parker J, Karginova O, Fan C, Livasy C, Herschkowitz J, *et al.* (2010). Phenotypic and molecular characterization of the claudin-low intrinsic subtype of breast cancer. *Breast Cancer Research* **12**(5): R68.

Quigley Iii JD, Martin KR, Dowlen HH (1995). Concentrations of Trypsin Inhibitor and Immunoglobulins in Colostrum of Jersey Cows. *Journal of Dairy Science* **78**(7): 1573-1577.

Reed JC (1999). Dysregulation of Apoptosis in Cancer. *Journal of Clinical Oncology* **17**(9): 2941.

Reis-Filho JS, Pusztai L (2011). Gene expression profiling in breast cancer: classification, prognostication, and prediction. *The Lancet* **378**(9805): 1812-1823.

Ribble D, Goldstein N, Norris D, Shellman Y (2005). A simple technique for quantifying apoptosis in 96-well plates. *BMC Biotechnology* **5**(1): 12.

Rigler R, Jr. (1966). Microfluorometric characterization of intracellular nucleic acids and nucleoproteins by acridine orange. *Acta Physiologica Scandinavica. Supplementum* **267**: 1-122.

Robbins E, Marcus PI, Gonatas NK (1964). DYNAMICS OF ACRIDINE ORANGE-CELL INTERACTION: II. Dye-Induced Ultrastructural Changes in Multivesicular Bodies (Acridine Orange Particles). *The Journal of Cell Biology* **21**(1): 49-62.

Roninson IB, Broude EV, Chang B-D (2001). If not apoptosis, then what? Treatment-induced senescence and mitotic catastrophe in tumor cells. *Drug Resistance Updates* **4**(5): 303-313.

Saeki T, Adachi I, Ogita M, Tabei T, Shin E, Tamura K, *et al.* (2000). Combination chemotherapy with vinorelbine and other cytotoxic agents for advanced breast cancer patients--a protocol of vinorelbine plus AC regimens used by the Japan Vinorelbin Study Group. *Gan to kagaku ryoho. Cancer & Chemotherapy* **27**(8): 1180-1184.

Salvesen GS, Duckett CS (2002). IAP proteins: blocking the road to death's door. *Nature Reviews Molecular Cell Biology* **3**(6): 401-410.

Sanchez-Alcazar JA, Ault JG, Khodjakov A, Schneider E (2000). Increased mitochondrial cytochrome c levels and mitochondrial hyperpolarization precede camptothecin-induced apoptosis in Jurkat cells. *Cell Death Differ* **7**(11): 1090-1100.

Saraste A, Pulkki K (2000). Morphologic and biochemical hallmarks of apoptosis. *Cardiovascular Research* **45**(3): 528-537.
Segawa K, Kurata S, Yanagihashi Y, Brummelkamp TR, Matsuda F, Nagata S (2014). Caspase-mediated cleavage of phospholipid flippase for apoptotic phosphatidylserine exposure. *Science* **344**(6188): 1164-1168.

Sharifi S, Barar J, Hejazi MS, Samadi N (2014). Roles of the Bcl-2/Bax ratio, caspase-8 and 9 in resistance of breast cancer cells to paclitaxel. *Asian Pacific Journal of Cancer Prevention* **15**(20): 8617-8622.

Siegel RL, Miller KD, Jemal A (2015). Cancer statistics, 2015. *CA Cancer J Clin* **65**(1): 5-29.

Simbayi LC, Shisana O, Rehle T, Onoya D, Jooste S, Zungu N, *et al.* (2014). *South African National HIV Prevalence, Incidence and Behaviour Survey, 2012* Pretoria: Human Sciences Research Council.

Simpson ER, Mahendroo MS, Means GD, Kilgore MW, Hinshelwood MM, Graham-Lorence S, *et al.* (1994). Aromatase Cytochrome P450, The Enzyme Responsible for Estrogen Biosynthesis. *Endocrine Reviews* **15**(3): 342-355.

Singletary SE, Allred C, Ashley P, Bassett LW, Berry D, Bland KI, *et al.* (2003a). Staging system for breast cancer: revisions for the 6th edition of the AJCC Cancer Staging Manual. *Surgical Clinics of North America* **83**(4): 803-819.

Singletary SE, Greene FL (2003b). Revision of breast cancer staging: the 6th edition of the TNM Classification. *Seminars in Surgical Oncology* **21**(1): 53-59.

Slee EA, Adrain C, Martin SJ (2001). Executioner Caspase-3, -6, and -7 Perform Distinct, Non-redundant Roles during the Demolition Phase of Apoptosis. *Journal of Biological Chemistry* **276**(10): 7320-7326.

Sobin LH (2001). TNM: principles, history, and relation to other prognostic factors. *Cancer* **91**(8 Suppl): 1589-1592.

Soldani C, Lazzè MC, Bottone MG, Tognon G, Biggiogera M, Pellicciari CE, *et al.* (2001). Poly(ADP-ribose) Polymerase Cleavage during Apoptosis: When and Where? *Experimental Cell Research* **269**(2): 193-201.

Soldani C, Scovassi AI (2002). Poly(ADP-ribose) polymerase-1 cleavage during apoptosis: An update. *Apoptosis* **7**(4): 321-328.

Song Q, Wei T, Lees-Miller S, Alnemri E, Watters D, Lavin MF (1997). Resistance of actin to cleavage during apoptosis. *Proceedings of the National Academy of Sciences* **94**(1): 157-162.

Sørlie T, Perou CM, Tibshirani R, Aas T, Geisler S, Johnsen H, *et al.* (2001). Gene expression patterns of breast carcinomas distinguish tumor subclasses with clinical implications. *Proceedings of the National Academy of Sciences* **98**(19): 10869-10874.

Sørlie T, Tibshirani R, Parker J, Hastie T, Marron JS, Nobel A, *et al.* (2003). Repeated observation of breast tumor subtypes in independent gene expression data sets. *Proceedings of the National Academy of Sciences* **100**(14): 8418-8423.

Strober W (2001). APPENDIX 3B Trypan Blue Exclusion Test of Cell Viability. In: *Current Protocols in Immunology*, John Wiley & Sons, Inc.

Swinney DC (2013). The Contribution of Mechanistic Understanding to Phenotypic Screening for First-in-Class Medicines. *Journal of Biomolecular Screening* **18**(10): 1186-1192.

Swinney DC (2014). The value of translational biomarkers to phenotypic assays. *Frontiers in Pharmacology* **5**(171).

Swinney DC, Anthony J (2011). How were new medicines discovered? *Nature Reviews Drug Discovery* **10**(7): 507-519.

Tardito S, Bussolati O, Gaccioli F, Gatti R, Guizzardi S, Uggeri J, *et al.* (2006). Non-apoptotic programmed cell death induced by a copper(II) complex in human fibrosarcoma cells. *Histochemistry and Cell Biology* **126**(4): 473-482.

Triglia RP, Linscott WD (1980). Titers of nine complement components, conglutinin and C3b-inactivator in adult and fetal bovine sera. *Molecular Immunology* **17**(6): 741-748.

Tsujimoto Y, Finger LR, Yunis J, Nowell PC, Croce CM (1984). Cloning of the chromosome breakpoint of neoplastic B cells with the t(14;18) chromosome translocation. *Science* **226**(4678): 1097-1099.

Twiddy D, Cohen GM, MacFarlane M, Cain K (2006). Caspase-7 Is Directly Activated by the ~700-kDa Apoptosome Complex and Is Released as a Stable XIAP-Caspase-7 ~200-kDa Complex. *Journal of Biological Chemistry* **281**(7): 3876-3888.

Uday Bhanu M, Kondapi AK (2010). Neurotoxic activity of a Topoisomerase-I inhibitor, camptothecin, in cultured cerebellar granule neurons. *NeuroToxicology* **31**(6): 730-737.

Umekita Y, Takasaki T, Yoshida H (1994). Expression of p53 protein in benign epithelial hyperplasia, atypical ductal hyperplasia, non-invasive and invasive mammary carcinoma: an immunohistochemical study. *Virchows Archiv: The European Journal of Pathology* **424**(5): 491-494.

US Food and Drug Administration (2010). FDA Expands Use of Approved Breast Cancer Drug. In: *News & Events* http://www.fda.gov/NewsEvents/Newsroom/PressAnnouncements/ucm199374.htm [accessed 31 July 2014]

Vaillant F, Merino D, Lee L, Breslin K, Pal B, Ritchie Matthew E, *et al.* (2013). Targeting BCL-2 with the BH3 Mimetic ABT-199 in Estrogen Receptor-Positive Breast Cancer. *Cancer Cell* **24**(1): 120-129.

Vakifahmetoglu H, Olsson M, Zhivotovsky B (2008). Death through a tragedy: mitotic catastrophe. *Cell Death & Diffeentiation* **15**(7): 1153-1162.

Vakifahmetoglu-Norberg H, Norberg E, Perdomo AB, Olsson M, Ciccosanti F, Orrenius S, *et al.* (2013). Caspase-2 promotes cytoskeleton protein degradation during apoptotic cell death. *Cell Death & Disease* **4**: e940.

Vakkala M, Lähteenmäki K, Raunio H, Pääkkö P, Soini Y (1999). Apoptosis during Breast Carcinoma Progression. *Clinical Cancer Research* **5**(2): 319-324.

van Slooten HJ, van de Vijver MJ, van de Velde CJ, van Dierendonck JH (1998). Loss of Bcl-2 in invasive breast cancer is associated with high rates of cell death, but also with increased proliferative activity. *British Journal of Cancer* **77**(5): 789-796.

Vanags DM, Pörn-Ares MI, Coppola S, Burgess DH, Orrenius S (1996). Protease Involvement in Fodrin Cleavage and Phosphatidylserine Exposure in Apoptosis. *Journal of Biological Chemistry* **271**(49): 31075-31085.

Vanden Berghe T, Grootjans S, Goossens V, Dondelinger Y, Krysko DV, Takahashi N, *et al.* (2013). Determination of apoptotic and necrotic cell death in vitro and in vivo. *Methods* **61**(2): 117-129.

Vařecha M, Potěšilová M, Matula P, Kozubek M (2012). Endonuclease G interacts with histone H2B and DNA topoisomerase II alpha during apoptosis. *Molecular and Cellular Biochemistry* **363**(1-2): 301-307.

Vaseva Angelina V, Marchenko Natalie D, Ji K, Tsirka Stella E, Holzmann S, Moll Ute M (2012). p53 Opens the Mitochondrial Permeability Transition Pore to Trigger Necrosis. *Cell* **149**(7): 1536-1548.

Venkitaraman AR (2001). Functions of BRCA1 and BRCA2 in the biological response to DNA damage. *Journal of Cell Science* **114**(20): 3591-3598.

von Minckwitz G, Untch M, Blohmer JU, Costa SD, Eidtmann H, Fasching PA, *et al.* (2012). Definition and impact of pathologic complete response on prognosis after neoadjuvant chemotherapy in various intrinsic breast cancer subtypes. *Journal of Clinical Oncology* **30**(15): 1796-1804.

Vorobiof DA, Sitas F, Vorobiof G (2001). Breast cancer incidence in South Africa. *Journal of Clinical Oncology* **19**(18 Suppl): 125S-127S.

Wagner AD, Thomssen C, Haerting J, Unverzagt S (2012). Vascular-endothelial-growth-factor (VEGF) targeting therapies for endocrine refractory or resistant metastatic breast cancer. *The Cochrane Database of Systematic Reviews* **7**: CD008941.

Wajant H (2003). Death receptors. *Essays In Biochemistry* **39**: 53-71.

Walerych D, Napoli M, Collavin L, Del Sal G (2012). The rebel angel: mutant p53 as the driving oncogene in breast cancer. *Carcinogenesis* **33**(11): 2007-2017.

Waring MJ (1965). Complex formation between ethidium bromide and nucleic acids. *Journal of Molecular Biology* **13**(1): 269-282.

Wei MC, Zong W-X, Cheng EH-Y, Lindsten T, Panoutsakopoulou V, Ross AJ, *et al.* (2001). Proapoptotic BAX and BAK: A Requisite Gateway to Mitochondrial Dysfunction and Death. *Science* **292**(5517): 727-730.

Weigel MT, Dowsett M (2010). Current and emerging biomarkers in breast cancer: prognosis and prediction. *Endocrine-Related Cancer* **17**(4): R245-R262.

Weigelt B, Horlings HM, Kreike B, Hayes MM, Hauptmann M, Wessels LF, *et al.* (2008). Refinement of breast cancer classification by molecular characterization of histological special types. *The Journal of Pathology* **216**(2): 141-150.

Wolf BB, Schuler M, Echeverri F, Green DR (1999). Caspase-3 Is the Primary Activator of Apoptotic DNA Fragmentation via DNA Fragmentation Factor-45/Inhibitor of Caspase-activated DNase Inactivation. *Journal of Biological Chemistry* **274**(43): 30651-30656.

Wong RS (2011). Apoptosis in cancer: from pathogenesis to treatment. *Journal of Experimental & Clinical Cancer Research* **30**(1): 1-14.

Woo M, Hakem R, Soengas MS, Duncan GS, Shahinian A, Kägi D, *et al.* (1998). Essential contribution of caspase 3/CPP32 to apoptosis and its associated nuclear changes. *Genes & Development* **12**(6): 806-819.

Wood ER, Truesdale AT, McDonald OB, Yuan D, Hassell A, Dickerson SH, *et al.* (2004). A Unique Structure for Epidermal Growth Factor Receptor Bound to GW572016 (Lapatinib): Relationships among Protein Conformation, Inhibitor Off-Rate, and Receptor Activity in Tumor Cells. *Cancer Research* **64**(18): 6652-6659.

Woolston C (2011). Avastin, the FDA and a question of effectiveness (not hope). In: *Los Angeles Times*. Los Angeles: Los Angeles Times. http://articles.latimes.com/2011/jun/30/news/la-heb-avastin-fda-20110630 [accessed 20 March 2013]

Yamamoto M, Hosoda M, Nakano K, Jia S, Hatanaka KC, Takakuwa E, *et al.* (2014). p53 accumulation is a strong predictor of recurrence in estrogen receptor-positive breast cancer patients treated with aromatase inhibitors. *Cancer Science* **105**(1): 81-88.

Yip KW, Reed JC (2008). Bcl-2 family proteins and cancer. *Oncogene* **27**(50): 6398-6406.

Yu S-W, Andrabi SA, Wang H, Kim NS, Poirier GG, Dawson TM, *et al.* (2006). Apoptosis-inducing factor mediates poly(ADP-ribose) (PAR) polymer-induced cell death. *Proceedings of the National Academy of Sciences* **103**(48): 18314-18319.

Zapata J, Krajewska M, Krajewski S, Huang R-P, Takayama S, Wang H-G, *et al.* (1998). Expression of multiple apoptosis-regulatory genes in human breast cancer cell lines and primary tumors. *Breast Cancer Research and Treatment* **47**(2): 129-140.

Zelenin AV (1966). Fluorescence Microscopy of Lysosomes and Related Structures in Living Cells. *Nature* **212**(5060): 425-426.

Chapter 7 – Appendix

Appendix A: Additional Documents

University
of the Witwatersrand,
Johannesburg

Human Research Ethics Committee (Medical)
(formerly Committee for Research on Human Subjects (Medical)

Secretariat Research Office, Room SH10005, 10th floor, Senate House • Telephone +27 11 717 1234 • Fax +27 11 339-1709
Private Bag 3, Wits 2050, South Africa

Ref: W-CJ-130311-2

11/03/2013

TO WHOM IT MAY CONCERN:

Waiver: This certifies that the following research does not require clearance from the Human Research Ethics Committee (Medical).

Investigator: **Dr L Harmse, Mr T Kurebwa (student no 303793).**

Project title: **The anti-cancer effects of azaindoles and imidazopyridines on breast cancer cells.**

Reason: This is a laboratory study using cell lines including K562, Jurkats, HL60, HEK93, MCF7, MDM, HT29 and Caco-2. No humans are involved.

UNIVERSITY OF THE WITWATERSRAND
2013 -03- 1 1

Professor Peter Cleaton-Jones
Chair, Human Research Ethics Committee (Medical)

copy: Anisa Keshav, Research Office, Senate House, Wits

R14/49 Dr Robyn L van Zyl

HUMAN RESEARCH ETHICS COMMITTEE (MEDICAL)

CLEARANCE CERTIFICATE NO. M140669

NAME: (Principal Investigator) Dr Robyn L van Zyl

DEPARTMENT: Pharmacy & Pharmacology
Medical School

PROJECT TITLE: The Chemotherapeutic Properties of Novel Synthetic and Natural Compounds (Renewal previously M090532)

DATE CONSIDERED: 29/05/2009 (Initial Approval) 26/06/2014 (Renewal)

DECISION: Approved unconditionally

CONDITIONS:

SUPERVISOR:

APPROVED BY: Professor PE Cleaton-Jones, Chairperson, HREC (Medical)

DATE OF APPROVAL: 26/06/2014

This clearance certificate is valid for 5 years from date of approval. Extension may be applied for.

DECLARATION OF INVESTIGATORS

To be completed in duplicate and **ONE COPY** returned to the Secretary in Room 10004, 10th floor, Senate House, University.

I/we fully understand the conditions under which I am/we are authorized to carry out the above-mentioned research and I/we undertake to ensure compliance with these conditions. Should any departure be contemplated, from the research protocol as approved, I/we undertake to resubmit the application to the Committee. **I agree to submit a yearly progress report**.

Principal Investigator Signature

Date 21-07-2014

PLEASE QUOTE THE PROTOCOL NUMBER IN ALL ENQUIRIES

UNIVERSITY OF THE
WITWATERSRAND
JOHANNESBURG

Private Bag 3 Wits, 2050
Fax: 027117172119
Tel: 02711 7172076

Reference: Ms Thokozile Nhlapo
E-mail: thokozile.nhlapo@wits.ac.za

25 August 2015
Person No: 303793
TAA

Mr TF Kurebwa
134 Coronation Avenue
Greendale
0000
Zimbabwe

Dear Mr Kurebwa

Master of Science in Medicine: Change of title of research

I am pleased to inform you that the following change in the title of your Dissertation for the degree of **Master of Science in Medicine** has been approved:

From:	**An In Vitro study of the effects of novel 7-azaindoles and 6-substituted imidazoles on breast cancer cells**
To:	**The effect of imidazole derivatives on MCF-7 and MDA-MB-231 breast cancer cells**

Yours sincerely

Mrs Sandra Benn
Faculty Registrar
Faculty of Health Sciences

UNIVERSITY OF THE WITWATERSRAND, JOHANNESBURG | FACULTY OF HEALTH SCIENCES

APPLICATION FOR CHANGE OF TITLE OF APPROVED RESEARCH REPORT, DISSERTATION OR THESIS

Student Surname and Initials: _____KUREBWA TF____ Student Number: ____303793___

Degree: ____MASTER OF SCIENCE IN MEDICINE (PHARMACOLOGY)_____

Department: ___PHARMACY & PHARMACOLOGY__ Telephone: __+27762551734_ E-mail: ___t.kurebwa@gmail.com__

Current Title: ___THE EFFECT OF IMIDAZOLE DERIVATIVES ON MCF-7 AND MDA-MB-231 BREAST CANCER CELLS

New Title: ___ The effect of imidazo[1, 2-a]pyridine amines on MCF-7 and MDA-MB-231 breast cancer cells

Motivation / Reason for title change: _____Upon discussion with our collaborators who synthesized the compounds we agreed that the new title better represents the nomenclature of the novel compounds

Approvals / signatures:

Student: _____ Date:__21/09/15_

Supervisor(s) names:__DR LEONIE HARMSE__ Departments: PHARMACY & PHARMACOLOGY

Supervisor(s) Telephone: 011 717 2542 Supervisor(s) E-mail: leonie.harmse@wits.ac.za

Supervisor 1 Signature _____

Supervisor(s) names:_____. Departments:

Supervisor(s) Telephone: _____ Supervisor(s) E-mail:

Supervisor 2 Signature _____

Supervisor(s) names:_____ Departments:

Supervisor(s) Telephone: _____ Supervisor(s) E-mail:

Supervisor 3 Signature _____

*HEAD OF DEPARTMENT / HEAD OF SCHOOL: *(Where the HOD is Supervisor, the HOS must sign)*

_____ _____ _____
(Name and Surname) (Signature) (Date)

DECISION OF CHAIR OF THE PG COMMITTEE: _____

Signature: _____ **Date:** _____

Appendix B: Standard Curves

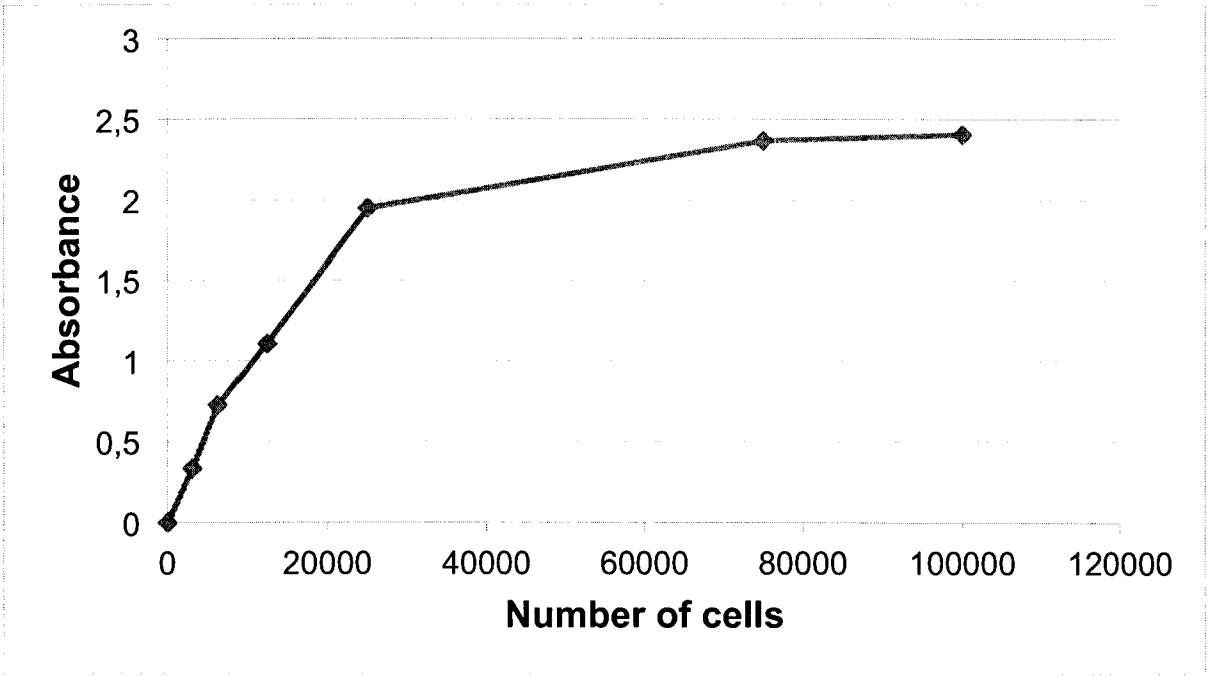


Figure B7.1 Standard curve for MCF-7 cells using the MTT assay

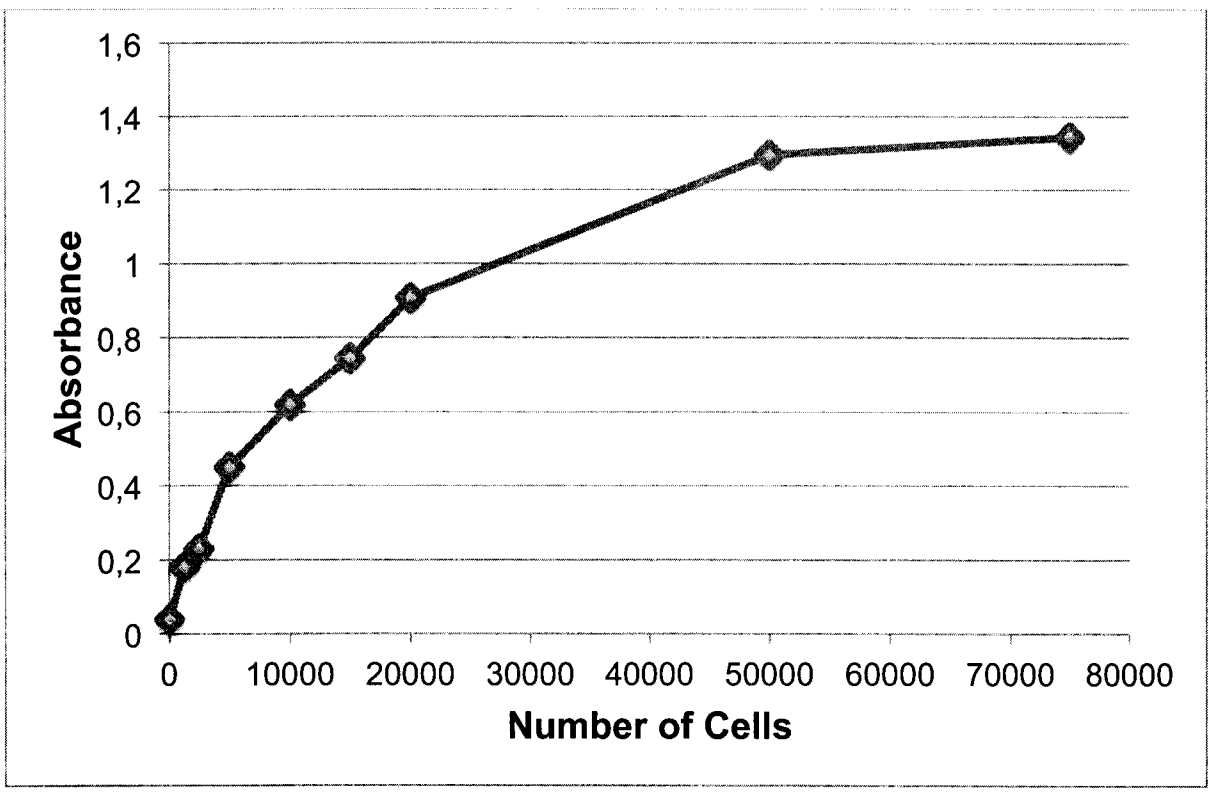


Figure B7.2 Standard curve for MDA-MB-231 cells using the MTT assay

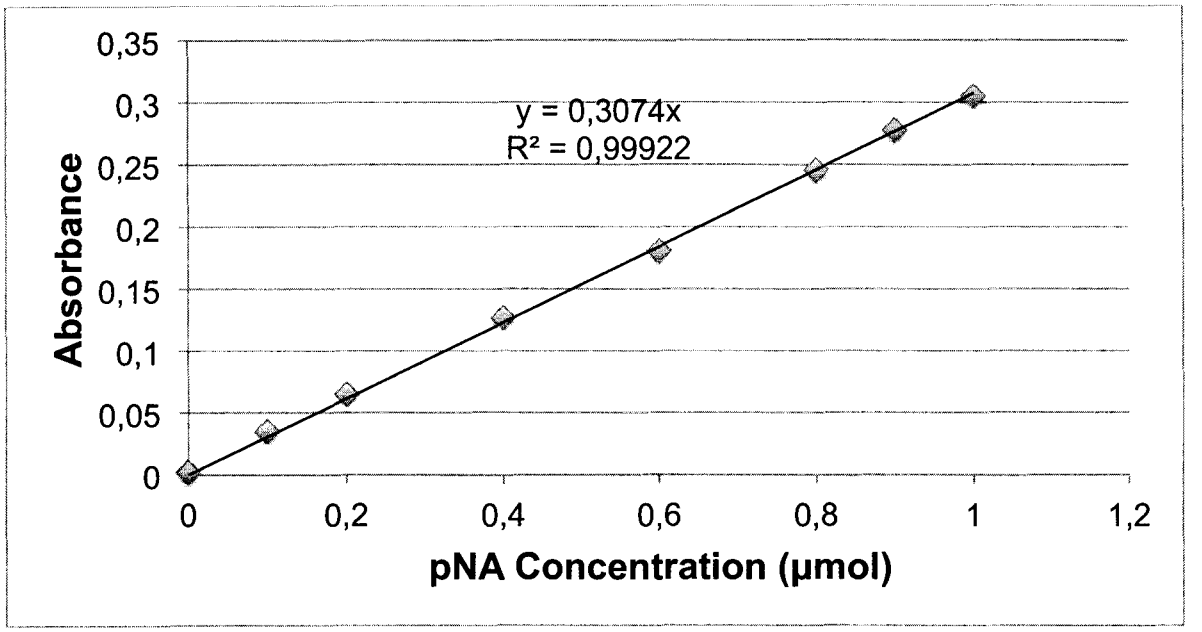


Figure B7.3 Caspase assay pNa standard curve

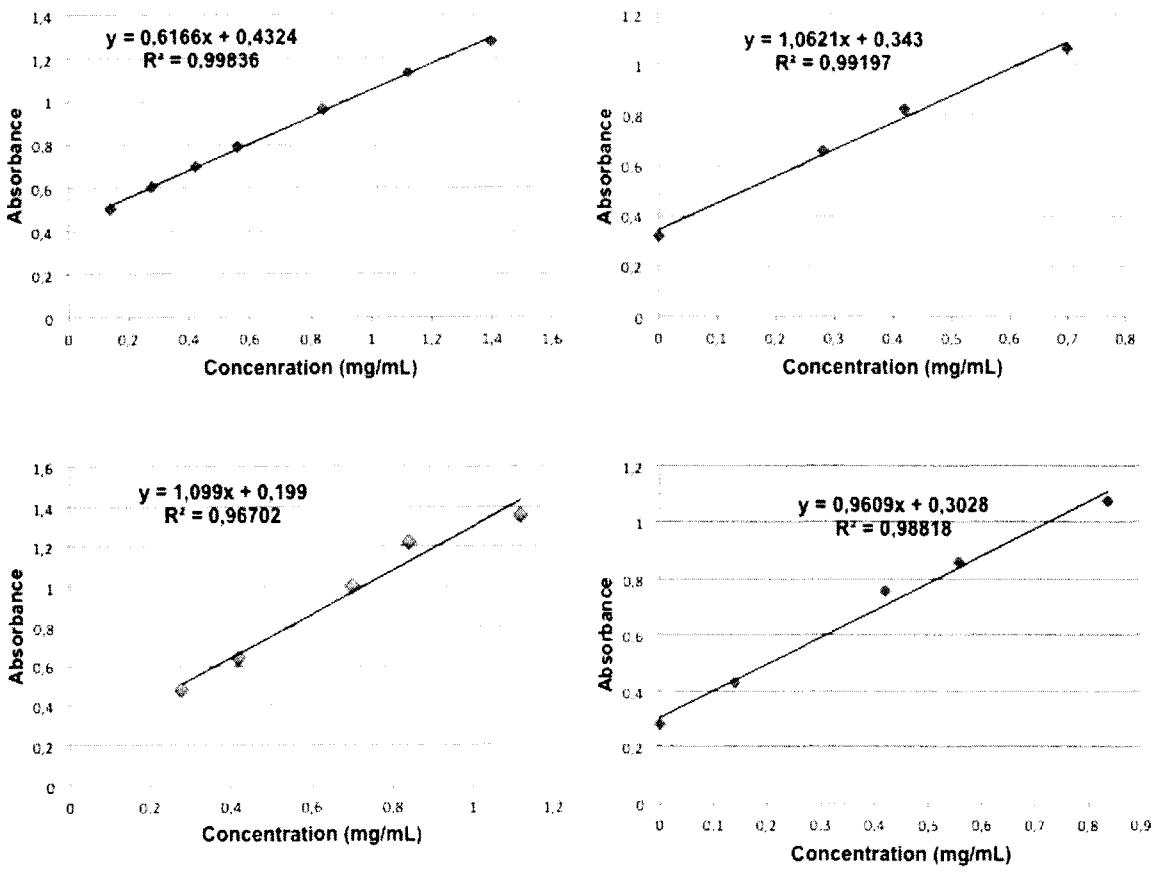


Figure B7.4 Standard curves for protein concentrations in the caspase assay (Experiment 1-4)

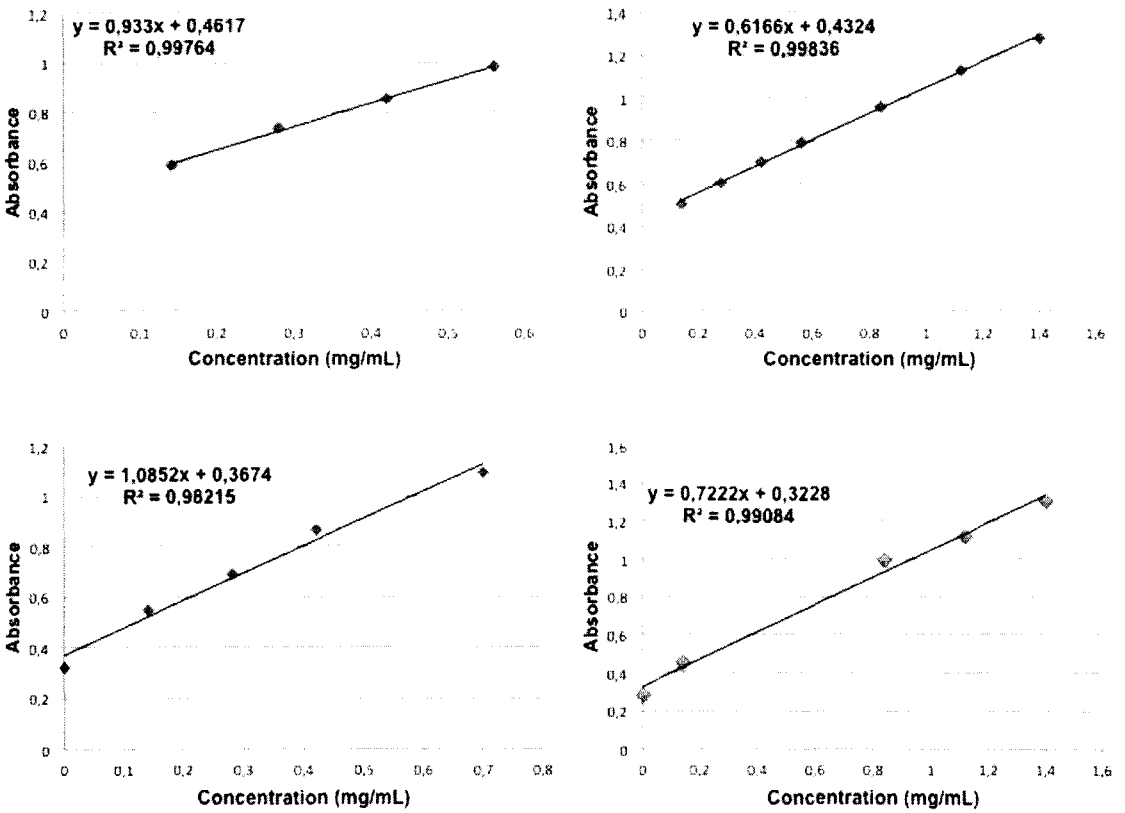


Figure B7.5 Standard curves for protein concentrations in the caspase assay (Experiment 5-8)

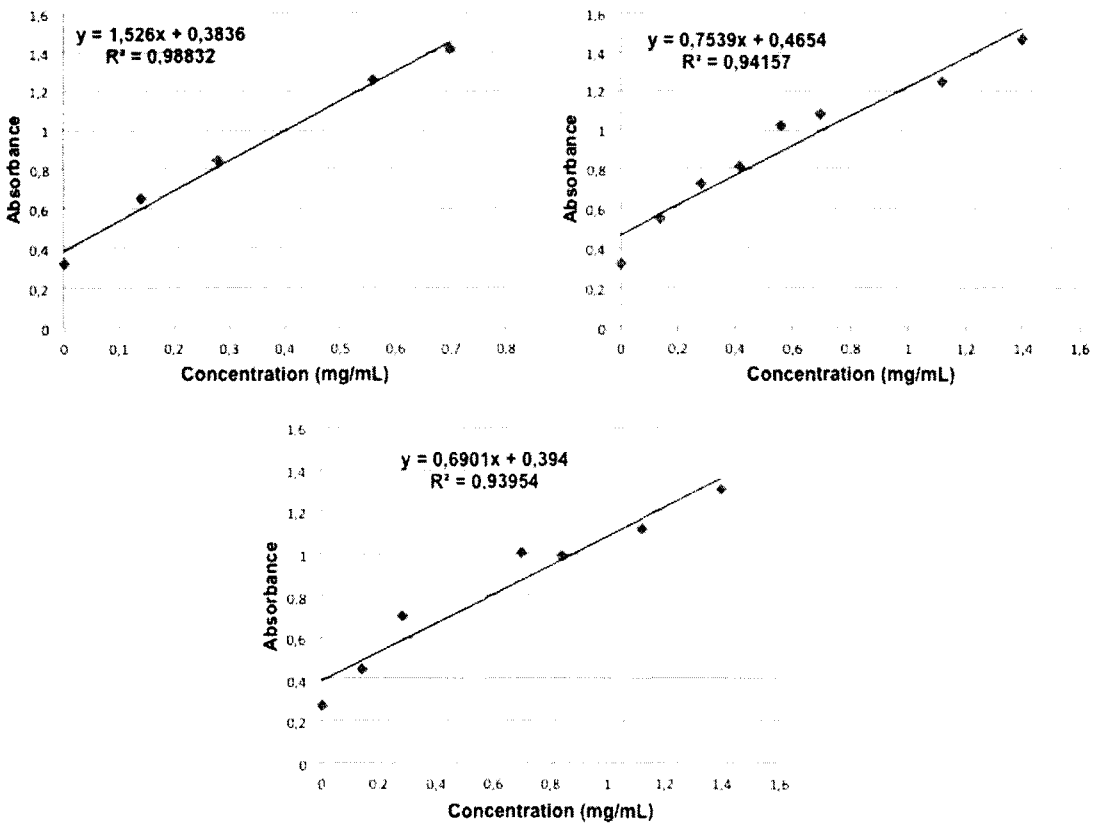


Figure B7.6 Standard curves for protein concentrations (Experiment 9-11)

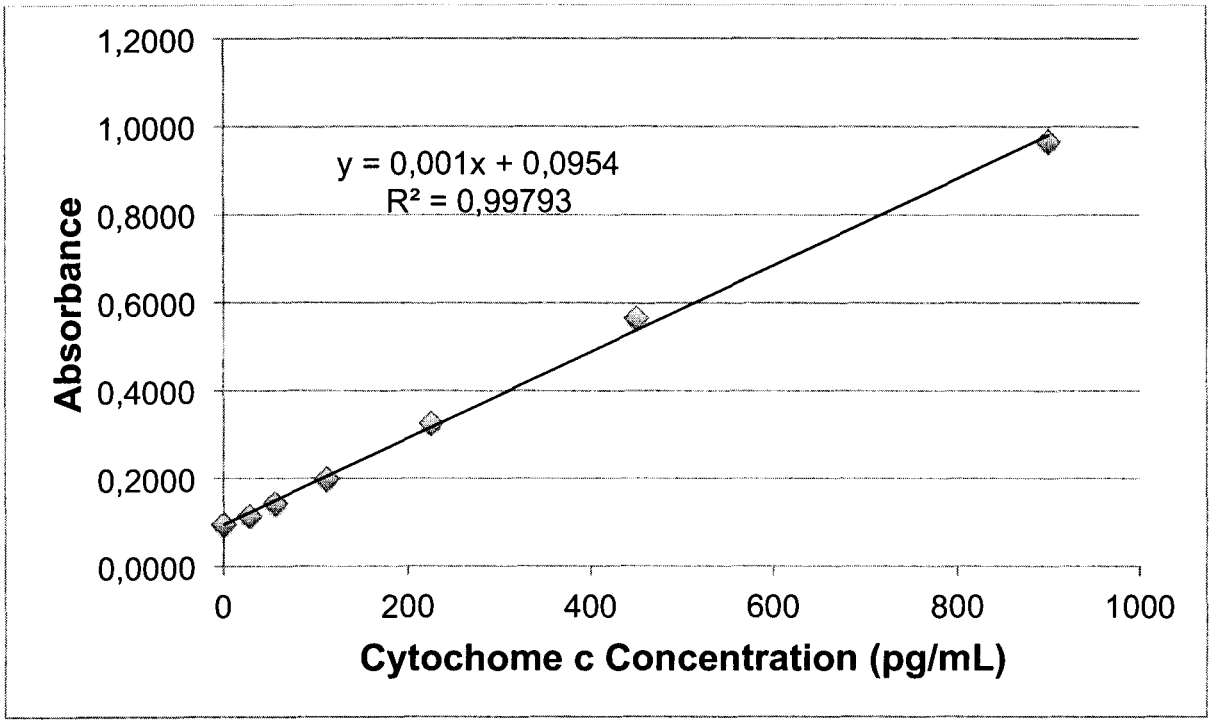


Figure B7.7 pNA standard curve for cytochrome c assay

Appendix C: Microscopy

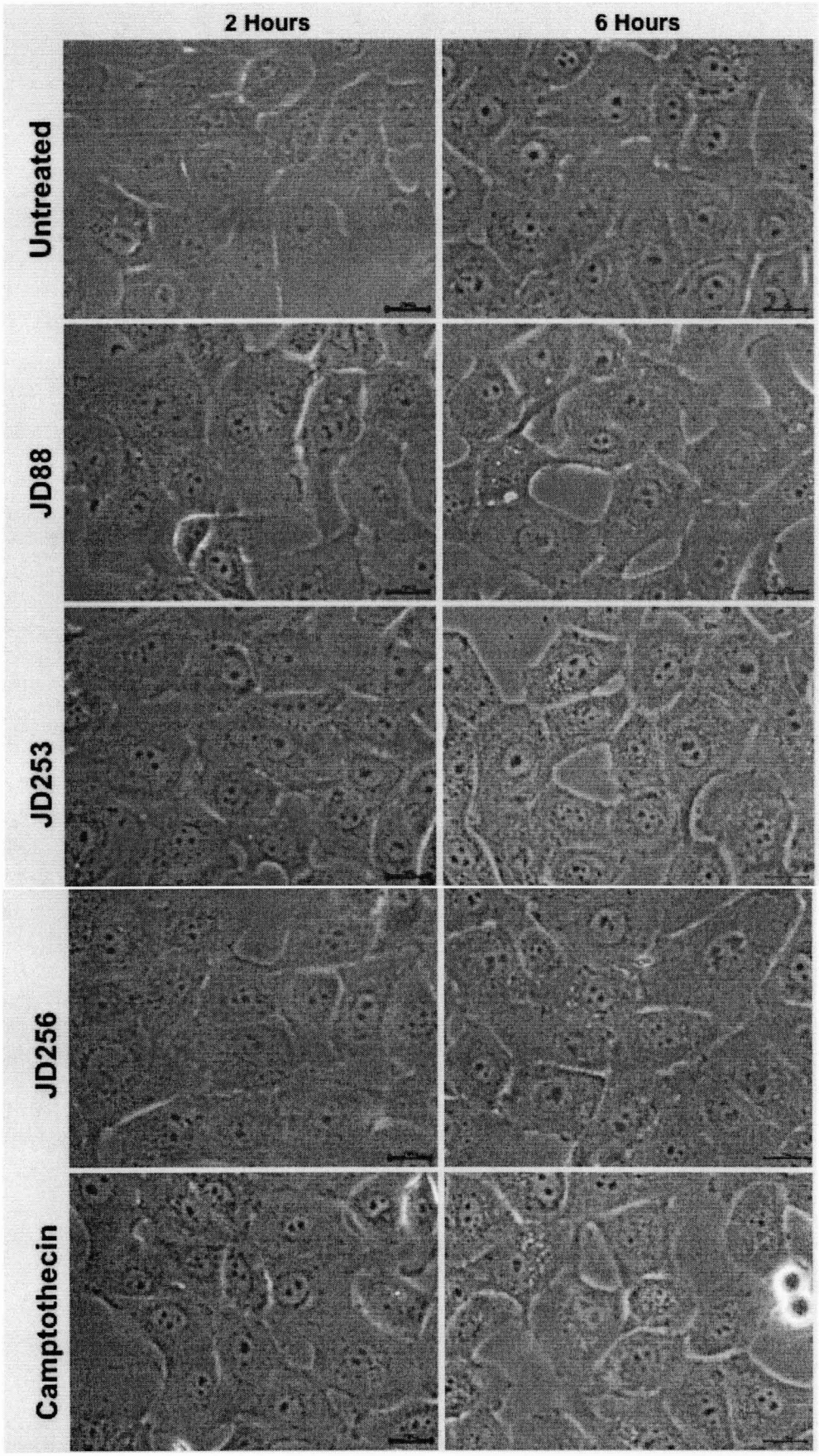


Figure C7.8 Effect of test compounds at IC_{50} values on MCF-7 cell morphology after 2 and 6 hours

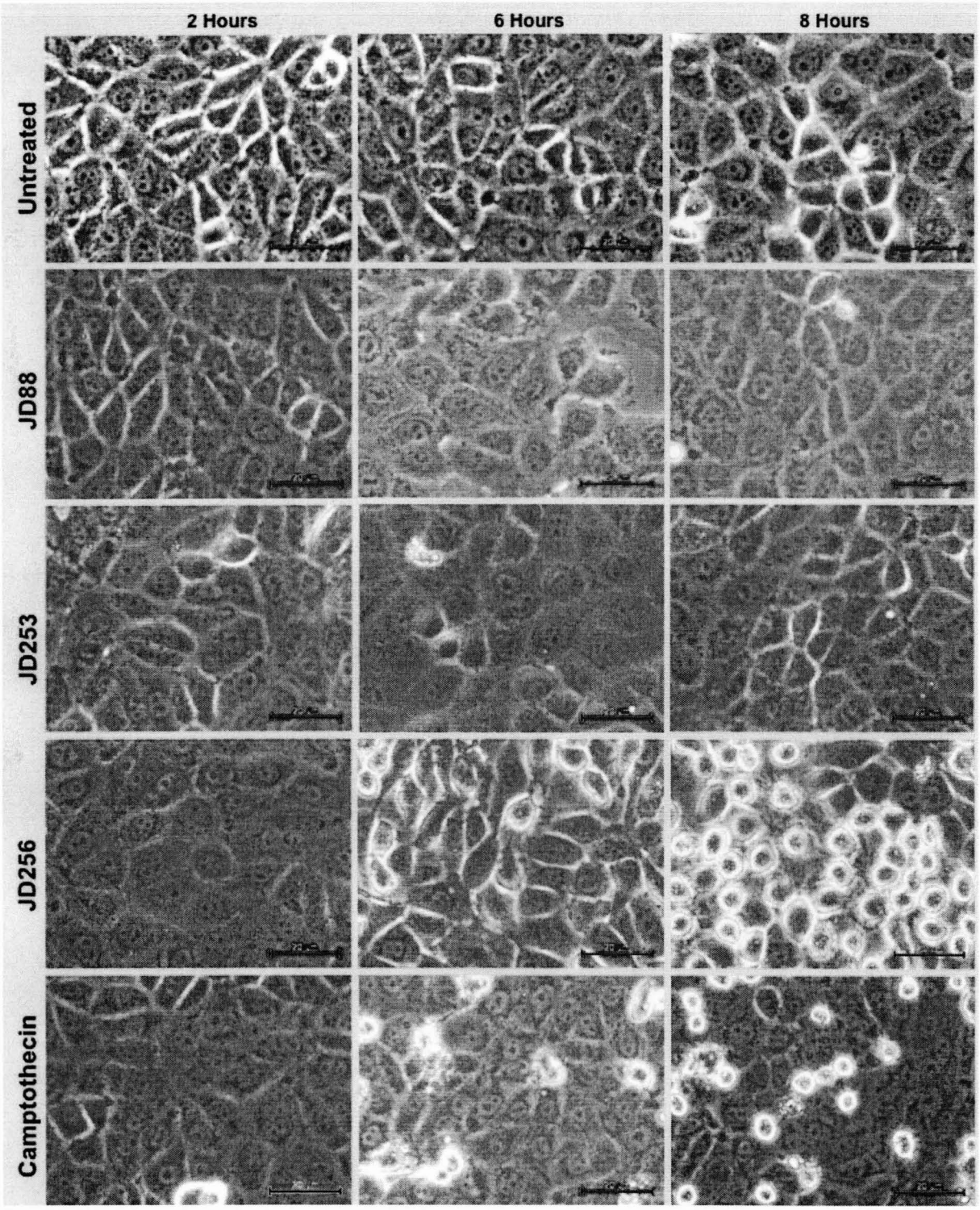


Figure C7.9 Effect of test compounds at 25 µM on MCF-7 cell morphology at 2, 6 and 8 hours

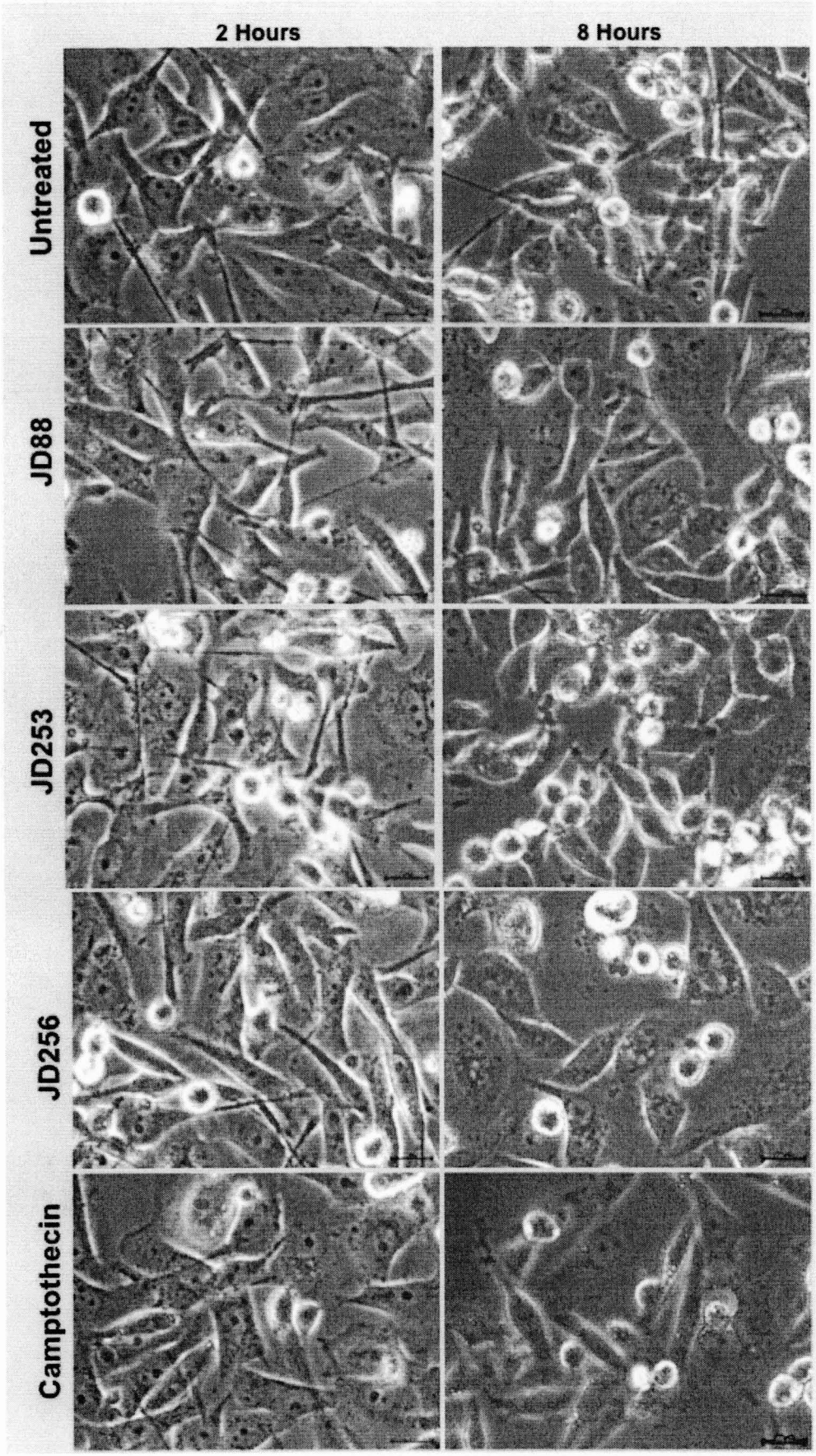


Figure C7.10 Effect of test compounds on MDA-MB-231 cell morphology at 2 and 8 hours

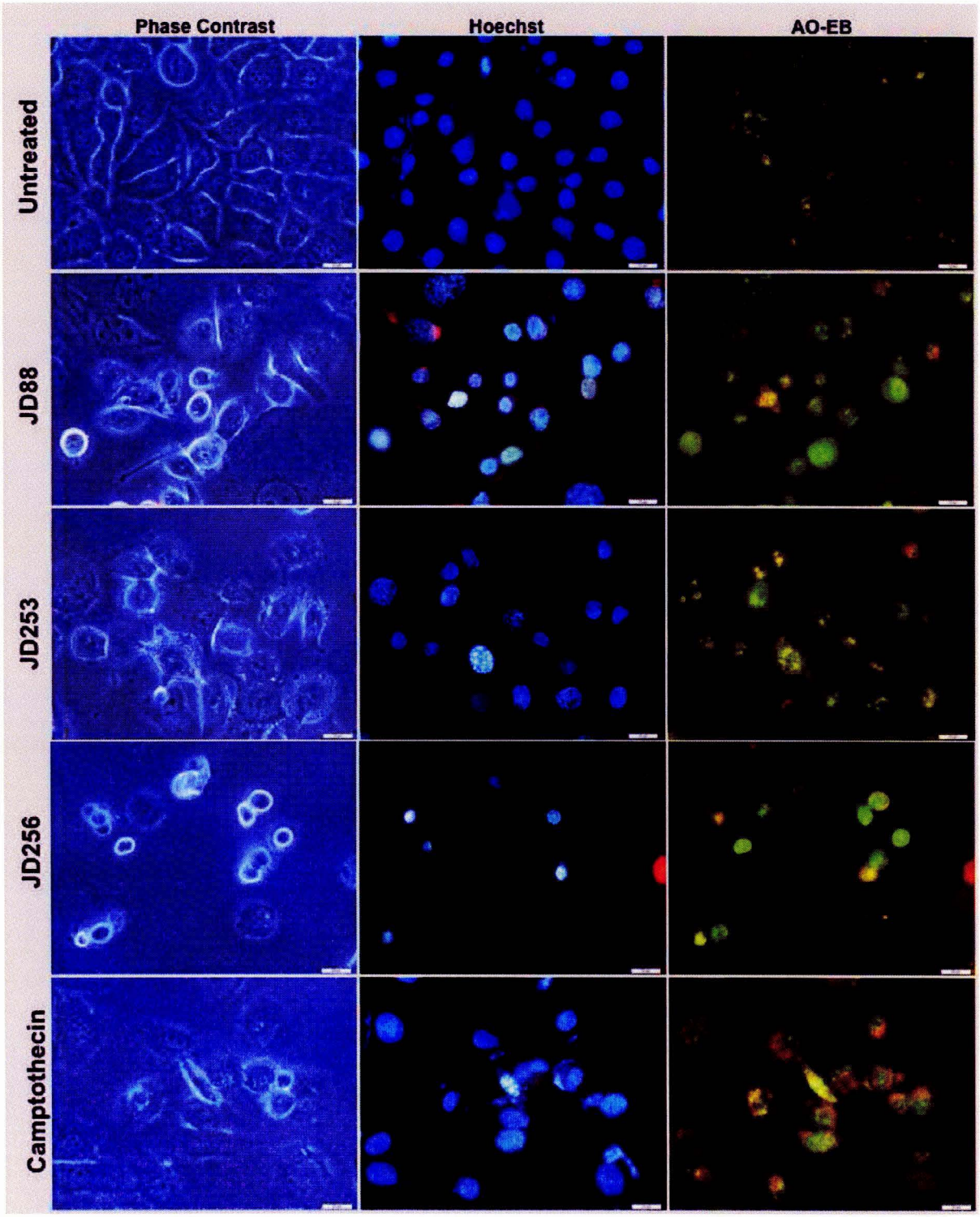


Figure C7.11 Effect of test compounds on nuclear morphology in MCF-7 cells at 24 hours

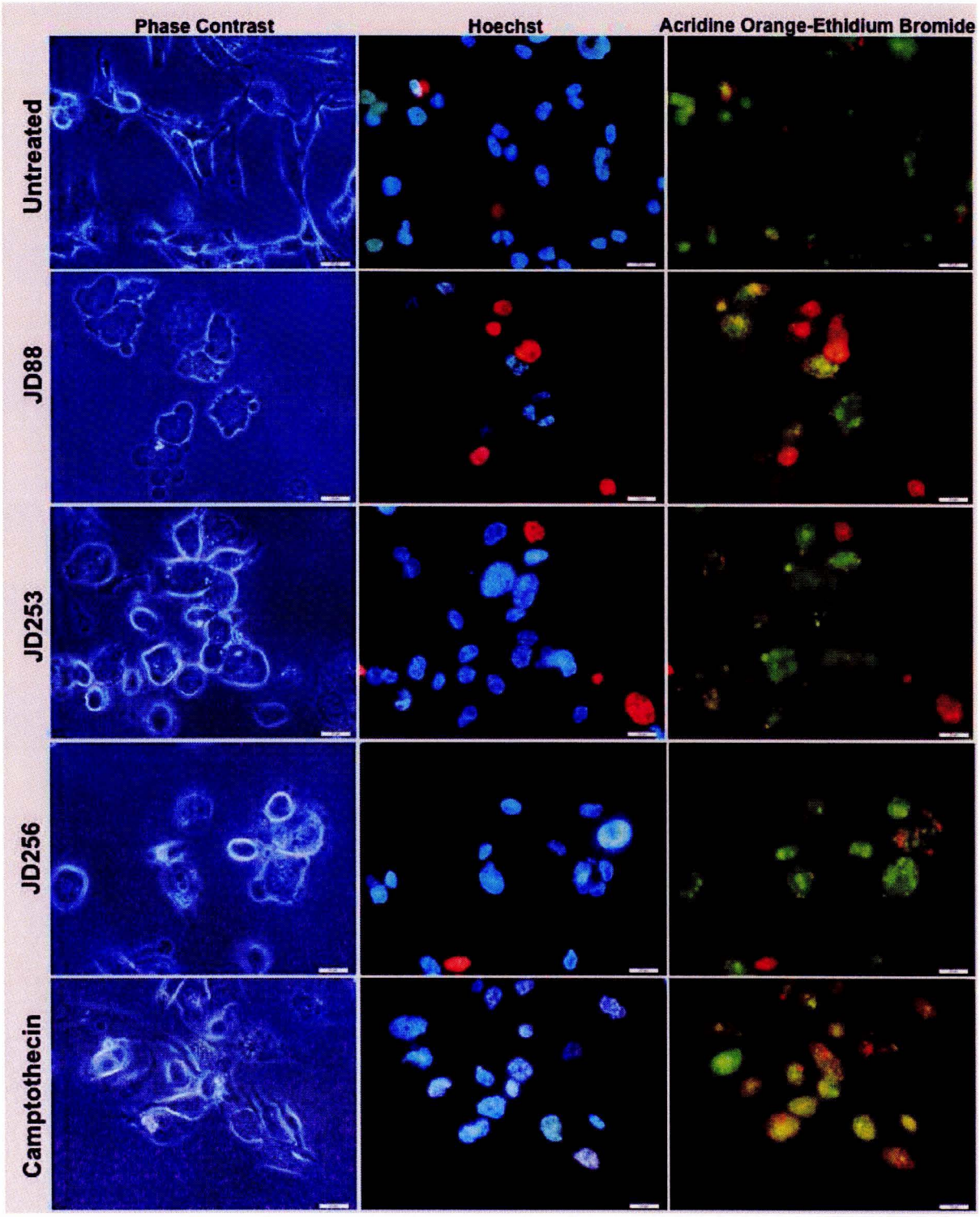


Figure C7.12 Effect of test compounds on nuclear morphology in MDA-MB-231 cells at 24 hours

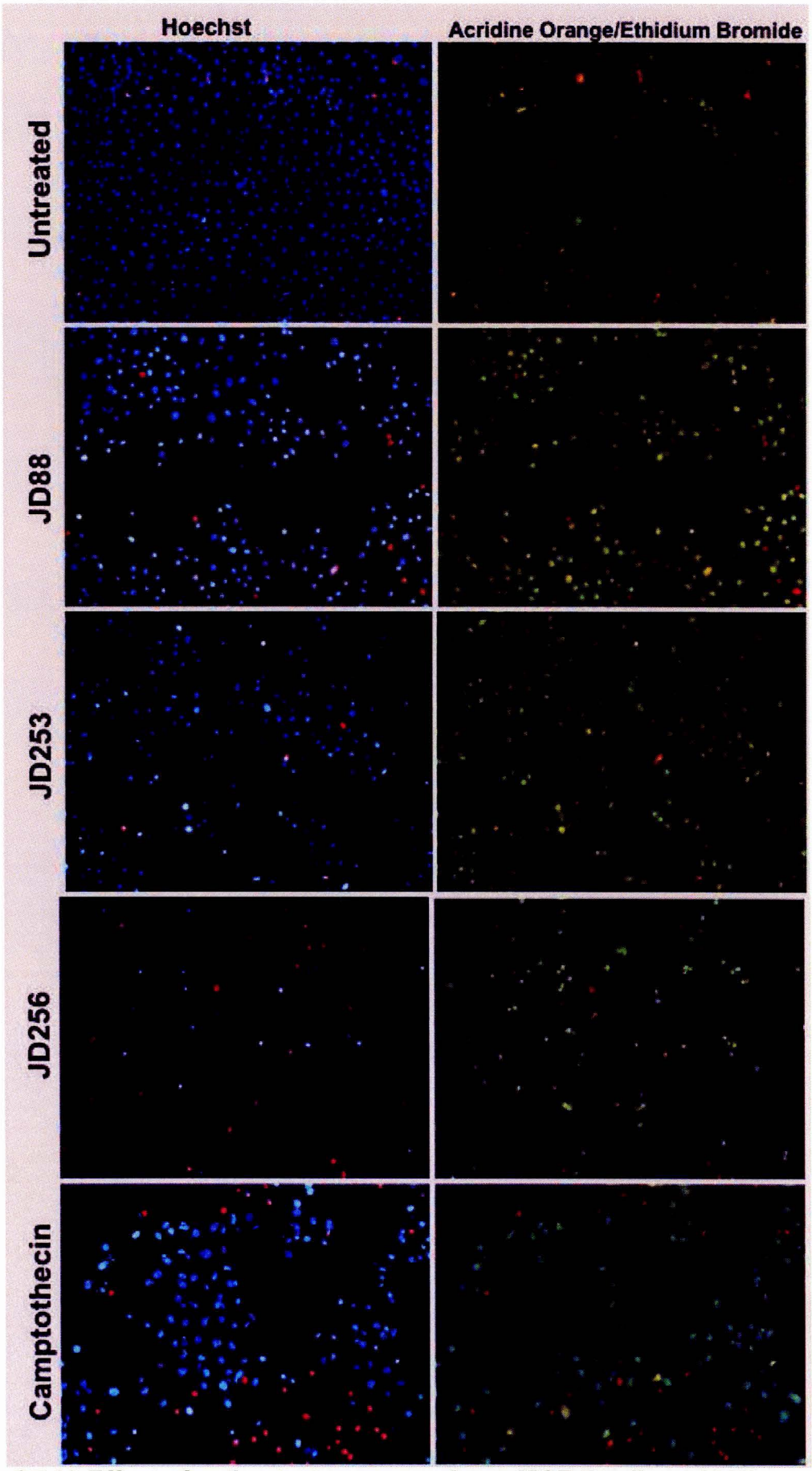


Figure C7.13 Effect of active test compounds on MCF-7 cells at 100X magnification Used to calculate the apoptotic and necrotic index

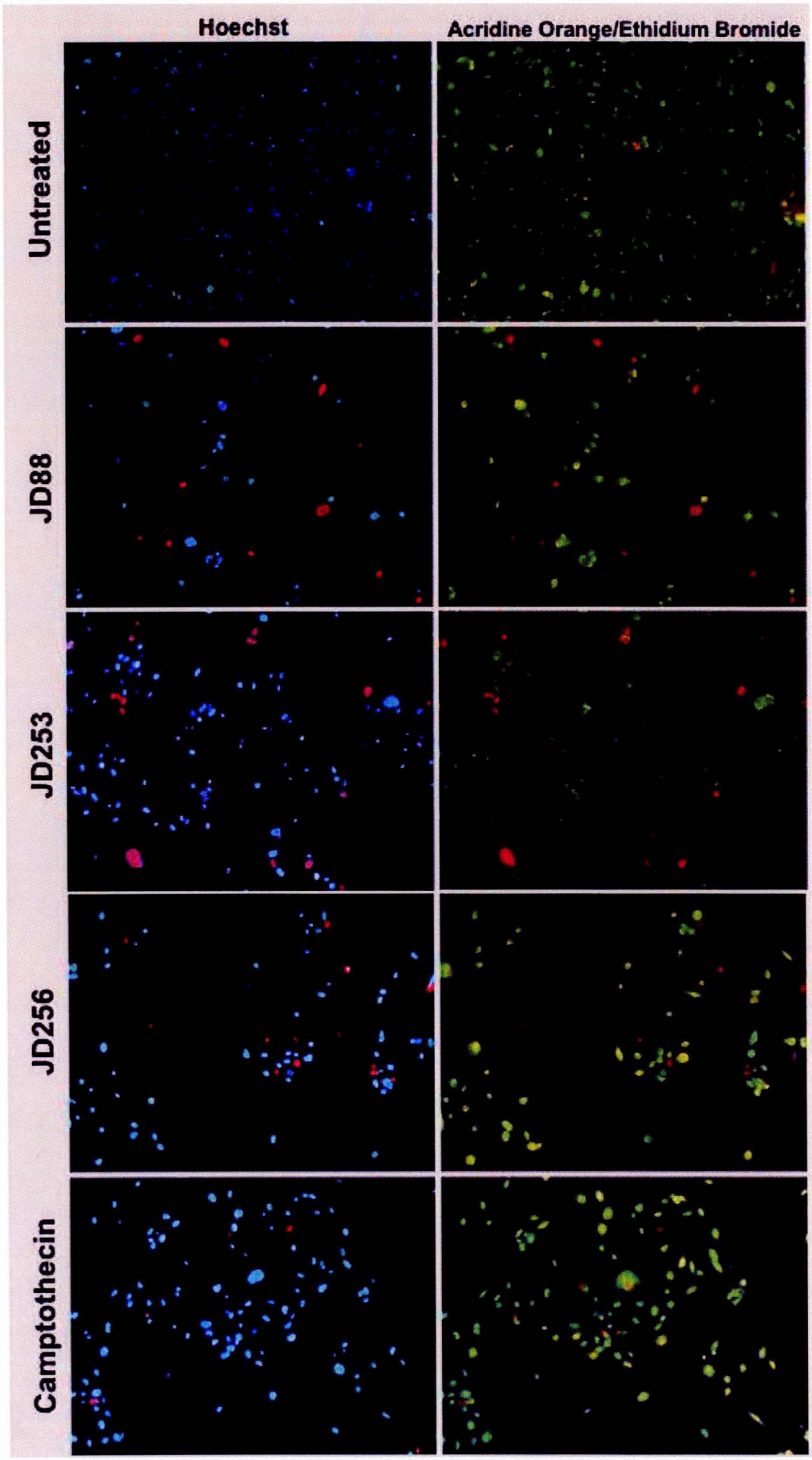


Figure C7.14 Effect of active test compounds on MDA-MB-231 cells at 100X magnification Used to calculate the apoptotic and necrotic index

Appendix D: Protein Concentration

Table D7.1 Effect of active test compounds on protein concentration in MCF-7 cells (caspase assay)

	Test Compounds				
Time (hours)	**Untreated**	**JD88**	**JD253**	**JD256**	**Camptothecin**
2	1.11 mg	1.05 mg	0.97 mg	1.17 mg	0.83 mg
8	1.06 mg	1.01 mg	0.95 mg	1.07 mg	0.77 mg
12	1,14 mg	0.92 mg	0.96 mg	1.04 mg	0.76 mg
18	1.24 mg	0.70 mg	0.67 mg	0.85 mg	0.64 mg
21	1.25 mg	0.70 mg	0.62 mg	0.70 mg	0.60 mg
30	1.33 mg	0.63 mg	0.55 mg	0.67 mg	0.55 mg

Table D7.2 Effect of active test compounds on protein concentration in MDA-MB-231 cells (caspase assay)

	Test Compounds		
Time (hours)	**Untreated**	**JD88**	**Camptothecin**
2	0.90 mg	0.95 mg	0.93 mg
6	0.94 mg	0.91 mg	0.87 mg
8	1,04 mg	0.92 mg	0.74 mg
12	1.29 mg	0.74 mg	0.69 mg
18	1.30 mg	0.72 mg	0.65 mg
24	1.39 mg	0.67 mg	0.64 mg